Elucidating the biological role of silicon

and

Designing a delivery system to enhance early bone mineralisation

by

Gurpreet Birdi

A thesis submitted to the School of

Chemical Engineering of the

University of Birmingham for the

degree of Doctor of Philosophy

School of Chemical Engineering

University of Birmingham

Edgbaston

Birmingham

B15 2TT

Abstract

Silicon has been shown to be an important trace element in bone formation and metabolism, and a decrease in silicon in the mammalian diet leads to abnormal bone formation. Consequently, silicon has been incorporated into many biomaterials to enhance bone generation around implants. Despite this, the mechanism of action has still not been elucidated and a therapeutic dosage has not been determined.

In this thesis, the optimum concentration of orthosilicic acid (OSA) to enable cell survival and early mineralisation has been identified. It was noted that a dosage of 5µg/ml of OSA enhanced bone nodule formation. The presence of OSA increased the expression of early osteogenic markers such as osteopontin, osteocalcin and type 1 collagen. In addition, increasing OSA concentration resulted in the development of a collagen fibril network of increasing complexity, up to supraphysiological OSA concentrations when the fibril network became fragmented. It was hypothesised that this may assist with mineral deposition.

A sustained delivery system was also developed using a combination of PLGA and calcium silicate. A sustained dose of orthosilicic acid ideal for cell survival was released from the PLGA micro-particles containing calcium silicate. As well as providing a source of OSA, the presence of the alkaline degradation products of calcium silicate aided in the neutralisation of the acidic degradation products of PLGA, which might enhance cell viability in the local environment. In addition to influencing cell behaviour, the OSA was shown to have a strong interaction with alginate, modifying its properties and preventing degradation. This finding is of importance as the molecules comprising alginate bear a structural resemblance to the glycosaminoglycans that are found in the majority of tissues.

Author Declaration

All the work submitted in this thesis for assessment is solely my work.

Gurpreet Birdi

Acknowledgements

I would like to express my deepest appreciation to my supervisor Professor Liam Grover for giving me the opportunity to carry out this work and his on-going guidance and inspiration throughout my PhD. I would also like to extend a special thank you to Dr. Richard Shelton, for all his help during my work at the School of Dentistry. In addition I express my gratitude to Dr. Rachel Bridson and Dr. Alan Smith for their support during their time at University of Birmingham.

Many thanks also go to the supporting staff at the Biochemical Engineering building, including Elaine Mitchell and David French for their assistance with various laboratory equipment and techniques.

I am very appreciative to all the members of L. Grover's group for all their help during the years, in their own unique ways, especially to Parastoo Jamshidi, for the very useful scientific discussions as well as the encouragement and lunch breaks. Many thanks also go to Dr. Jennifer Paxton for her helpful comments and guidance throughout my research.

Finally I would like to thank my mum, dad and Harraj, for their on-going encouragement not only through this PhD but throughout everything I have chosen to do. To my Fiancé Nav, thank you for the late night pick- ups and the amazing motivational speeches. I could not have done it without you all.

I dedicate this thesis to the most inspiring person in my life, my late grandfather, Diwan Singh Birdi, who would have been very proud to see me graduate.

TABLE OF CONTENTS

LIST OF FIGURES

List of Tables

List of Abbreviations

AFM	Atomic force microscope
ALP	Alkaline phosphate
BCP	Biphasic calcium phosphates
BMPs	Bone morphogenetic proteins
Calcium silicate/PLGA	CS/PLGA
cDNA	Complementary DNA
Coll- 1	Collagen Type 1
DMEM	Dulbecco's Modified Eagle's Medium
DMP-1	Dentin matrix protein-1
EDTA	Ethylenediaminetetraacetic acid
FBS	Foetal bovine serum
GAPDH	Glyceraldehyde-3-phosphate dehydrogenase
GH	Growth hormone
GPI	Glycosylphophatidylinositol
HA	Hydroxyapatite
IGFs	Insulin-like growth factors
L-Glut	L-Glutamine
MSCs	Mesenchymal stem cells
MEPE	Matrix extracellular phosphoglycoprotein

OCN	Osteocalcin
OM	Osteogenic mediators
OPN	Osteopontin
OSA	Orthosilicic acid
P/S	Penicillin/streptomycin
PCL	Poly-ε-caprolactone
PCNA	Proliferating cell nuclear antigen
Pi	Inorganic phosphate
PLA	Polylactic acid
PLGA	Poly lactic-*co*-glycolic acid
PPi	Inorganic pyrosphosphate
rBMSCs	Rat bone marrow cells
SBF	Stimulated body fluid
s-DMEM	Supplemented DMEM
SEM	Scanning electron microscope
Si-HA	Silicon substituted hydroxyapatite
TAE	Tris Acetate EDTA
TGF-β	Transforming growth factor-beta
XRD	X-ray diffraction
XRF	X-ray fluorescence

α-MEM	α-Minimum Essential Medium
α-or-β- TCP	α-or-β Tricalcium phosphates

1. Introduction

Bone related diseases such as osteoporosis and rheumatoid arthritis have an immense impact on an individual's health as well as the population at large, resulting in high financial costs to national economies (Harvey et al. 2010). With a global shift towards an aging population, there is a large increase associated with bone related diseases. Consequently this has led to a demand for biomaterial-based treatments in orthopaedics (Stevens 2008).

A large volume of bone may be removed for the treatment of disease (Raisz 1999), genetic abnormalities (Rucci 2008) or trauma (Arcos & Vallet-Regí 2010). Bone grafts are used to enhance the healing process as well as prevent fibrosis occurring within the defect (Palmer et al. 2009). Two million bone grafting procedures are undertaken annually, with most of them using the 'gold standard' autograph procedure (Walschot et al. 2012). Allografts (Lavernia et al. 2004) and xenografts (Navarro et al. 2008) are other biological bone grafts often used in treating bone defects. Although these bone grafting procedures have been shown to be successful in the augmentation of bone defects they still have major disadvantages, such as, immune rejection and disease transmission (Rupani et al. 2012). This has stimulated research into the development of novel approaches to replace tissue bone grafting.

Many synthetic materials such as polymers (Gunatillake & Adhikari 2003), metals (Matsuno et al. 2001), hydrogels (Hunt et al. 2010), glass (Hench 2009) and cement (Ohtsuki et al. 2009) have been investigated as bone replacement materials. An ideal biomaterial for bone replacement should enhance the healing of the bone tissue and yet resorb without non-cytotoxicity (Hing 2004), as well as performing a mechanical role by supporting the surrounding tissues. To date, however, autografts are still being used as the materials of

choice for bone replacements as they stimulate bone growth and healing, resulting in good clinical results (Jones 2013).

Many ions have been detected in the body at trace levels and have been shown to elicit strong biological responses. For example, copper has been shown to promote blood vessel formation (Sen et al. 2002), zinc has been shown to enhance healing in fractured bone (Towler et al. 2009) and silicon has been shown to play a key role in the calcification of young bone (Carlisle 1976). This has therefore led to an increase in investigations incorporating silicon into various biomaterials, with a number reaching the market as promising bone replacement materials. Xynos et al (2000) demonstrated the effect of silicon from a phosphosilicate glass (Bioglass®) and showed the osseointegration of the material within the implanted site without the occurance of fibrosis (Xynos et al. 2000). Others have attempted to incorporate silicon into the hydroxyapatite lattice (Patel et al. 2002) and other calcium phosphate ceramics (Ni et al. 2008). These materials have been shown to have a significant effect on osteogenesis when compared to the non-modified ceramics. There is no complete consensus, however, as to how silicon functions to enhance mineralisation. Previously it has been reported by Reffit et al (2003) that the soluble form of silicon; orthosilicic acid enhances collagen 1 expression (Reffitt et al. 2003). At the same time little work has been done to determine the local release of orthosilicic acid from these biomaterials *in vitro* and *in vivo.* Therefore, the therapeutic dose of orthosilicic acid released from these materials, which will maximise hard tissue formation, has yet to be established.

The work reported in this thesis systematically evaluated the effect of silicon in its soluble form, orthosilicic acid (OSA), on cell viability, collagen excretion and formation, as well as mineral deposition. By identifying the role of silicon and the therapeutic dosage of silicon a delivery system was developed to release a sustained dosage of orthosilicic acid over a period

of time. Work has also been undertaken to determine how orthosilicic acid may interact with and modify the structures of a number of biomaterials, including alginate.

2. Literature review

2.1 Bone Biology

In the past, the skeleton has often had a reputation of being an inert and static material. However, given that bone tissue has the ability to repair itself and its capacity to rapidly mobilise mineral stores on metabolic demand it is in fact a 'smart' material (Sommerfeldt & Rubin 2001), and a dynamic biological system. Bone is a dense multi-phase composite made up of cells embedded in a matrix composed of organic and inorganic elements. Its structure usually differs widely, depending on age, site and history leading to its classifications by mechanical and functional characteristics (Hing 2004). Although bone's primary role is to maintain the body's structure it is also responsible for maintaining mineral homeostasis, and acts as a source of haematopoietic stem cells. Bone in its natural environment is involved in a continuous cycle of resorption and renewal, therefore always undergoing a chemical exchange and structural remodelling, due to internal hormonal regulation and external mechanical demands (Grosland 2001). The mineral storage however, can exceed the structural function resulting in the loss of the bone structure.

2.2 Bone structure

Bone is a complex and dynamic living tissue that is continually reshaped and remodelled to provide dynamic mechanical support and facilitate for movement in vertebrates. It also acts as protection for internal organs against injury, for example the ribs protect all the organs in the thoracic cavity. Morphologically bone is divided into two types on the basis of porosity and the microstructure:

Trabecular/ cancellous bone: make up only 20% of the skeleton – Trabecular bone is mainly made up of a loosely organised porous matrix of interconnecting columns and these spaces are filled with bone-marrow (Tuan et al. 2003). The mechanical properties of cancellous bone are mostly dependent upon porosity and architecture, both which vary due to the location and age of the bone. In addition, cancellous bone is often anisotropic due to the orientation of major trabeculae along the lines of principle stress (Kuo & Carter 1991).

Cortical / compact bone; Cortical bone comprises of 80% of the mass of the skeleton. Compact bone is dense with a porosity ranging between 5% - 10%. It is primarily found in the diaphyses of long bones and forms the outer shell around the cancellous bone at the end of joints and vertebrae (Grosland 2001). Cortical bone is arranged in a series of concentric rings known as osteons, which surround the central Haversian canal, this consists of blood vessels which are laterally linked by Volkmann's canals (Hogan 1992). Osteocytes surrounded by the osseous matrix are found in pores within the osteons and enable the exchange of nutrients, growth factors and factors responsible for maintaining mineral levels within the body (Figure 1.1) (Hing 2005)

Figure 2.1: Sectioned human femoral head, showing the differences in bone structure (a). Structure of the cortical bone including Haversian canal and interconnecting Volksmann canal (b) (National Cancer Institute, 2012)

Both cortical and cancellous bones are surrounded by fibrous connective tissue known as the periosteum (Figure 2.1b). The periosteum provides a blood supply and innervation on the bone surface, in addition it is the main store of osteoprogenitor cells and osteoblasts, and therefore plays a vital role in fracture repair (Rowe & Tracey 2005).

Cortical bone is mainly known for its protection and load –bearing capabilities to bone while trabecular bone is responsible for metabolic functions of bone. Cortical bone appears in various shapes such as:

1. Long bones: these have a greater length than width and consist of a shaft and a variable number of endings; their primary function is strength and examples include, femur, tibia, fibula, humerus, ulna and radius.

2. Flat bones: have a thin structure and provide considerable mechanical protection and large surfaces for muscle attachment, examples include cranial bones (that protect the brain), the sternum and ribs (protecting the organs in the thorax) and the scapulae, also known as, shoulder blades.

Cancellous bone can be further classified into coarse and fine; coarse cancellous bone is characteristic of a healthy adult mammalian skeleton, while fine cancellous bone is often found in the foetal skeleton or early fracture callus.

Bone also functions in mineral homeostasis and stores several vital minerals, especially calcium and phosphorous, which it can release into the bloodstream to maintain critical mineral balances. Furthermore bone can suffer from pathological conditions for example cancer, and can degrade as a result of age and disease, that is, osteoporosis.

2.2.1 Cell types in bone metabolism

Various cell types are responsible for the continuous remodelling and resorption of bone tissue. These distinct lineages can be found within the bone: osteoblasts and osteocytes, these are responsible for mineral deposition and homeostasis respectively and osteoclasts are involved in bone resorption process.

2.2.1.1 Osteoblasts

Osteoblasts are mononucleated cells derived from multipotent mesenchymal stem cells. They can be differentiated into various mesenchymal lineages, such as fibroblasts, chondrocytes, myoblasts and adipocytes, depending on the activated transcription signalling pathways (Yamaguchi et al. 2000).

Several specific transcription factors are responsible for the commitment of multipotent mesenchymal cells into the osteoblast cell lineage. Core binding factor α 1 (Cbfα-1) , also known as, Runx – 2, a transcription factor part of the *runt* domain gene family, plays a critical role in osteoblast differentiation. It is involved in the production of bone matrix proteins and it is able to up-regulate the expression of major bone matrix protein genes, such as type 1 collagen, osteopontin, bone sialoproteins and osteocalcin (Fukuoka et al. 2007) leading to an increase in the number of immature osteoblasts from multipotent stem cells.

Differentiated osteoblasts are responsible for bone formation process and in the mineralisation of the extracellular bone matrix. They play an important role in the modulation of bone remodelling as well as in the regulation of the metabolic activity of other bone cells via the receptor activator of nuclear factor κ – B ligand and osteoprotegrin (OPG). Inadequate osteoblastic function is responsible in the number of human bone related diseases such as osteoporosis and rheumatoid arthritis.

2.2.1.2 Osteocytes

Osteocytes are fully differentiated, non-proliferating cells, and are localised in the mineralised bone matrix and in newly synthesised osteoids. They are derived from active osteoblasts, which become encased within the bone matrix during bone formation, after the completion of ECM synthesis and mineralisation, 10-20% of osteoblasts differentiate into osteocytes (Andreassen & Oxlund 2001). Several studies showed that osteocytes express specific markers for bone formation and phosphate homeostasis. Dentin matrix protein 1 (DMP1), matrix extracellular phosphoglycoprotein (MEPE) and sclerostin are gene markers that are involved in phosphate homeostasis. They are also key endocrine regulators for bone metabolism, and are sensitive to parathyroid hormone and calcitonin, and are therefore responsible for maintaining plasma calcium levels in the body (Matsuo & Irie 2008). Osteocytes secrete signalling molecules such as nitric oxide and prostaglandin E_2 to initiate bone remodelling (Guo & Bonewald 2009).

Osteocytes are also involved in the maintenance of the dynamic equilibrium between osteoblast and osteoclast cells, and therefore play a vital role in the bone remodelling and bone resorption processes.

2.2.1.3 Osteoclasts

Osteoclast cells are continuously ‘destroying’ the very organ that the body is trying to form (Phan et al. 2004). Osteoclasts are multinucleated cells, derived from haemopoetic cells lines of the monocyte/macrophage lineage (Rucci 2008). The differentiation of osteoclasts occurs with close contact to stromal cells and the interaction between monocyte precursors and osteoblasts shown in Figure 2.2. The production of two haematopoetic factors, from stromal cells, the TNF-related cytokine RANKL and the polypeptide growth factor CSF-1 assist in

promoting osteoclast genesis and for the activation of RANKL on the surface of haematopoetic precursor cells (Fox & Lovibond 2005).

Osteoclasts lie in the Howship's lacunae, small conical cavities within the bone matrix (Raisz 1999). An actin ring creates a tight junction between the cell and the surface of the bone and the osteoclasts begin to form a polarised morphology. Proton pumps such as the ATPase ion pump in osteoclasts, pumps hydrogen ions against a high concentration gradient into the cavities acidifying (Equation 2-1) and dissolving the mineralised bone matrix into Ca^{2+}, H_3PO_4, H_2CO_3 and H_2O (Francis et al. 2002).

$$H_2O + CO_2 \rightarrow HCO_3^- + H^+$$

Equation 2-1

Additionally several hydrolytic enzymes including collagenase and cathepsin K are released in the lacuna via lysosomes to degrade the organic matrix (Matsuo & Irie 2008). This leads to debris of calcium salts and protease products which are endocytosed by the cell and form vesicles in the cytoplasm before excretion. Regulation of osteoclastic differentiation and activity is monitored by various hormones, such as parathyroid hormone (PTH), calcitonin and Interleukin 6 (IL-6) (Hadjidakis & Androulakis 2006).

Imbalances between osteoblastic and osteclastic activity can result in various bone related diseases such as Paget's disease occurs due to osteoclasts over activity and osteopetrosis due to insufficient osteoclast activity (Raisz 1999).

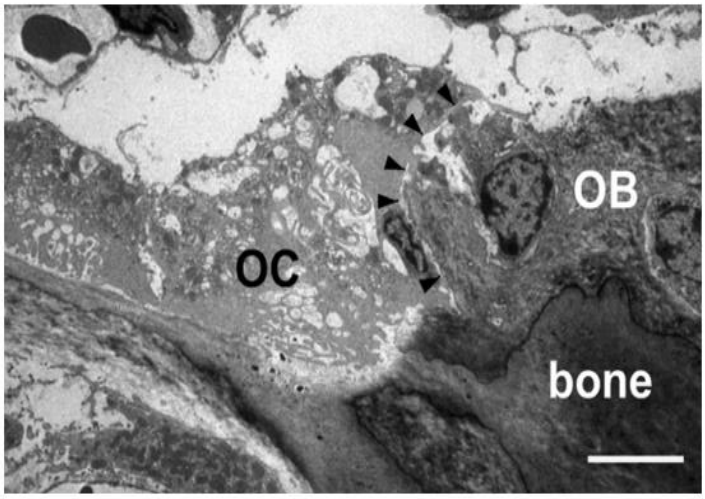

Figure 2.2: TEM image of osteoclast – osteoblast contact in 14 week old mouse tibial bone. Arrows show contact surface between osteoclasts (OC) and osteoblasts (OB). Scale bar 5μm (Matsuo & Irie 2008)

2.2.2 Bone remodelling

2.2.2.1 Bone formation and metabolism

Bone formation is first observed when undifferentiated mesenchymal cells or pre-osteoblasts take on the appearance of osteoblasts which begin to secrete a specialised extracellular matrix. The matrix starts to mineralise and the pre- osteoblasts surrounded by the matrix are differentiated to osteocytes, this type of bone formation is known as intramembranous ossification. Osteoblasts initially produce bone during embryonic development and continue to metabolise bone during bone growth and remodelling including tissue trauma, such as myositis ossificans, whereby calcification occurs within a muscle after trauma or fracture. Mature bone is formed by the highly organised mineralisation of the bone matrix secreted by the osteoblast cells (Buckwalter et al. 2010). Long bones, however, are formed through endochondral ossification; this is whereby the cartilage is initially formed from differentiating chondrocytes, and later replaced by bone through morphogenesis (Gerber et al. 1999)

Osteoblasts have been shown to produce various growth factors, which are regulated by both hormones and local mechanical stress. Growth factors have been shown to increase bone formation *in vivo* by regulating proliferation and differentiation of osteoblasts at different stages of the cell cycle and therefore significant for local regulation of bone formation. Bone morphogenetic proteins (BMPs) and Insulin-like growth factors (IGFs) are growth factors that are involved in the bone modelling process;

Bone morphogenetic proteins (BMPs) are involved in various development and pathophysiological processes of bone formation. BMPs are synthesised by osteoblasts and are secreted within the extracellular bone matrix. *In vitro*, differentiation of mesenchymal stem cells (MSCs) into osteoblastic phenotypes occurs in the presence of BMPs. *In vivo*, BMPs initiate the complete pathway of bone formation, starting from the migration of MSCs through to the differentiation into osteoblasts (Kempen et al. 2010).

Insulin growth factors (IGFs) have shown to increase the proliferation and migration of MSCs and osteoprogenitor cells *in vitro*, leading to new bone formation and mineralisation**.** IGFs have an anti-apoptotic effect on pre-osteoblasts and enhance bone matrix synthesis. *In vivo* IGF treatment increased bone formation, bone volume as well as bone turnover in animal models and clinical trials for osteoporosis (Niu & Rosen 2005).

2.2.2.2 Bone resorption

Bone homeostasis relies on the delicate balance between bone deposition by osteoblasts and bone resorption by osteoclasts. Initial osteogenesis occurs in the embryonic skeleton, and hereon osteoblasts and osteoclasts begin the simultaneous processes of bone modelling and remodelling. During skeletal growth, bone remodelling takes place at a rapid pace. The rate of bone turnover of the skeleton approaches nearly 100% in the first year of life, and decreases to approximately 10% per year in early adulthood and remains at this rate throughout life (Barrère et al. 2006). The intercellular communication between both osteoblasts and osteoclasts is essential to maintain this balance (Phan et al. 2004).

Osteoclasts are derived from the haematopoietic cell lines of the macrophage/monocyte lineage and are differentiated within the bone microenvironment. Once differentiated, multinucleated osteoclasts attach to the bone matrix via integrin receptors and undergo various morphological changes. The cells polarise at 4 domains known as; the ruffled border, the basolateral domain, the functional secretory domain and the sealing zone, illustrated in Figure 2.3. The osteoclasts initiate bone resorption, by degrading the inorganic component of the bone matrix, hydroxyapatite. This is demineralised by the acidification of the intercellular vesicles known as resorption lacunae, which secrete hydrochloric acid leading to the dissolution of the mineral crystal allowing for the digestion of the bone matrix. As the bone undergoes resorption, various growth factors such as growth hormone (GH) and transforming growth factor – β (TGF-β), within the bone matrix are released at the same time, to recruit osteoblasts in the resorbed area as illustrated in Figure 2.3 (Rucci 2008).

Growth Hormone (GH) functions as a growth factor for bone remodelling in two ways; via direct interactions with GH receptors on osteoblasts and via the induction of IGF-1. Direct interaction of GH stimulates the proliferation of osteoblasts. In recent *in vitro* studies, it has

been shown that GH also regulates osteoclast formation in bone marrow cultures (Ohlsson et al. 1998). *In vivo* studies have shown that GH administration increases bone formation and resorption and thus enhancing bone mass and mechanical strength (Andreassen & Oxlund 2001).

Transforming Growth Factor – β (TGF- β) is mainly expressed by osteoclast and osteoblasts, and is therefore considered an important regulator for their activity. It has been suggested that TGF-β couples both bone formation and resorption during the remodelling cycle. It directly enables osteoclast formation by antagonising inflammatory signalling; this stimulates a state in which various precursors are resistant to the inflammatory response created by the osteoclasts. In contrast the role of TGF-β is also to suppress osteoclast formation to prevent excessive resorption. This indirect role of TGF-β is as a result of it regulating the osteoblastic signalling pathway, involving RANKL (receptor activator of NF_kB ligand) expression. An increase in RANKL expression reduces the rate of osteoclastic differentiation and therefore reduces the rate of resorption (Fox & Lovibond 2005).

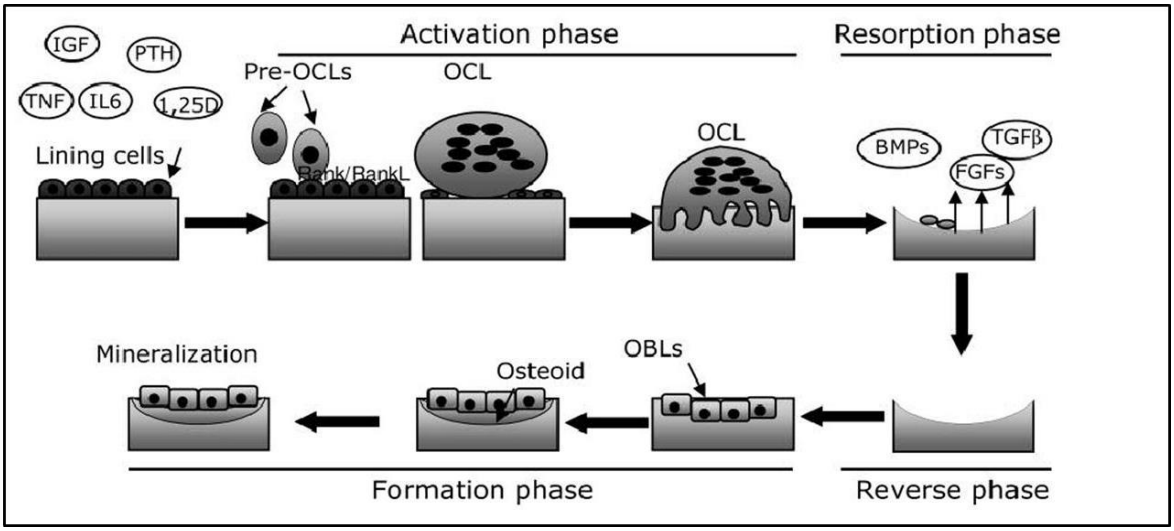

Figure 2.3: Schematic representation of the bone remodelling process; Activation phase is where bone remodelling begins when lining cells are activated by various signals and increase the expression of RANKL. RANKL triggers osteoblast (OBL) differentiation. Resorption phase – osteoclasts (OCL) resorb bone and factors stored within the bone matrix are released, thus recruiting osteoblasts in the reabsorbed area. Formation phase – osteoblasts produce a new bone matrix and stimulate mineralisation therefore completing the remodelling process (Rucci 2008).

2.2.3 Molecular biology

Osteoblasts are continuously developing from a proliferating immature cell to a mature osteoblastic cell that synthesises specific bone proteins which are characterised by a specific sequential expression of tissue specific genes. These specific genes identify the three distinct periods of osteoblast phenotype development; proliferation, maturation and the synthesis of the extracellular matrix and matrix mineralisation (Neve et al. 2011). Differentiated and mature osteoblasts express the proteins as described below.

2.2.3.1 Collagen

Collagen is the most common protein found in nature and is present in many tissues in the human body such as bones, skin, lungs and scar tissue as it is the major constituent of the extracellular matrix. Collagen has many functions, the major function among them being its capacity to mineralise in tissues such as bone, tendon and dentin. Mineralised collagen acts as the framework for the mechanical support as of the skeleton and acts a reservoir for ions and small molecules as well as a means of strain energy storage (Landis et al. 2006).

The defining feature of collagen is the right handed triple helix formed from a structural motif of 3 parallel polypeptide strands in a left-handed, polyproline-II-type (PP-II) helical confirmation which coil around each other and is stabilised by hydrogen bonding (Shoulders & Raines 2010). The triple helix configuration is made up of repetitive triplet of Gly-X-Y, where X is often proline and Y is usually hydroxyproline. Glycine is always required in every third position as it is the smallest amino acid that occupies a limited space in the centre of the triple helix (Viguet-Carrin et al. 2006).

The triple helix form collagen fibrils of approximately 300nm in length and 1.5nm in diameter are bordered with short telopeptides. Collagen fibrils are synthesised and transported into the extracellular matrix in the form of procollagens - soluble precursors of collagen. The biosynthesis of procollagen is a complex process in which several enzymes and molecular chaperones assist its folding and trimerisation. Synthesised procollagen chains are associated in trimers via their C-propeptides, leading to nucleation and folding in a C-to-N direction and forming the triple helix. Protein disulphide isomerase induces the formation of inter and intrachain disulphide bonds within the c-propeptide allowing the association between procollagen chains (Viguet-Carrin et al. 2006).

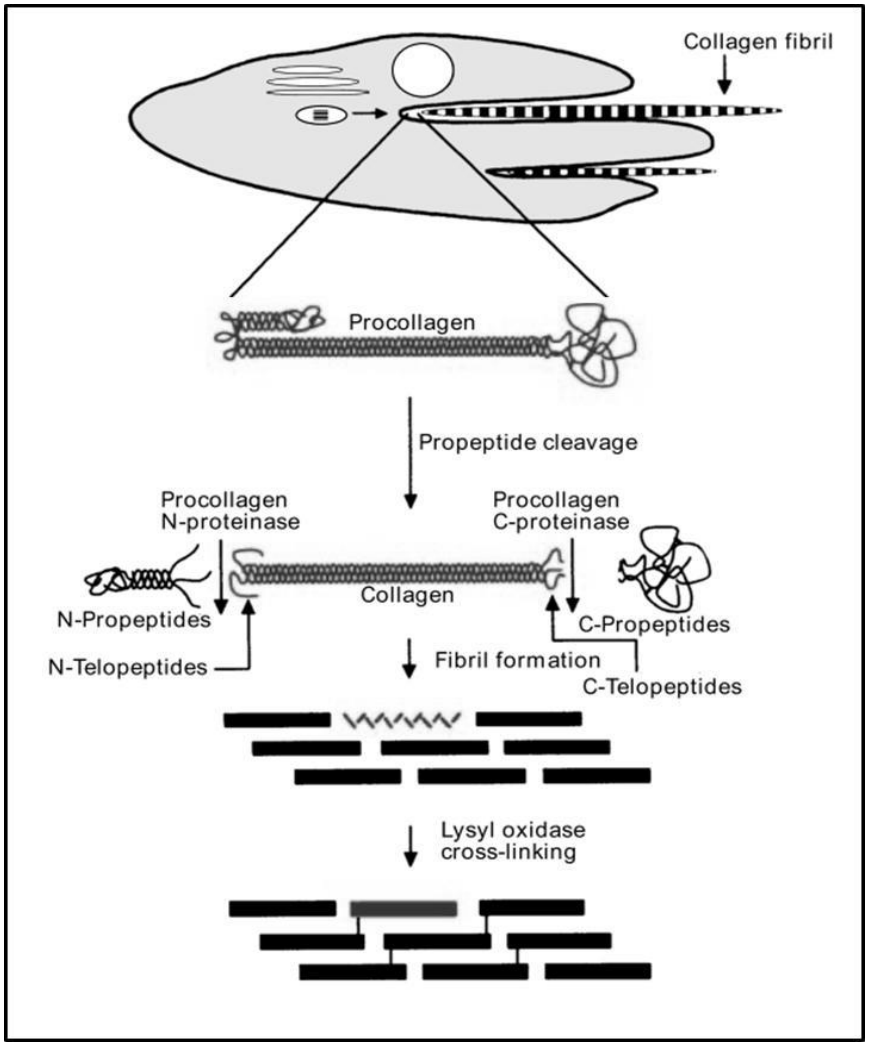

Figure 2.4: Schematic diagram illustrating the process in which procollagen is converted to collagen after it is released from cells (Kadler et al. 1996).

Procollagen bordered by a trimeric globular C – propeptide domain (right hand side of Figure 2.4) and the trimeric N-propeptide domain (left hand side of Figure 2.4) is secreted from cells and converted to collagen by the removal of the C and N propeptides by procollagen proteinases. Once the collagen is formed it spontaneously self assembles into striated fibrils that are present in the ECM of connective tissues. These fibrils are stabilised via covalent cross-linking which is limited by oxidative deamination of specific lysine and hyroxylysine residues in the collagen by lysyl oxidase.

Approximately 80% of the total proteins in bone are collagen, whereby 95% of this collagen is type 1 collagen. Bone matrix has the unique ability to mineralise, as crystals of hydroxyapatite are found on the collagen fibres and within them. The crystals are often oriented in the same direction as the collagen fibres. type 1 collagen is known for its mechanical function, providing elasticity and structure in bone tissue. Several studies indicate collagen plays a key role in its capacity to absorb energy, while the mineral content, HA, is mainly involved in determining bone stiffness.

Abnormalities of collagen structure can be caused by genetic mutations such as osteogenesis imperfecta – a disease which causes brittle bones due to the lack of connective tissue, the amino acid sequence of type 1 collagen is altered which results in the formation of branched fibres responsible for brittle bones and abnormal mineralisation (Rupani et al. 2012).

2.2.3.2 Osteopontin

Osteopontin (OPN) is made up of approximately 300 amino acids and is a negatively charged hydrophilic protein, which is acidic in nature. The OPN molecule undergoes considerable post-translational modification, and is phosphorylated and glycosylated. OPN has an arginine –glycine-aspartic acid (RGD) cell binding sequence, a calcium binding site and two heparin binding domains (Mazzali et al. 2002).

OPN is closely involved in the regulation of both physiological and pathological mineralisation and is expressed by both osteoclast and osteoblasts. OPN influences bone homeostasis both by inhibiting mineral deposition, by promoting osteoclast differentiation and by enhancing osteoclast activity (Rosenthal et al. 2007). OPN is one of the major non-collagenous proteins in bone. The electronegative RGD residues and the Ca^{2+} binding sites allow OPN to tightly bind to HA, therefore making OPN a potent inhibitor of the mineralisation process. Osteopontin is secreted into all body fluids and plays a key role in angiogenesis as well as immune function (Standal et al. 2004).

2.2.3.3 Alkaline Phosphatase

Alkaline phosphatase (ALP, orthophosphoric-monoester phosphohydrolase – EC 3.1.3.1) is a metalloenzyme which is expressed in various tissues, such as the intestine, placenta, liver, kidney and bone. The ALP gene corresponding to the liver, kidney and bone is the tissue-nonspecific alkaline phosphatase (TNAP) (Mornet et al. 2001). ALP is anchored to the membrane via glycosylphosphatidylinositol (GPI) by means of postransational modification (Golub et al. 2007).

High levels of ALP are present in bone as it is known to increase the local concentration of inorganic phosphate (Pi) (Golub et al. 2007). ALP is among the first non-collagenous genes expressed in the process of calcification, as it hydrolyses inorganic pyrophosphate (PPi) to generate Pi, which stimulates the formation of hydroxyapatite. ALP expression is therefore a good predictor neotissue osteogenesis (Orimo 2010)

Mutations on the TNAP gene have been linked with hypophosphatasia a rare inherited bone disease, which is characterised by hypomineralisation of hard tissues (Whyte 2010).

2.2.3.4 Osteocalcin

Osteocalcin (OCN) makes up 25% of the non-collagenous proteins of the bone matrix. It is a highly conserved (has the same sequence in most invertebrates) extracellular protein composed of 49-51 amino acid residues, with a molecular weight of 5-6kDa (Lepage et al. 1990). Its transcription occurs in three steps, initially it is regulated by 1,25 – dihydroxy – vitamin D3, here the molecule is made up of 3 parts, a signal peptide cleaved during translation, a propeptide which targets the protein for γ-carboylation and a mature protein. The second step involves translation of osteocalcin by vitamin K1, this acts as co-factor for the post-translation γ-carboxylase enzyme, this is where a second carboxyl group is added to a specific glutamyl residue (Glu) forming γ-carboxyglutamyl residues (Gla). This modification stabilises the osteocalcin protein and promotes its binding to calcium and hydroxyapaptite (Lee et al. 2000). Osteocalcin has also shown to delay nucleation of HA (Hunter et al. 1996) and therefore acts to regulate bone remodelling, previous studies have shown that mice deficient with respect to OCN have increased bone formation (Ducy et al. 1996).

2.2.3.5 Osteonectin

Osteonectin is a 32kDa protein expressed by osteoblastic cells. It is a single chain polypeptide containing two glycosylation sites that can bind up to eight Ca^{2+} ions making it a protein that binds strongly to hydroxyapatite. In the presence of high concentration of hydroxyapatite, osteonectin has the ability to inhibit HA crystal growth, this may aid in the remodelling of bone tissue. Osteonectin is also significantly present in non-mineralising tissues such as platelets and endothelial cells therefore its function cannot be limited to calcified tissue (Kelm et al. 1994). Osteonectin is present in the basement membrane matrix of actively proliferating and remodelling sites such as embryonic and adult tissues. It is also shown to bind to type 1 collagen (Termine et al. 1981), it is therefore suggested that osteonectin is involved in cell-matrix interactions rather than mineralisation directly (Termine et al. 1981).

2.2.4 Bone mineralisation and development of the skeleton

The inorganic mineral, hydroxyapatite makes up nearly 70% of calcified bone. Hydroxyapatite is a calcium phosphate mineral with a chemical formula $Ca_{10}(PO_4)_6(OH)_2$. Its morphology is mainly plate-like with a length of 30-50nm. Early X-ray fluorescence spectroscopy patterns show that crystalline HA has a Ca/P ratio of 1.67, however, it has recently been demonstrated that this ratio may vary in biomineralised HA as bone is continuously being remodelled to maintain homeostasis with regards to calcium, phosphate and magnesium ions (Palmer et al. 2009).

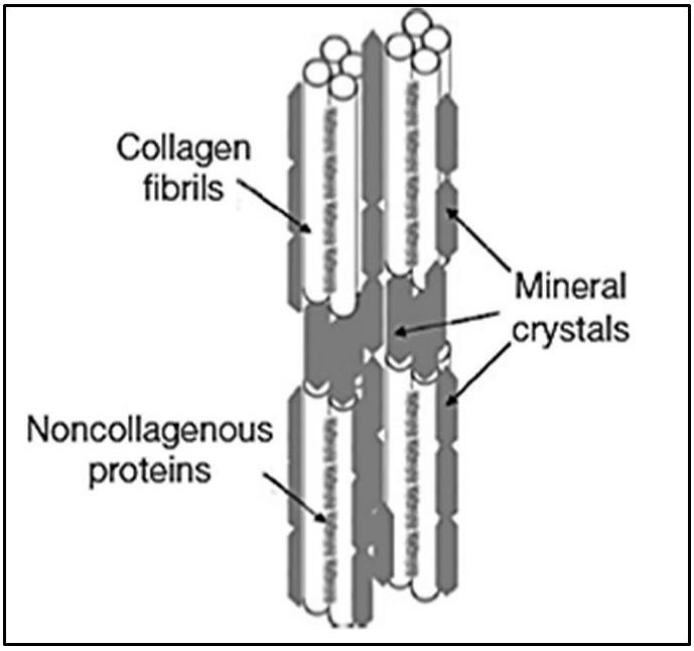

Figure 2.5: HA mineral and non-collagenous proteins can be found in-between and within collagen fibres (McNamara 2011)

Prior to osteoid mineralisation the organic matrix primarily consists of collagen, non-collagenous proteins such as osteocalcin, osteopontin and osteonectin as well as growth factors and signalling molecules (Figure 2.5). The organic matrix starts to mineralise 10-15 days after it has been synthesised in the collagen fibrils (Sommerfeldt & Rubin 2001).

The mineralisation process is initiated by matrix vesicles, which are 30-100nm in diameter and are lipid bi-layer organelles originating from chondrocytes or osteoblasts. Matrix vesicles are made up of several proteins such as alkaline phosphatase and annexins II, V and VI. Annexin V plays a key role in the functioning of matrix vesicles especially during the beginning of calcification when the first HA phase is formed in the vesicle lumen. Annexin V causes an influx of Ca^{2+} ions into the vesicle which therefore results in the mineral growth form the existing nucleation complex. Inorganic ions Ca^{2+} and inorganic PO_4^{3-} are accumulated within the matrix vesicles as shown in Figure 2.6. Annexin V also binds to collagen types II and X; this facilitates the anchoring of the vesicles to the extracellular matrix. The vesicles' membrane ruptures and releases HA crystals into the extracellular fluid, where they further grow and spread and become part of the ECM. The balance between PO_4^{3-} to crystalline HA is regulated by the extracellular $P_2O_7^{4-}$ (pyrophosphate), which inhibits the ability of PO_4^{3-} to crystallise in the presence of calcium(Sapir-Koren & Livshits 2011).

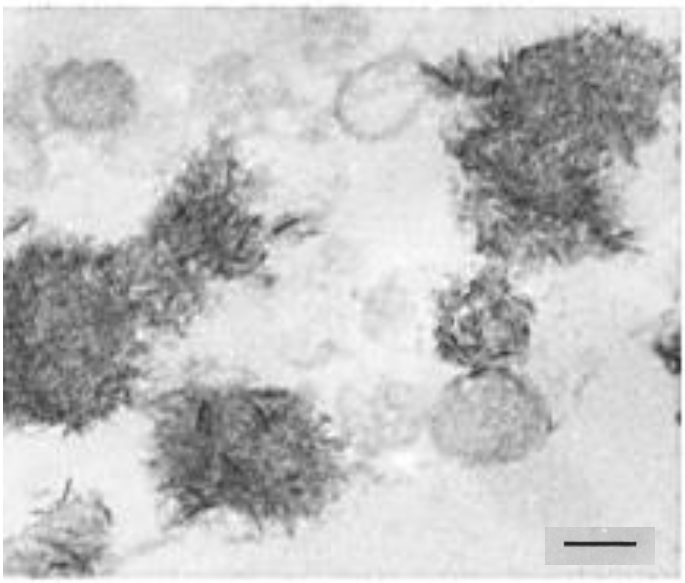

Figure 2.6: Electron micrographs of matrix vesicles exhibiting needle-like crystal structures of HA therefore indicate the process of calcification. Bar denotes 100μm (Kirsch et al. 1997).

Various studies have been carried out to investigate the structure and the components that begin mineralisation, it has been suggested that the presence of proteoglycans in the cartilage may also provide these nucleation sites. In this mechanism mesenchymal stem cells are differentiated into chondrocytes to form a firm model of the cartilage. The proteoglycans have a high negative charge density which allows them to bind a significant amount of Ca^{2+} ions, which are then displaced by inorganic phosphate leading to mineral deposition into the collagen matrix which acts as a scaffold for the growth of bone (Kirsch et al. 1997)

2.2.5 Bone fracture and healing

Although bone has the innate ability to remodel and repair itself through a lifetime, some traumatic injuries and pathological diseases such as osteoporosis, osteogenensis imperfecta and Paget's disease, can result in a loss of these normal functions, which increase the likelihood of bone fractures. Fracture healing is a process that takes place with the assistance of osteoprogenitor, chondroblast and osteoblast cells (McNamara 2011).

The fracture healing process is similar to that of bone formation in the embryo indicating that similar mechanisms occur for both bone formation in mature bone and embryonic skeletons. Bone formation occurs in two processes, intramembranous and endochondral ossification, depending on the type of bone being formed. Intramembranous ossification occurs when a high concentration of mesenchymal cells are transformed into osteoprogenitor cells and immediately into osteoblasts, leading to the direct formation of bone. Endochondral ossification, on the other hand occurs via a two-step process, whereby, initially the mesenchymal cells are differentiated to chondroblasts, which produces the collagenous template which is ossified by osteoblasts (Hing 2004).

Bone healing usually occurs via the endochondral ossification process. A bone fracture initially leads to the formation of a haematoma (blood clot) which occurs because of injury to the periosteum. The periosteum consists of blood vessels and is the area of bone where soft tissues, tendon and muscle attach. In response to the haematoma, inflammatory cells are recruited to the site. The inflammatory response is linked with pain, heat, swelling and the release of several growth factors and cytokines at the site of fracture. Bone repair begins 3-7 days after the inflammatory response this is whereby the cells present at the damaged site start to differentiate into either osteoblasts or fibroblasts (Carano & Filvaroff 2003).

Cells such as macrophages and fibroblasts are also recruited so as to remove the tissue debris and to express the extracellular matrix proteins, respectively. Osteoblasts begin to produce woven bone, which rapidly produces a periosteal and marrow callus. The soft callus fills the gaps of the fracture as illustrated in Figure 2.7.

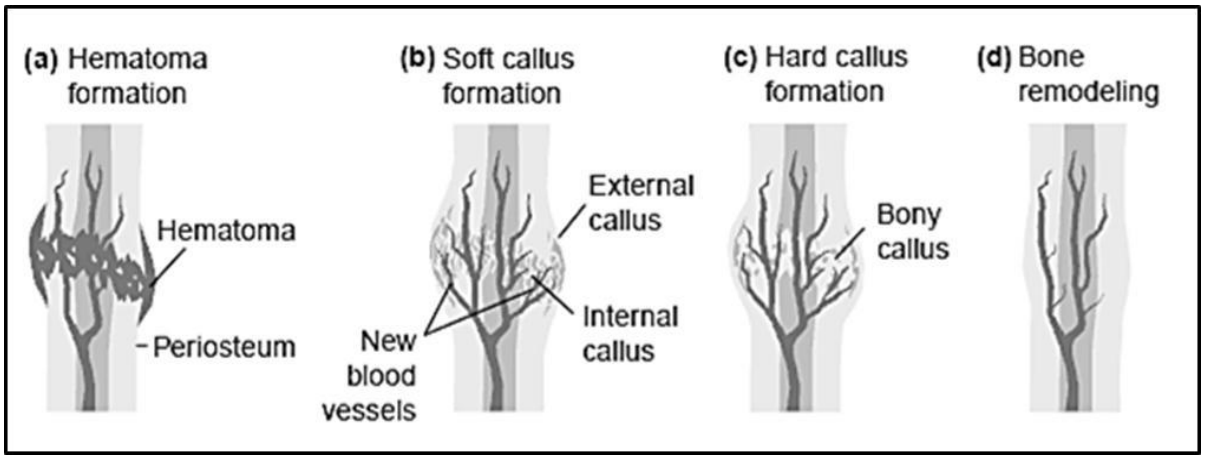

Figure 2.7: Schematic diagram illustrating the processes of bone healing. As a result of injury, blood vessels are damaged and a haematoma forms (a). Angiogenesis occurs and a soft callus is formed (b). The soft callus starts to calcify forming woven bone (c). The fractured site starts to remodel to recapitulate the original bone (Carano & Filvaroff 2003).

Fibroblasts induce angiogenesis within the granulated site and chondrocytes form the collagenous cartilage. The woven bone is remodelled into lamellar bone and by the process of endochondral ossification the cartilage is converted to mineralised tissue. The newly formed callus is constantly being remodelled by osteoclasts until the bone reaches its original morphology and mechanical strength and stiffness (McNamara 2011).

2.3 Tissue Engineering

Every year there are approximately 20,000 organ transplants and around 2 million implantations of organs and parts (Nerem & Sambanis 1995). There are not enough organs, however, available for transplantation, which leads to patients dying with some not even making the organ waiting list. Consequently, this has led to an increase in the demand for 'artificial' organs and biomaterials that cannot be met by transplantation on its own.

Tissue engineering is a multidisciplinary research field that focuses on the formation of biomaterials used for repairing/treating of damaged or diseased tissue. Medicine, biology, material science and engineering all play vital roles in the development of an ideal scaffold to be implanted in the body. The main aim of tissue engineering is to overcome the limitations encountered during conventional treatments based on organ transplants. Tissue engineering can potentially lead to the supply of tissue substitutes which can be tolerated by the immune system and last a lifetime with a patient. Tissue engineering is a permanent solution in treating organs or tissues, without the need for additional treatments and therefore making this a cost effective treatment over a longer period (Sachlos & Czernuszka 2003).

2.3.1 Bone tissue engineering

As previously described, bone has the unique ability to restore to a healthy tissue depending on the size of a fracture or defect (Hing 2005). Pathological condition such as cancer or degenerated bone due to age or disease however, can often only be restored by surgical procedures. Bone grafting was first recognised in the 1800s, whereby damaged or diseases bone was either replaced by autografting, that is when a healthy tissue is taken from the patient's own body, or allografting, a healthy tissue obtained from a donor (Lavernia et al. 2004).

Autografting is often used in orthopaedics; however this is restricted by the amount of bone that can safely be removed from the patient. Other disadvantages include, the demand for healthy bone often exceeds the supply and healing can often be inconsistent. Consequently, this has led to an increase in the demand for biomaterials-based treatments that would avoid these complications.

Initially the materials created were designed to act as load bearing scaffolds only, however material scientists have now moved to forming bioactive materials that can be combined with biological molecules to promote tissue regeneration (Stevens 2008).

An ideal material for bone regeneration should exhibit load bearing mechanical properties that are suitable for the desired site of implantation which is often determined by its porous structure. The scaffold being designed as a bone replacement composite must be able to provide the mechanical stability to the constructs in load bearing sites prior to the deposition of the extracellular matrix by the cells. A scaffold with an interconnected porous structure with a high porosity but less than 90% allows for the cells to penetrate through the material as

well as allowing for tissue in-growth and making nutrients available to the new tissue being formed.

Often biomaterials produced for bone tissue engineering act as a cell delivery scaffolds whereby the material is able to support cells as well as promote attachment, proliferation and differentiation of the osteogenic cells. As new bone tissue starts to develop around the scaffold, appropriate degradation of the composite *in vivo* is required so as to promote tissue regeneration. Another key characteristic for bone replacement therapies is the ability to tailor the scaffold, that is, the material should be adaptable and easily malleable so as to be incorporated into various shape defects, which are indeed unique to each patient.

Many bone substitutes are designed to substitute autologous or allogenic bone replacements and the most common bone biomaterials investigated are; bioactive ceramics, bioactive glasses, biological and synthetic polymers and various composites of these (Stevens 2008).

2.4 Trace elements in bone

The importance of trace elements was first noticed during the 19th century when zinc was identified in micro-organisms such as *Aspergillus niger* and later the relevance of iron in haematopoiesis and anaemia was discovered (Prasad 1991). In the late 1970s it was noticed that trace elements also play an essential role in bone architecture. These trace elements include; silicon (Si), copper (Cu), manganese (Mn) and zinc (Zn) (Calomme et al. 2006). Although various cellular and molecular markers influence the synthesis and maintenance of bone, trace elements play an essential role in bone metabolism and act as cofactors for specific enzymes (Towler et al. 2009). In this section the role of silicon in bone biology and its addition into various biomaterials is discussed.

2.5 Silicon

2.5.1 Silicon in the environment

Silicon is the second most abundant element in the Earth's crust at 28% wt, when combined with oxygen it forms silicates which form the largest and most abundant groups of minerals (Anvir et al. 2006). Silicon dioxide (SiO_2) is often in the form of ordinary sand; however it also exists as quartz, rock crystal, rhinestone and opal (Douthitt 1982). It is also the main element of glass, cement and some ceramics.

2.5.2 Diatoms and radiolarians

The silicon mineral in the form of hydrated amorphous silica is one of the major minerals made by organisms, after carbonate minerals which occur in abundance. Amorphous silica plays a significant role in most plant biology, as its primary function is to strengthen cell walls for support and to provide skeletal functions for protection such as in radiolarian and diatoms (Figure 2.8).

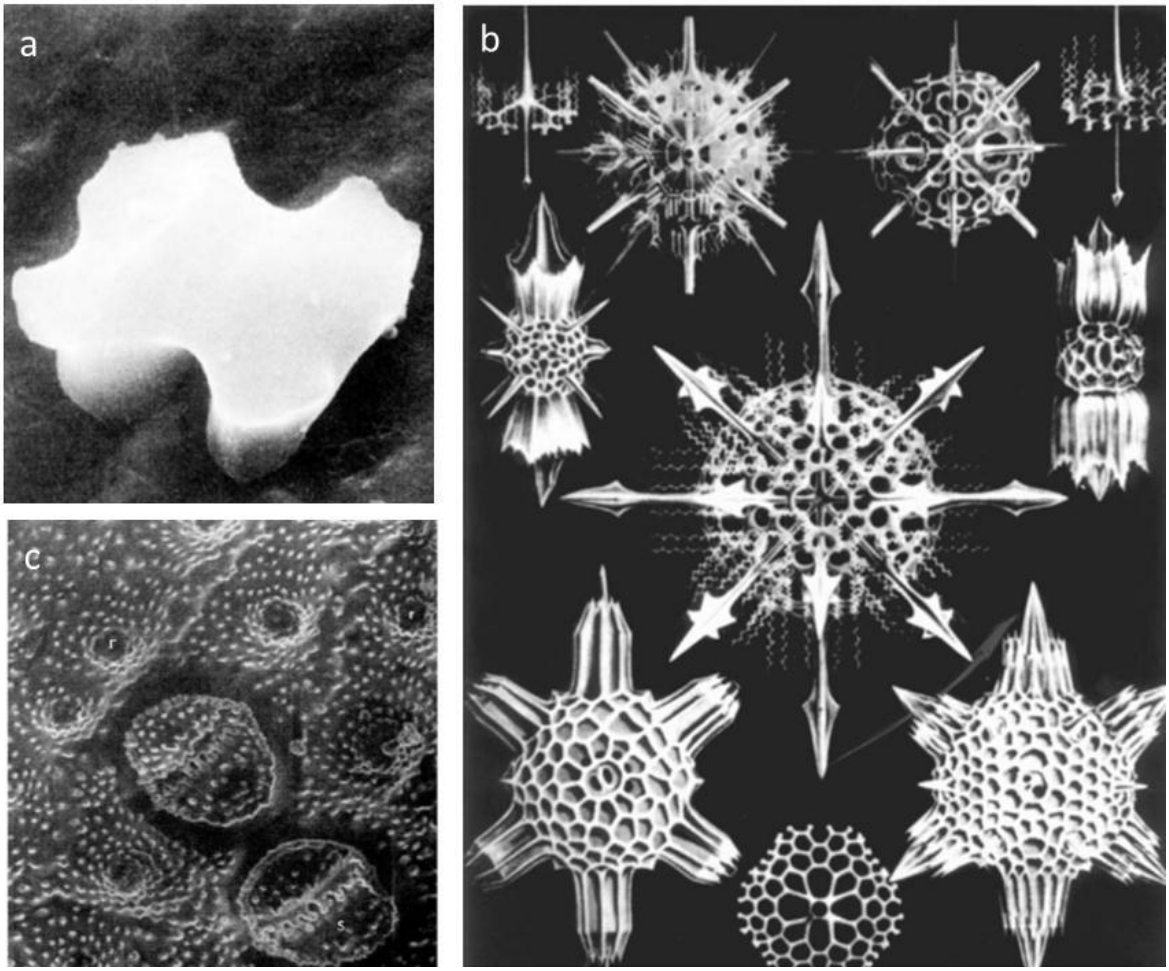

Figure 2.8: Images of; (a) silica cells from higher plants such as *Oryza sativa* a type of rice, which can be up to 7μm in diameter. (b) The structure of radiolarians and diatoms which can be nearly several hundreds of micrometres in diameter. (c) Silicified cell wall stromal structures from *Equistetum arvense* a field horsetail at 20μm in diameter (Perry 2010).

Diatoms are single celled organisms that have the most unique feature of their highly organised siliceous walls. The presence of silicon in these microorganisms is vital for photosynthesis and metabolic processes such as the synthesis of proteins and DNA, whereby the cell cycle is dependent on the presence of amorphous silica (Theriot et al. 2012).

2.5.3 Silicon in higher animals

Silicon was an overlooked trace mineral until the late 1970s, and was considered to be inert in the biological system. It is, however, proving to be an essential component in the human body, for maintaining bone and skin health. Humans store nearly 2-5g of silica in various tissues and body fluids. Silica binds via glycosaminoglycans in tissues and is found as orthosilicic acid in the blood. The main source of silicon for the human body is predominantly from the diet, these include; drinking water containing orthosilicic acid, the ingestion of plants and animals as well as drinking beverages such as beer (Jugdaohsingh et al. 2002).

Animal studies in the in the 1970s showed that dietary silicon is necessary during the mineralisation process of growing bone (Carlisle 1976; Schwarz 1973). Various research groups over the last 30 years have added to these findings and show that dietary silicon is important for formation and bone health.

2.5.4 Silicon is essential for bone formation

In vivo studies conducted by Carlisle (1975), found that silicon is required for normal growth and development in the chick. From this study it has been suggested that silicon is associated with calcium in an early stage of bone formation. The Carlisle study showed that chicks fed on a diet without silicon had a decreased growth rate, when compared to chicks fed on a supplemented diet. The chicks on the non-supplemented diet appeared to much smaller and stunted. The bones of the deficient birds show a smaller circumference and a thinner cortex, and also tend to fracture easily. The beak and comb were also more flexible in the deficient group, shown in Figure 2.9. These findings strengthen the fact that silicon is vital in early bone formation.

Figure 2.9: Four week old chicks showing normal growth when silicon is present in the diet (left) and abnormal growth in a non-silicon diet (right), (Carlisle 1972).

In vivo experiments were also carried out on rats which concur with the results from the chicks' study, where the relationship between silicon and calcium in bone formation was investigated (Schwarz 1973). Schwarz et al (1973) showed that silicon is involved in the development of the glycosaminoglycan network, by forming cross-links via silanolate bonding (R-O-Si-O-R) which stabilises the structure and function of the polysaccharide. Silicon has been identified within early bone growth in young mice and rats and its concentration increases simultaneously with the increase in calcium concentration, within the bone matrix. It has been noticed, however, that as the bone matures with time the levels of detectable silicon decrease as the bone becomes fully mineralised. This suggests that silicon is essential in the initial growth of the organic matrix and may act as an initiator for the process of calcification.

2.5.5 Polymerisation of silicon

Silicon on its own is an insoluble solid, and is mainly present as an oxide, most commonly known as silica (SiO_2), which is also just partially soluble in water. Silica at pH 10, however, is present as silicate ions which are soluble in water, and hydrolyses to form orthosilicic acid. Orthosilicic acid in solution exists as $Si(OH)_4$, formed from silica (Equation 2-2).

$$SiO_{2\,(S)} + 2H_2O_{(l)} \rightarrow Si(OH)_{4\,(aq)}$$

Equation 2-2

Orthosilicic acid is highly hydrophilic and is difficult to isolate, because it is a weak acid that exists in dilute aqueous solutions as it polymerises when it is concentrated. It is the soluble form of silica that is in equilibrium with the solid phase. It has been demonstrated that the acid dissociates in two steps when in the presence of water (equation 2-3);

$$Si(OH)_4 + H_2O \rightarrow SiO(OH)_3^- + H_3O^- \quad Pka = 9.8$$

$$Si(OH_3)^- + H_2O \rightarrow SiO_2(OH)_3^- + H_3O^- \quad Pka = 11.8$$

Equation 2-3

(Greenberg 1959)

Orthosilicic acid ionises in alkaline solutions at approximately pH 10, in the presence of hydroxyl ions (Equation 2-4),

$$Si(OH)_4 + OH^- \rightarrow HSiO_3^- + 2H_2O$$

Equation 2-4

(Iler 1955)

The condensation of silanol groups leads to polymerisation, and as polymerisation continues it forms hydrated colloidal particles which have a higher affinity with organic molecules and can form complexes with inorganic compounds, for example, aluminium and calcium oxide.

The solubility of orthosilicic acid increases as the temperature increases (Figure 2.10), it was demonstrated that amorphous silica solubility occurs at 100°C (Rimstidt & Cole 1983), however later found that it dissolves at even higher temperatures of 350°C (Gunnarsson & Arnórsson 2000).

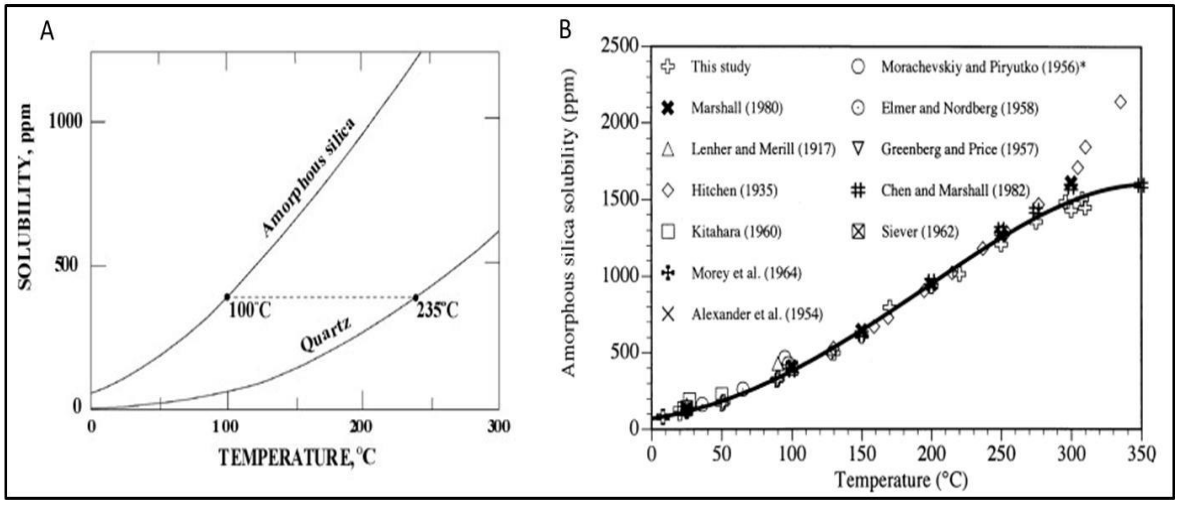

Figure 2.10: Determination of the solubility of amorphous silica and quartz was carried out at various temperatures and showed that at 100°C amorphous silica and quartz started to dissolve and form orthosilicic acid (A) (Rimstidt & Cole 1983). This has been confirmed by various other researchers (B) (Gunnarsson & Arnorsson 2000).

2.6 Silicon containing biomaterials

There is a constant increase in the number of people who suffer every year from bone traumas and diseases (Harvey et al. 2010). Autografts and allografts are the 'gold standard' procedures often used to treat/repair the damaged bone. These grafts however, possess various risks for example the risk of disease transmission and implant failure, particularly if being applied for a long time. This has led to an increased interest in fabricating synthetic bone substitutes, which can eliminate these risks and enhance bone growth onto the implanted surface. Materials such as metals and cements have been used extensively, as they exhibit ideal properties for bone replacement. During the past two decades, however, these biomaterials have also been used for drug delivery by inserting bioactive components within the material to enhance the growth of new bone. In this section, materials containing silicon as a bioactive agent have been discussed, the most popular of them being hydroxyapatite, Portland cements, Bioglass® and natural and synthetic polymers.

2.6.1 Silicon substituted hydroxyapaptite

Synthetic hydroxyapatite, a hydrated calcium phosphate is the most commonly used biomaterial in bone and dental applications (Gibson et al. 1999), and has been used as a coating on hip replacements and as acts a filler in bone cavities (Barrère et al. 2006). It has a similar composition and crystallographic structure to the natural bone mineral; it is also an osteoconductive material, as it supports the attachment of new osteoblasts and therefore allows direct bone formation across its surface by attachment, proliferation and differentiation of bone cells (Patel et al. 2002).

Natural bone mineral often contains various ionic substitutes in its lattice, which most synthetic HA composites do not have, this therefore makes synthetic HA less integrated with natural bone tissue, when implanted. This limitation can be overcome by substituting ionic

components such as silicon within the lattice as it plays a significant role in the biochemistry of tissue growth. One of the early fabrications of silicon substituted HA (Si-HA) was carried out by Gibson et al (1999), whereby Si-HA was formed by a simple aqueous precipitation method and sintered at 1200^{o}C which resulted in HA without any secondary phases such as calcium oxide and tricalcium phosphate. This method substitutes phosphate in the HA lattice with silicate (Gibson et al. 1999).

In vitro studies carried out by Thian et al (2006) coated titanium (Ti) surfaces with Si-HA and compared the response of human osteoblast cells (HOB) to nanocrystalline Si-HA thin coatings of different silicon compositions and that of uncoated titanium surfaces. There was a significant increase in cell growth density, including differentiation and it was found that cells on the silicon coated surfaces formed an extensive extracellular matrix and bone minerals were also observed on cell membranes. High concentrations of silicon coating (4.9%), however showed to inhibit cell attachment as it was noticed there was fast dissolution of Si from the material, which was not ideal for cells at the early time points (Thian et al. 2006).

The *in vivo* behaviour of Si-HA was demonstrated by Patel et al (2002) where they fabricated granules of pure phase HA and Si-HA and assess the bone growth of the granules. It was shown that Si-HA increased *in vivo* bone growth when compared to phase pure HA granules. This strengthened the evidence the silicate ions in low concentrations are an improved alternative to just phase pure HA for bone tissue engineering (Patel et al. 2002)

2.6.2 Bioactive glass ceramics

Bioactive glass ceramics were first discovered by Hench et al in 1969, whereby it was noticed that when the phosphosilicate glass was implanted it joined with bone without forming a fibrous scar. The bioactive glass was trademarked Bioglass 45S5® and is formed from 45% SiO_2, 24.5% Na_2O, 24.5% CaO and 6% P_2O_5 wt% (Xynos et al. 2000). Bioglass® has been classified into the Class A bioactivity index as they exhibit both osteogenic and osteoconductive properties. They also have the ability to bond to both bone and intramuscular sites (Lai et al. 2002). This led to a series of experiments whereby the surface chemistry of the glass ceramic was evaluated and *in vitro* investigations carried out to determine the effect of this bioactive glass on a cellular level.

In vitro analysis showed that Bioglass 45S5® has an effect on the cell cycle of human osteoblast cells resulting in an increase in osteoblast turnover, which produces a population of mature bone cells leading to the formation of bone nodules in a relatively short time of 12 days (Xynos et al. 2000). This is due to the dissolution of various ions from the glass ceramic which also contains a surface gel consisting of calcium phosphate and reactive silica, which leads to the formation of bone-like tissue.

Bosetti et al (2002) studied the effect of three bioactive glass composites containing various amounts of silica on HOB cell behaviour, focussing especially on the expression of collagen and the matrix associated non-collagenous protein alkaline phosphatase. It was demonstrated that there was a significant increase in collagen secretion by the osteoblasts when cultured on the Bioglass 45S5® surface. It has previously been suggested that the cross-linking of collagen chains and the precipitation of hydroxyapatite are pH dependent. The dissolution of the glass ceramic caused alkalisation in the culture media, and since collagen formation is pH

dependent, increased the production of collagen and crosslinking as well as increasing the formation of hydroxyapatite (Bosetti et al. 2003).

2.6.3 Calcium phosphate cements and Portland cements

Calcium phosphate ceramics have been the most common biomaterials used as exogenous grafts in bone regeneration. Calcium phosphate as a biomaterial in both bone and dental applications has the unique characteristic for bone substitution when compared to other biomaterials as its chemical composition is similar to that of the biological bone mineral, apatite. Calcium phosphates also known more accurately as calcium orthophosphates, are salts of orthophosphoric acid (H_3PO_4). The advantages of using calcium phosphate cements is that they are self-hardening and are able maintain sufficient mechanical strength for repairing damaged hard tissues (Guo et al. 2007). The limiting factors of calcium phosphates, however, are the unpredictable setting times and degradability (Verron et al. 2010).

Synthetic calcium phosphates such as α- or β- tricalcium phosphates (α- or β- TCP) and biphasic calcium phosphates (BCPs) are widely used as biomaterials in bone tissue repair. β-TCPs are bioresorbable ceramics that are well tolerated in the body and have shown to be osteoconductive. *In vivo*, however, β-TCP, shows a reduced rate of bone formation and osseointegration, this limits its potential use as a bone replacement biomaterial. To enhance the function of the β-TCP, Ni et al (2007) synthesised calcium silicate, ($CaSiO_3$, CS, Portland cement) and β-TCP composites and evaluated apatite formation and *in vitro* response of osteoblasts to the composite (Ni et al. 2008). β-TCP/CS composites increased in mechanical properties such as compressive strength and bending strength when compared to β-TCP composites only. *In vitro* cell cultures showed increased adhesion, growth and ALP activity of the osteoblast cells when cultures on the modified composite containing 50% CS.

In vivo experiments with calcium silicate have shown that dissolution of both calcium and silicon ions from the material improved osteogenesis, by having a direct effect on the genes which regulate the induction and progression of the cell cycle (Guo et al. 2007).

2.6.4 Natural and synthetic polymers

Natural and synthetic polymers are widely used in tissue engineering, as scaffolds, in orthopaedic surgery such as rods, screws and pins and sutures, cell delivery carriers and drug delivery vesicles. Naturally derived polymers are often used as they have a similar structure to the ECM and do not cause inflammation or immunological reactions and toxicity within a biological environment (Mano et al. 2007).

Biodegradable synthetic polymers have a number of advantages such as; their mechanical properties and degradation properties can be altered to suit for their desired application. Desired pore sizes as well as shapes can also be achieved that will allow for its specific application. Chemical functional groups can also be incorporated within the polymers so as to induce tissue growth (Gunatillake & Adhikari 2003).

Biopolymers such as chitin are widely investigated as scaffolds in bone tissue engineering. Chitin is a biopolymer composed of β -1,4 glycan of N-acetyl – D – glucosamine units and is present in two crystalline forms, α – chitin and β – chitin. Chitin is used in various applications like wound dressings due to its wound healing, antibacterial and anti – inflammatory properties. Although chitin has various properties such as biocompatibility, biodegradability, non- toxicity and haemostatic property, it is not a bioactive material and therefore cannot induce bone regeneration. Madhumathi et al (2009), show that the addition of silica can improve the bioactivity of chitin *in vitro* using stimulated body fluid (SBF) it was

seen that the crystalline hydroxyapatite was formed on and in the scaffolds after being immersed in SBF for 14 days (Madhumathi et al. 2009).

Lee et al hybridised chitosan with a silica xerogel to form a chitosan – silica xerogel hybrid membrane. Silica xerogels act as biologically active agents and are useful as a bone substitute and drug delivering particulate carrier. The chitosan – silica xerogel hybrid membrane has shown excellent ability to form bone like apatite. The faster mineralisation of the hybrid membrane releases ions which induce degradation of the membrane. Calcium and phosphorous ions lead to the supersaturation of the SBF solution around the hybrid membrane and this increased the formation of apatite. The chitosan-silica xerogel hybrid membrane showed a higher degradation rate than that of pure chitosan membrane, this is observed in *in vitro* tests. The hybrid is also seen to increase the bone healing process and also plays a positive role in the stimulation of bone forming cells (Lee et al. 2009).

Sodium alginate is a linear polysaccharide derived from brown seaweed composed of (1-4) linked β-D-mannuronic acid (M unit) and α-L-guluronic acid (G unit) (for further information see section 4.1.1*). It has often been used for the encapsulation of cells and biomolecules as it forms a soft gel matrix under mild conditions. Alginate's internal structure resembles that of the extracellular matrix, and is often used as a synthetic ECM in tissue engineering and as a cell delivery vehicle, organising the cells in a three-dimensional hydrated structure (Rowley et al. 1999) keeping them viable and maintaining a normal cellular function in order to produce the desired tissue found in the body(Hunt et al. 2010)

Lim et al (2009), developed silica-coated alginate beads and encapsulated proteins *in vitro.* The silica coat provided the alginate beads with a protective shield resistant to chemical and environmental stresses. The silica beads prevented the beads from disintegration and

maintained the activity of the proteins encapsulated within the alginate beads for 70h, which was five times longer than the length of activity on the non-coated beads (Lim et al. 2009). This external membrane prevents leakages of the biological components such as cells, which have been entrapped, however did not prevent the diffusion of essential ions into the beads.

Type 1 collagen has recently been used as a biomaterial in bone regeneration, since collagen is the most abundant protein in mammals and it forms most of the structural framework for tissues. It is an ideal hydrogel to be used in bone regeneration due to its practical aspects, that is, it is easy to prepare as well as having a widespread occurrence in nature. Collagen has ideal characteristics as a biomaterial as it gradually degrades in the body as it is being replaced by the host tissue (Stenzel et al. 1974), it also has a high affinity for water, low antigenicity, and is virtually non-toxic *in vivo* which favour its use as a biomaterial. Collagen also has also shown to promote cellular attachment, growth and differentiation (Landis et al. 2006). Heinemann et al (2007) developed a silica-collagen xerogels to be an alternative scaffold used in hard tissue. The xerogels showed structural homogeneity and sufficient mechanical strength as well as supporting the attachment, proliferation and osteogenic differentiation of human mesenchymal stem cells (Heinemann et al. 2007).

The local release of drugs in a desired site is one of the major on-going research areas in orthopaedics. The advantage of using localised drug delivery means that the drug can be maintained at the desired therapeutic range with just a single dose, without being toxic or ineffective. Polymers such as poly-ϵ-caprolactone (PCL), poly lactic-*co*-glycolic acid (PLGA) and polylactic acid (PLA) have been combined with ceramics and are widely used as drug delivery mechanisms for bone filling due to their ability to integrate with bone. The main disadvantage encountered with using localised drug delivery is when the drug ‘particles’ are adhered within the polymer matrix, this causes initial ‘dumping’ of the drug within the

localised area and hence does not allow for a sustained delivery of the drug, for more than a few days.

To overcome the disadvantage of an initial burst release of drugs once implanted in the desired site, Xue et al (2004), formed PLGA/mesoporous silica composites for the sustained delivery of the antibiotic gentamicin. Gentamicin was entrapped in mesoporous silica particles and then encapsulated in PLGA. The release of gentamicin was more sustained in the hybrid structure, that is, PLGA/mesoporous silica composites, than that of mesoporous silica alone. The release lasted for up to 5 weeks and more importantly the initial burst of release was reduced significantly in the hybrid structure (Xue & Shi 2004). Another advantage of having mesoporous silica within the composite is the release of orthosilicic acid as the particles degrade. This promotes mineralisation by increasing the deposition of calcium as well as neutralising the acidic by-products of PLGA therefore creating an ideal environment both *in vitro* and *in vivo* (Fan et al. 2012).

2.7 Aims of this investigation

The overall aim of the research presented here is to develop a controlled release system for the release of silicon in the form of orthosilicic acid as a potential biomaterial to be applied in bone tissue engineering.

The primary aims of this investigation include;

- To elucidate the biological pathway of orthosilicic acid on osteoblast cells and *in vitro* mineralisation.
- To fabricate a release system for the dissolution of a therapeutic dosage of orthosilicic acid after evaluating the ideal concentration of orthosilicic acid required for cell survival.

3. *IN VITRO* ASSESSMENT OF ORTHOSILICIC ACID ON OSTEOBLAST BEHAVIOUR

3.1 Introduction

Nutritional silicon deficiency leads to skeletal deformities such as abnormal skull development and long bones, as well as poorly formed joints with decreased cartilage content (Perry & Keeling-Tucker 1998). Absorption studies have shown that 50% or less of bioavailable orthosilicic acid is absorbed in humans in any ingested dose. Normally fasting concentrations of Si in plasma are 2-10μM and rise to 20-30μM after meals and 700μM/day are excreted (Reffitt et al. 2003). The earliest work on the role of silicon in bone dates back to the early 1970s where it has been reported that silicon at 0.5wt% *in vivo* was present within the active mineralising osteoid regions, that is, the sites undergoing active calcification. Abnormal shaped bones and inadequately formed cartilagenous tissue were formed with lack of Si in the diet of new born chicks and rats (Carlisle 1976; Schwarz 1973), however, this was reversible upon the addition of soluble Si to their diet. This suggested that silicon may play a key role in the metabolism and stabilisation of the connective tissue present in bone and cartilage although its effect on calcification may be an indirect phenomenon through its interaction with matrix components.

Although the addition of silica into various biomaterials has been carried out for several decades, the optimum concentration of orthosilicic acid required for cell mineralisation *in vitro*, is yet to be established. The dissolution of silicon from these biomaterials into the local environment could affect protein secretion, cell survival and apoptosis. Reffit et al (2003) demonstrated that type 1 collagen synthesis in human osteoblast-like cells was enhanced in the presence of 10-20μM of orthosilicic acid (Reffitt et al. 2003). Arumugram et al showed

that 5 to 50μM of orthosilicic acid significantly increased the expression of type 1 collagen mRNA in osteoblasts, however the concentration – response relationship is still debated as well as the significance of Si in cell behaviour (Arumugam et al. 2003).

In this chapter a series of experiments were carried out to evaluate the response of osteoblasts to 0, 5 and 20 μg/ml concentrations of orthosilicic acid prepared using sodium metasilicate. The cell viability and mineralisation was established in osteoblasts, followed by the effect of OSA on various osteogenic markers when cells were cultured with osteogenic mediators or without osteogenic mediators. Collagen fibrillogenesis was also evaluated with various concentrations of OSA.

3.2 Materials and methods

3.2.1 Cell isolation and cell culture

All cell culture procedures were conducted in aseptic conditions within a laminar hood (BSB 3-S, Gelaire ICN Biomedicals, UK). Equipment was disinfected with 70% ethanol.

3.2.1.1 Culturing MC-3T3-E1

Transformed mouse calvarial osteoblasts (MC3T3-E1) were obtained from LGC (Middlesex, UK) and stored in liquid nitrogen (N_2). When needed the cells were thawed rapidly in a water bath at 37^{o}C and added into fresh Dulbecco's Modified Eagle's Medium (DMEM) supplemented with 10% foetal bovine serum (FBS), 2.5% HEPES, 1% penicillin/streptomycin (P/S), 2.5% L-glutamine (L-Glut) and centrifuged at 1000rpm for 3min. The old medium was aspirated and discarded, and replaced with fresh supplemented DMEM (s-DMEM), the cells were suspended evenly in the culture media and seeded in 75ml flasks and maintained at 37^{o}C in a humidified atmosphere of 95% air and 5% CO_2 (Sanyo Electric Co. LTD, Japan)

3.2.1.2 Isolation and culturing of rat bone marrow cells

Rat bone marrow cells (rBMCs) were isolated from the femora of adult albino Wistar rats using the method described by Maniatopolous et al (Maniatopoulos et al. 1988). The femora were dissected out and the adherent soft tissue was removed. The femora were placed in transport medium consisting of: Minimum Essential Medium (α-MEM), 10% P/S, 2.5% HEPES and 1% amphotericin, until required. The epiphyses were removed and the femora were flushed with supplemented α-MEM containing, 10% FBS, 2.5% HEPES, 10% P/S, 10% L-Glut and 1% amphotericin. The cells were centrifuged at 1000rpm from 3min to form a pellet of cells. The supernatant was aspirated and replaced with fresh supplemented medium. The cells were incubated in a 75ml flask in a humidified atmosphere of 95% air and 5% CO_2 at 37^{o}C. The media for all cultures and experiments was changed three times weekly.

3.2.2 Determining the optimum concentration for cell survival

MC-3T3-E1 cells at passage 15 were dissociated from the flasks with 0.25% trypsin – 0.02% EDTA (Sigma, UK). Trypsin-EDTA was dispensed into the flasks to completely cover the monolayer of cells and placed in an incubator at 37^{o}C for 3 minutes, until all the cells had detached from the surface of the flask, excess culture media was added to the detached cells to de-activate the trypsin. The cells were centrifuged at 1000rpm for 3 minutes before re-suspension in S-DMEM at a density of 2x10^{4}cells/ml. The cells were seeded in a 12 well plate and left to attach overnight. After overnight attachment, s-DMEM containing various concentrations of sodium metasilicate solution was added to the cells. Viability was assessed using either the MTT assay (section 2.2.3), calcein AM and propidium iodide staining (section 4.2.4) or trypan blue as described in section 2.2.5. The MTT assay and trypan assay were used to obtain quantitative data whereas calcein AM and propidium iodide staining was used to obtain qualitative data.

3.2.3 MTT assay

The MTT (3-(4,5-Dimethylthiazol-2-yl)-2,5-diphenyltetrazolium bromide) assay is a colourmetric assay used to assess viable cells number in proliferation and cytotoxicity studies. MTT is based on the cleavage of the yellow tetrazolium salt to form a soluble blue formazan salt by mitochondrial enzymes. The amount of formazan produced is directly proportional to the number of living cells present during the MTT exposure.

A stock solution of sterile – filtered 5mg/ml MTT (Sigma, UK) in phosphate buffer saline (NaCl 138mM; KCl 27mM, PBS (Sigma, UK) was prepared and stored at 4^{o}C in the dark. 10% volume, of the MTT stock solution was added to the cells for analysis. In this case 200µL of the MTT stock solution was added to the cell cultures and incubated for 4 hours at 37^{o-}C for the formation of the purple formazan crystals. The MTT solution was removed and 1ml of hydrochloric acid and isopropanol, in a ratio of 1:25, was added to dissolve the formazan crystals and further incubated at 37^{o}C for 45 minutes. The optical absorbance of the solution was measured at 650nm using a microplate reader (Promega, UK). The absorbance was converted to cell number, determined from a calibration of different known cell numbers, assayed with the MTT assay as described.

3.2.4 Calcein-AM and Propidium Iodide staining

Calcein acetoxymethylester (Calcein-AM) is highly lipid soluble and rapidly penetrates the plasma membrane of the cells. Initially it is not fluorescent, however, when the ester bonds are cleaved by the intracellular esterases of viable cells it becomes hydrophilic and emits a green fluorescence indicative of live cells (Kaneshiro et al. 1993).

Propidium Iodide (PI) is a membrane impermeant and does not penetrate through the membrane of viable cells, instead enter the cells via damaged membranes. It binds to the

DNA double helix and emits a red fluorescence and is used to identify dead cells in a cell population. Both Calcein-AM and PI are excited at 490nm and therefore can be viewed simultaneously using a fluorescence microscope.

50µg/mL stock solution was prepared in DMSO, PI (Invitrogen, Paisley, UK) was diluted in water, at a concentration of 100µg/ml. 7µL of Calcein-AM and 25µL of PI were added to the cultures and left for 5 minutes in the dark. The stained cultures were observed using a fluorescence microscope fitted with a mercury lamp (Carl Zeiss Ltd, Hertfordshire, UK) at a magnification of X20. Images of live and dead cells were taken using a digital camera (Powershot G5, Canon UK Ltd, Surrey, UK) attached to a light microscope (Carl Zeiss Ltd, Hertfordshire, UK).

3.2.5 Trypan Blue assay

Trypan blue is derived from toluidine and is also referred to as the dye exclusion method, whereby it passes through by the damaged membrane of the cells, staining them blue. The viable cells exclude the dye leaving them white. In order to determine cell viability and cell number, a Neubauer haemocytometer (Beckman Coulter Ltd, UK) was used. Trypsinised cells were suspended in a small amount of culture medium and mixed with 0.2% w/v solution of trypan blue (Sigma, UK) in a ratio of 1:1. The haemocytometer was viewed using a light microscope and the number of blue (dead cells) and white cells (live cells) were counted. The approximate number of viable cells present was calculated using equation 3.1;

Cells/ml = Number of white cells x multiplication factor (2000) x dilution factor (2)

Equation 3-1

3.2.6 Von Kossa assay

The formation of mineralised nodules in osteoblastic-like cells can be assessed using the Von Kossa histochemical assay. This method is based on the binding of silver ions to the anions of calcium salts such as phosphates. The presence of phosphate ions therefore reduces the silver ions to form dark brown or black metallic silver staining in the presence of light illumination, indicating mineralised nodules in cell monolayers or tissues (Wang et al. 2006)

Cell cultures for analysis were washed with PBS and fixed with 10% (v/v) paraformaldehyde for 30 minutes. The cultures were serially dehydrated in 70%, 95% and 100% ethanol and air dried. 2% (v/v) silver nitrate solution was added and the samples were exposed to UV light for 45 minutes. The samples were further rinsed with distilled water and sodium thiosulphate (5% v/v) was added to the cultures and left to stand for 2 minutes. The samples were then rinsed twice with distilled water and 95% ethanol and left to dry for image analysis (Bonewald et al. 2003). Digital images were captured using an inverted light microscope with a digital camera attached (CETI, Medline Scientific Limited, UK), for quantitative analysis the % area of mineralisation was determined using the image processing and analysis software ImageJ 1.43 (National Institutes of Health, USA).

3.2.7 Alizarin Red S staining

Alizarin Red S or 1,2-dihydroxyanthraquinone is a histochemical assay, used to evaluate calcium deposits in cells in culture. Alizarin Red S has an affinity for calcium and upon binding to calcium gives a red/orange stain.

40mM Alizarin Red S (Sigma Aldrich, UK) was prepared and adjusted to pH 4.2 with 10%(v/v) ammonium hydroxide (Fischer Scientific, UK). The cultures were fixed with 10% (v/v) paraformaldehyde for 30 minutes at room temperature and washed with PBS. Alizarin Red S stain was added to the cultures and left in room temperature for 20 minutes. Excess stain was removed and the cultures were washed with PBS. The stained monolayers were visualised using an inverted light microscope (Zeiss, UK) and images were captured using a digital camera (Canon F2.0, UK). For quantitative analysis the % area of mineralisation was determined using the image processing and analysis software ImageJ 1.43 (National Institutes of Health, USA).

3.2.8 Reverse-transcription polymerase chain reaction (RT-PCR)

Total cellular RNA was isolated from rat BMSC cells following incubation with 0, 5 and 20μg/ml of orthosilicic acid (source: sodium metasilicate) for 3, 7 and 10 days.

RNA isolation was carried out following manufacturer instructions in the Rneasy Kit (Qiagen, UK), briefly, the cell monolayers were lysed with beta-mercaptoethanol, a reducing agent used for nuclease inhibition, prepared in RLT buffer at a 1/100 (v/v) ratio. Contaminating DNA was removed using DNAse. mRNA was quantified and evaluated using a spectrophotometer (BioPhotometer, Eppendorf, UK) and by electrophoresis. Electrophoresis was carried out on an agarose gel (1% w/v), prepared by dissolving agarose in Tris Acetate EDTA (TAE) buffer. For the visualisation of the bands on the gel when exposed to fluorescent light, SYBR gold (Invitrogen, UK) a stain used for RNA gels was added to the agarose/Tris acetate mixture prior to setting. The agarose gel was poured into a mould and the combs used to create the wells were placed in the gel and was allowed to set for 25 minutes at room temperature until solidified. The gel was immersed in TAE buffer in an electrophoresis tank and the gel loaded with the RNA samples as well as the HyperLadder IV (Bioline, UK), which provides the molecular weight markers. The gel was run for approximately 30min at 120 volts.

Reverse transcription of mRNA to complementary DNA (cDNA) was carried out using the omniscript DNase kit (Qiagen, UK), using Oligo dT primer (0.5μg/ml) and DNase inhibitor (40units/μL) from Promega (UK). Concentration of the cDNA was carried out using micron filters (Millipore, UK). Samples were prepared for PCR with the addition of REDTaq® ReadyMix™ mastermix consisting of 12.5μl of REDTaq®, 2μl of forward and reverse primer mix, 1μl of template DNA and 9.5μl of RNAse free water per sample. PCR was carried out

using a Mastercycler thermal cycler (Eppendorf, UK) and typical cycling conditions were as follows; 94^{o}C for 5 minutes, followed by 30 cycles consisting of 94^{o}C for 20 seconds for denaturing the template, 60^{o}C for 20 seconds to anneal the primers and 72^{o}C for 20 seconds to polymerise the DNA. Finally, the samples were incubated at 70^{o}C for 10 minutes and the temperature was held at 4^{o}C after completion. The primers used are listed in Table 3.1. Following PCR the products were electrophoresed in 1.5% (w/v) agarose gels (described earlier) and visualised by ethidium bromide staining (3μL from the stock solution, 10mg/ml). All samples were kept on ice throughout the experiment.

Band intensities were quantified using Genesnap/Genetool (Syngene,UK). Band intensities for each studied gene were normalised against the house keeping gene glyceraldehyde-3-phosphate dehydrogenase (GAPDH) for each time point and concentration. These normalised cDNA intensities were converted to relative transcription levels using equation 3.2.

$$\text{Relative transcription} = \frac{\text{Sample normalised cDNA intensity}}{\text{Normalised cDNA intensity of untreated sample at day 3}} \times 100$$

Equation 3-2

Table 3.1: Primers used for RT-PCR

Primer	Primer – Full name	Sequence of Primers Forward (F) Reverse (R)	Product Length (bps)
rGAPDH	Glyceraldehyde - 3 Phosphate Dehydrogenase	F- CGA TCC CGC TAA CAT CAA AT R- GGA TGC AGG GAT GAT GTT CT	227
rOcalcin	Osteocalcin	F- TCC GCT AGC TCG TCA CAA TTG G R- CCT GAC TGC ATT CTG CCT CTC T	215
rOpontin	Osteopontin	F- AAG CCT GAC CCA TCT CAG AA R- GCA ACT GGG ATG ACC TTG AT	445
rAlkPhos	Alkaline Phosphatase	F- CTC CGG ATC CTG ACA AAG AA R- ACG TGG GGG ATG TAG TTC TG	499
rColl-1α	Collagen Type 1	F – AAA AGG GTC ATC GTG GCT TC R – ACT CTG CGC TCT TCC ACT CA	336
rPCNA	Proliferating Cell Nuclear Antigen	F- TTG GAA TCC CAG AAC AGG AG R- CGA TCT TGG GAG CCA AAT AA	389

3.2.9 Extraction of Type 1 Collagen

Type 1 collagen was extracted from Wistar rat tail tendons and processed in 0.5M acetic acid solution for 48 hours at 4^{o}C. Dialysis tubes were prepared by simmering in ethanol (50% v/v) for 1 hour and for another hour in a 10mM sodium bicarbonate ($NaHCO_3$) / 1mM EDTA solution. The dialysis tubes were further simmered for 1h in distilled water and stored at 4^{o}C until required. The extracted rat tail tendons were sterile filtered and poured into the dialysis tubes and dialysed against 0.1x DMEM for 24h at 4^{o}C. The solution was centrifuged at 10,000 rpm for 24h at 6^{o}C (Beckman Coulter, UK), and transferred into glass bottles and stored at 4^{o}C. The autoclaved glass-ware was used throughout the experiments.

3.2.10 Collagen fibrillogenesis (turbidity experiments)

Kinetic analysis of collagen fibril formation was examined in the presence of different concentrations of sodium metasilicate, by carrying out studies of the turbidity of the gelling collagen (loss of transparency) over a period of time.

Prior to forming the gel, all solutions were placed on ice. 0.3% (w/v) collagen gels were prepared with 10X DMEM and 0.4M sodium hydroxide (NaOH) at a 2:1 ratio. Various concentrations of sodium metasilicate were added to the gel solution. 1/1000 (v/v) acetic acid was added to make up the desired volume and concentration of the gel. The pH was adjusted with 1M NaOH to 8.0-8.5. Phenol red present in the DMEM solution was used as a pH indicator, which turns pink between pH 8.0 – 8.5. 1ml of the solution was quickly added into a cuvette (1cm) and placed in a UV-VIS spectrophotometer (Cecil Instruments, UK) and the absorbance was set at 553nm. The kinetics study was started immediately (t= 0min) and the temperature was maintained at 37^{o}C and a turbidity-time profile was determined. Turbidity experiments were carried out in triplicate to ensure good reproducibility.

3.2.11 Atomic Force Microscopy to determine collagen self-assembly

The atomic force microscope (AFM) allows for the direct measurement of intermolecular forces with atomic-resolution characteristics. It has often been used in place of other conventional microscopes such as the scanning electron microscope (SEM) and transmission electron microscopy (TEM) as it has many advantages in imaging from the nano-scale to the molecular scale. It is used when analysing various materials, such as the homogeneity of polymers, glasses and composition changes in ceramics as well as imaging biological macromolecule interactions.

A typical AFM system consists of a micro-mechanical cantilever probe and a sharp tip mounted onto a piezoelectric scanner and a sensitive photo-detector for receiving a laser beam to provide cantilever deflection feedback illustrated in figure 3.1. The AFM probes the sample with a sharp tip, usually made of silicon, and makes measurements in 3 dimensions (x,y and z), normal to the sample surface.

The principle of AFM is to scan the tip over the sample surface with feedback mechanisms which allow the piezoelectric scanner to maintain the tip at a constant force or height above the sample. AFM relies on the forces between the tip and sample and is measured by Hooke's law (equation 3-2) whereby F is the force, k is the stiffness of the cantilever and z is the deflections of the lever.

$$F = -kz$$

Equation 3-3

Typical forces between probing tip and sampling range from 10^{-11} to 10^{-6}N. AFM can be operated in various modes for example, contact mode, intermittent contact mode and phase imagings are a few. For the analysis of collagen fibres, the intermittent contact was operated, this is whereby the stiff lever is oscillated close to the sample and the tip intermittently touches the surface of the sample (Jalili & Laxminarayana 2004).

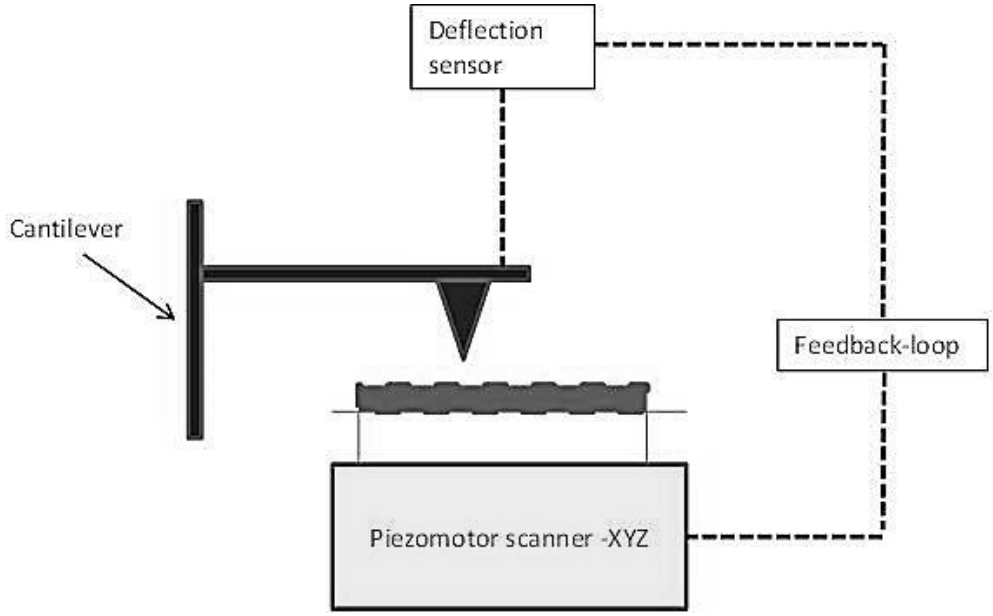

Figure 3.1: Schematic diagram illustrating the functioning of an AFM. A laser beam from the deflection sensor is focussed on the back of the cantilever which deflects and the signal changes to an electric signal (Jalili & Laxminarayana 2004).

Collagen gels were prepared as described in section 3.2.10, with different concentrations of OSA and before gelling the sample was swabbed onto clean silicon substrates. The sample was left to air dry for 20 minutes and rinsed three times in distilled water to remove any excess salts.

Surface morphology was determined using a NanoWizard II atomic force microscope (JPK Instruments, UK) operating in intermittent contact mode at a tip velocity of 2 μm/s, employing pyramidal tipped Si cantilevers (PPP-NCL, Windsor Scientific, UK).

3.3 Results

3.3.1 Determining the maximum concentration of OSA without cell death

Initial studies were carried out to determine the optimum concentration of OSA needed before MC-3T3 cell death. MC-3T3 viability was determined by MTT and calcein AM assays, Figure 3.2 shows the cell viability of MC-3T3 osteoblasts doped with 0 – 1.5mg/ml of OSA using the 3-(4,5-dimethylthiazol-2-yl)-2,5-diphenyltetrazolium bromide (MTT) assay. The cells were analysed after 72h of incubation and it can be seen the cell viability decreased when the concentration of OSA was 0.2mg/ml and further decreased as the concentration of OSA increased. There was no difference however, in the high concentrations of OSA and cell viability.

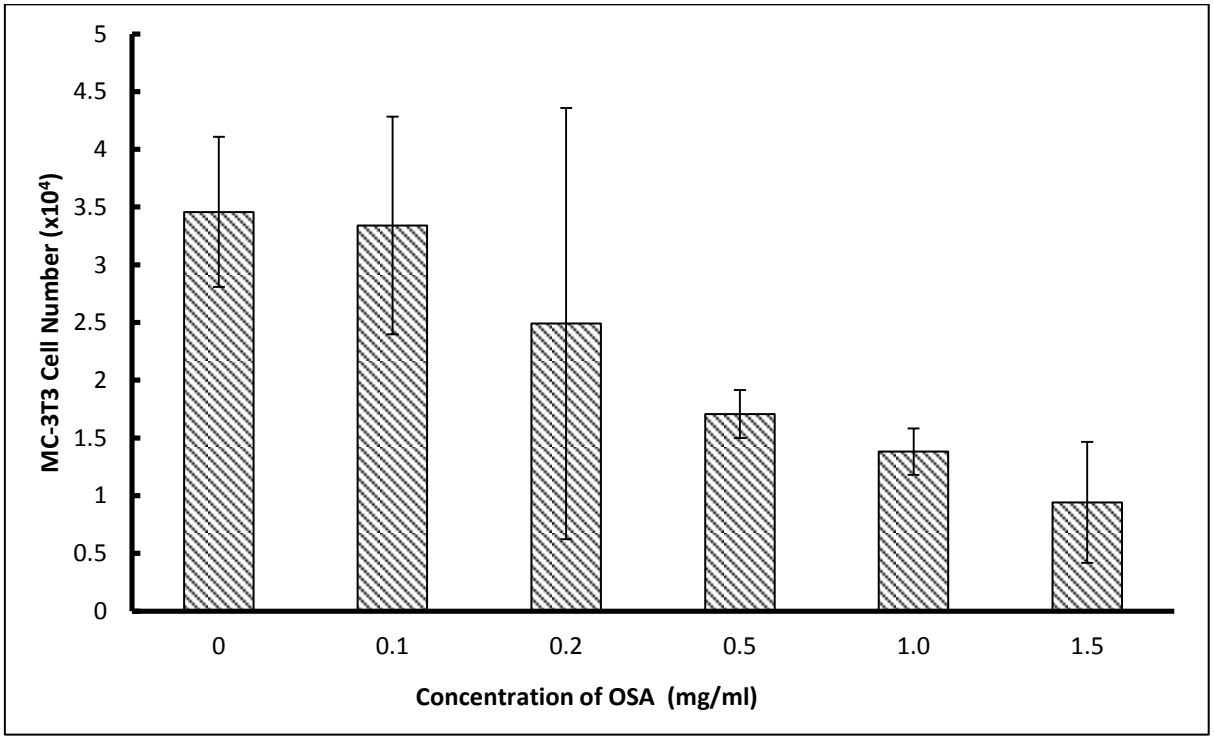

Figure 3.2: Viability of MC-3T3 osteoblasts cultured in media containing 0-1.5mg/ml OSA for 72H, shows that viability decreased when the concentration of OSA increased.

It was also noted the colour of the supplemented DMEM changed from orange to yellow as the concentrations of OSA increased, indicating that the environment was too acidic for the cells to survive (Figure 3.3).

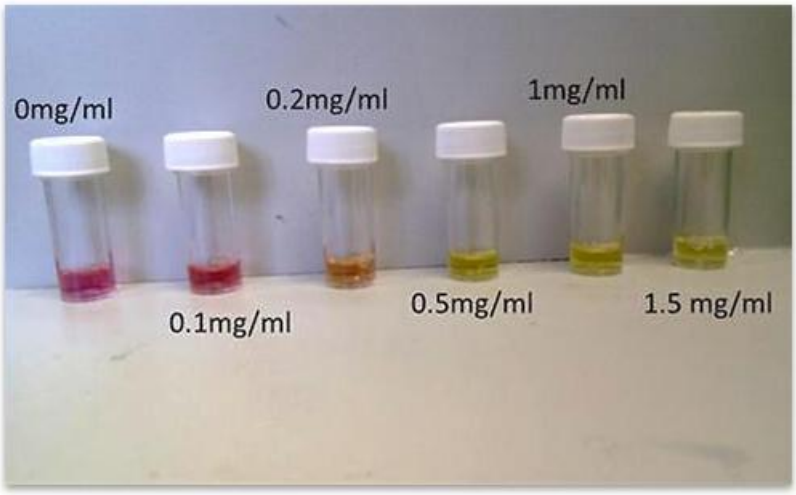

Figure 3.3: Indicates the colour of supplemented DMEM with increasing concentrations of OSA from 0-1.5mg/ml.

Osteoblasts cultured in lower concentrations of OSA, that is, between 0-20µg/ml showed an increase in cell viability. This too was determined using the MTT assay (Figure 3.4) as well as Calcein AM and Propidium Iodide staining to examine cell viability (Figure 3.5)

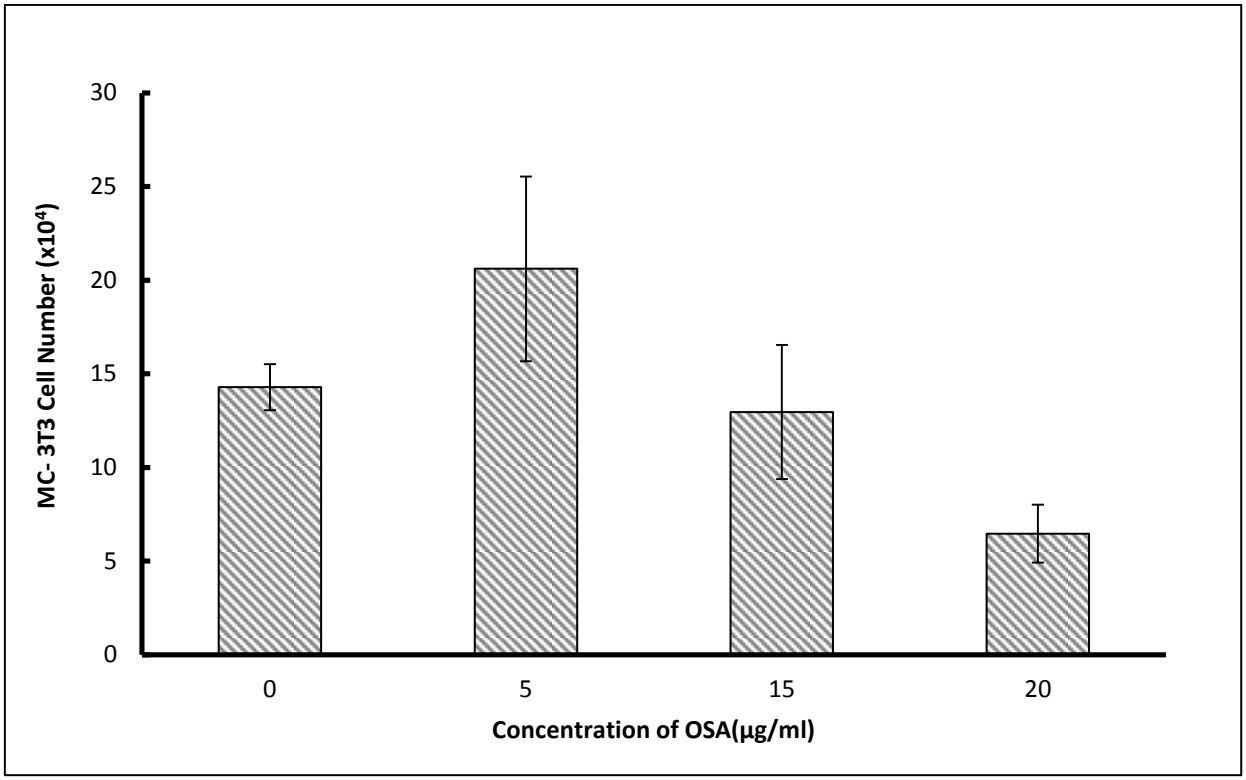

Figure 3.4: MC-3T3 viability assessed in the presence of 0-20µg/ml OSA for 72H, indicates that MC-3T3 cell viability significantly increased ($p<0.05$) in the presence of 5µg/ml of OSA, however viability decreased as the OSA concentration is increased above 15µg/ml, this was determined using the MTT assay.

MC-3T3 cell survival relied on the concentration of OSA, it was noted that concentrations of OSA below 5µg/ml showed an increase in cell number (Figure 3.4). Cells cultured without OSA showed a cell count of $14x10^4$ after 72h whereas there were approximately $21x10^4$ cells in the presence of 5µg/ml of OSA. Cell number decreased, to $13x10^4$ and $6x10^4$ however, when the concentration of OSA was increased for 15µg/ml and 20µg/ml of OSA, respectively.

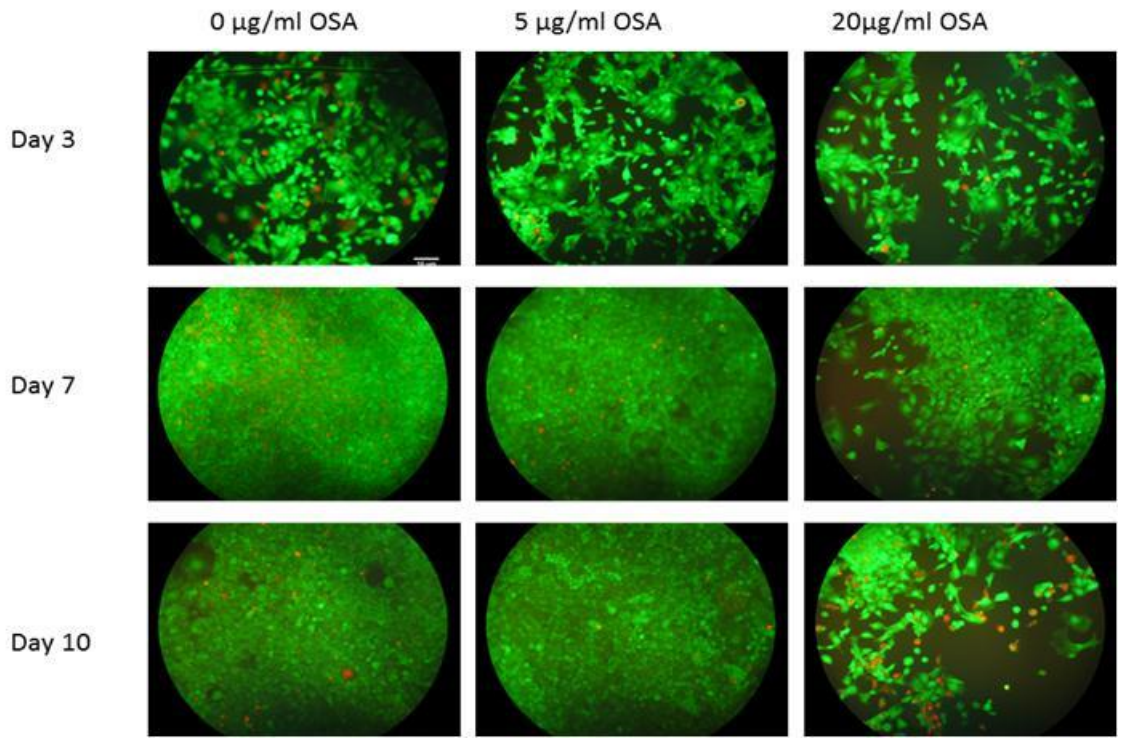

Figure 3.5: Live/dead fluorescent images of MC-3T3 cells doped with 0-20µg/ml of OSA using the Calcein AM (green) and Propidium Iodide (red) assays. Images indicated that high concentrations of OSA decreased cell viability. Scale bar denotes 10µm.

Live/dead fluorescent images show the viability of MC-3T3 cells for 3, 7 and 10 days when doped with 0, 5 and 20µg/ml of OSA (Figure 3.5). A decrease in the number of live cells was seen over the 10 days with cells cultured with 20µg/ml OSA. Cells with no OSA and 5µg/ml OSA illustrated more live cells (green staining) than dead cells (red staining) and the reached confluency over the 10 day period.

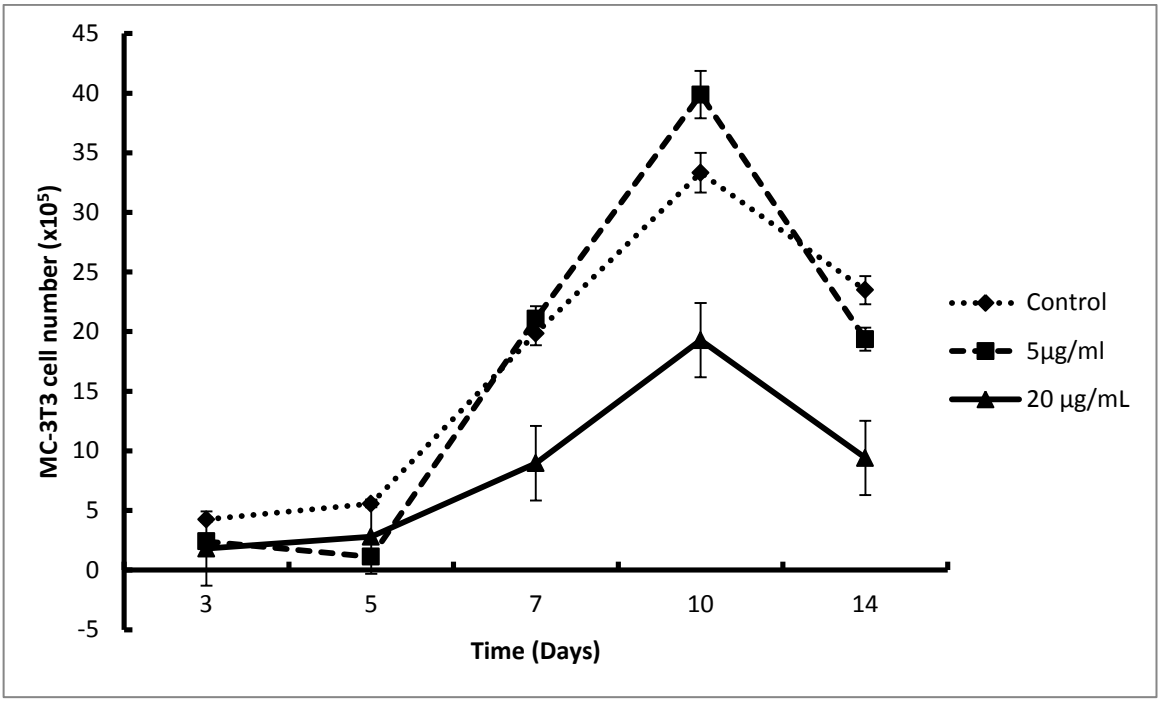

Figure 3.6: 14 day growth curve for MC-3T3 cells doped with various concentrations of OSA, indicating that cell number was significantly increased ($p<0.05$) in the presence of 5µg/ml OSA when compared to cells doped with no OSA and with 20µg/ml. This was determined using the Trypan blue assay.

A growth curve was determined to identify the effect of OSA on the attachment and proliferation of MC-3T3-E1 cells with time. Cell viability was significantly ($p<0.05$) higher when cells were treated with 5µg/ml OSA on day 7 and 10, when compared with untreated cells. Cells cultured with 20µg/ml of OSA showed a decrease in cell number, where only $1.9x10^6$ cells were viable on day 10 (Figure 3.6). At day 14, however, there was a decrease in cell number when cells were treated with 5µg/ml and 20µg/ml OSA concentration as well as the untreated samples. This could be attributed to the cells reaching 100% confluency at this time point and reducing the surface area for further cells proliferation.

3.3.2 Determining mineralisation in the presence of OSA

The quantification of inorganic phosphate and calcium were examined using Von Kossa and Alizarin Red respectively. The stains were used to examine mineralisation *in vitro* of cells doped with various concentrations of OSA only. Cells were not cultured in the presence of osteogenic mediators, so as to evaluate the effect of OSA on mineralisation.

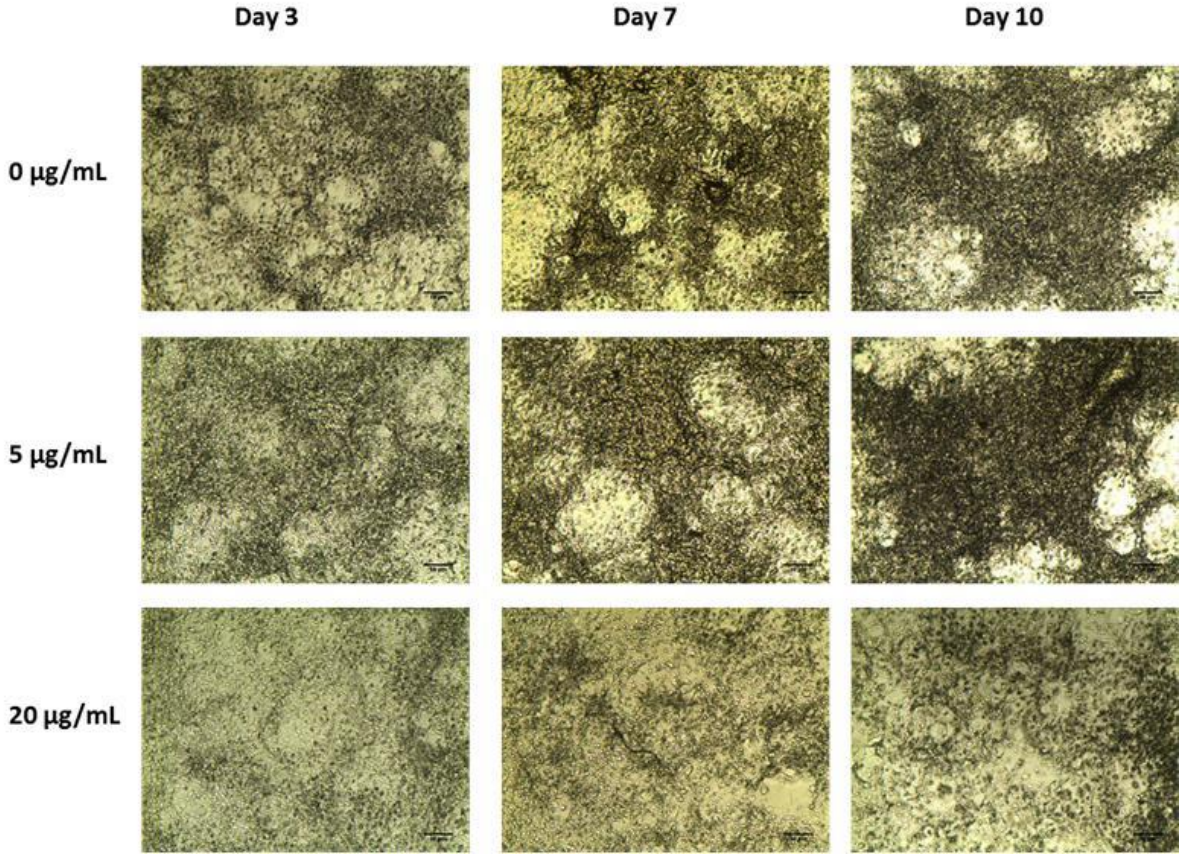

Figure 3.7: Deposition of inorganic phosphate when cells are doped with 5ug/ml and 20ug/ml of OSA over time. Scale bars denote 50µm.

The deposition of inorganic phosphate was determined *in vitro* using the Von Kossa assay. It was seen that there was the least phosphate deposition, when cells were doped with 20µg/ml of OSA (Figure 3.7). The decrease in phosphate deposition suggests mineralisation is concentration dependent and this agrees with the cell viability results whereby there is a decrease in cell number when cells are exposed to high concentrations of OSA.

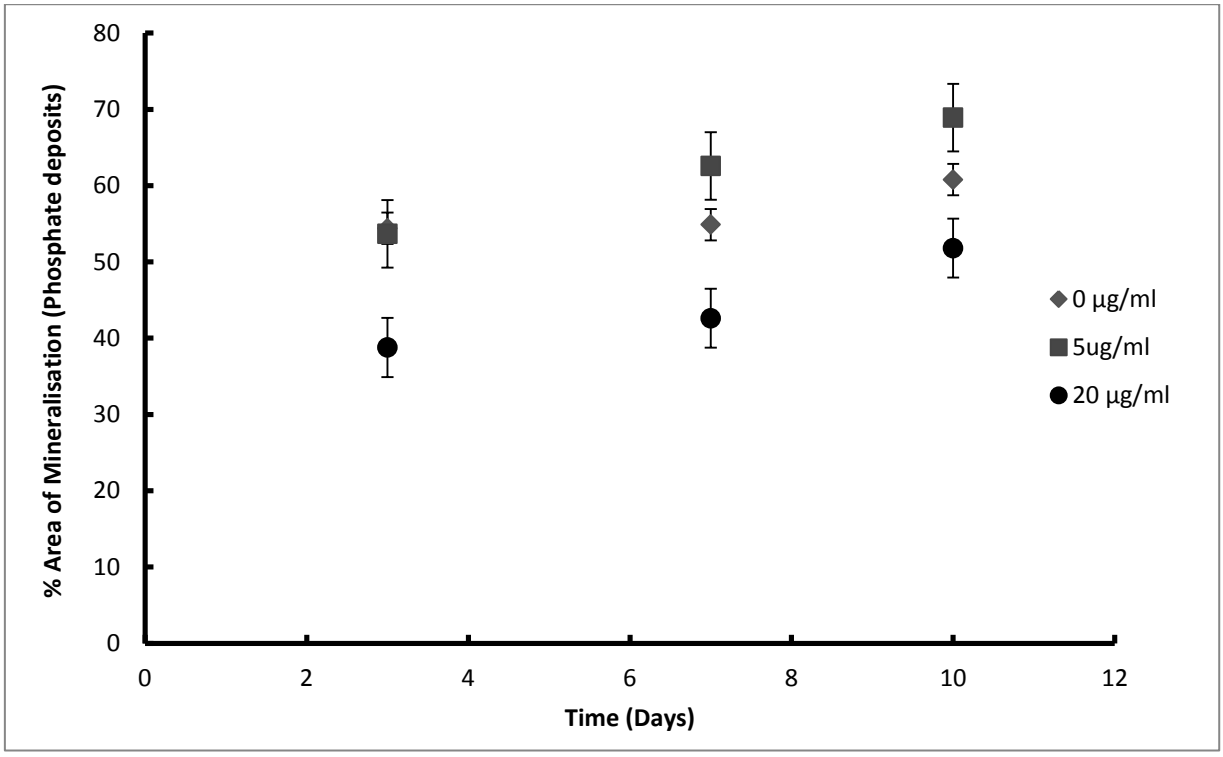

Figure 3.8: Quantitative analysis of phosphate deposits determined with the Von Kossa assay, the % area of mineralisation was measured using the software ImageJ.

Phosphate deposition significantly increased ($p<0.05$) when cells were treated with 5µg/ml of OSA. The % area of mineralisation is 63% and 68% on both day 7 and 10, respectively, when compared to cells cultured without OSA where on day 7 the % area of mineralisation is 55% and 60.8% on day 10 (Figure 3.8).

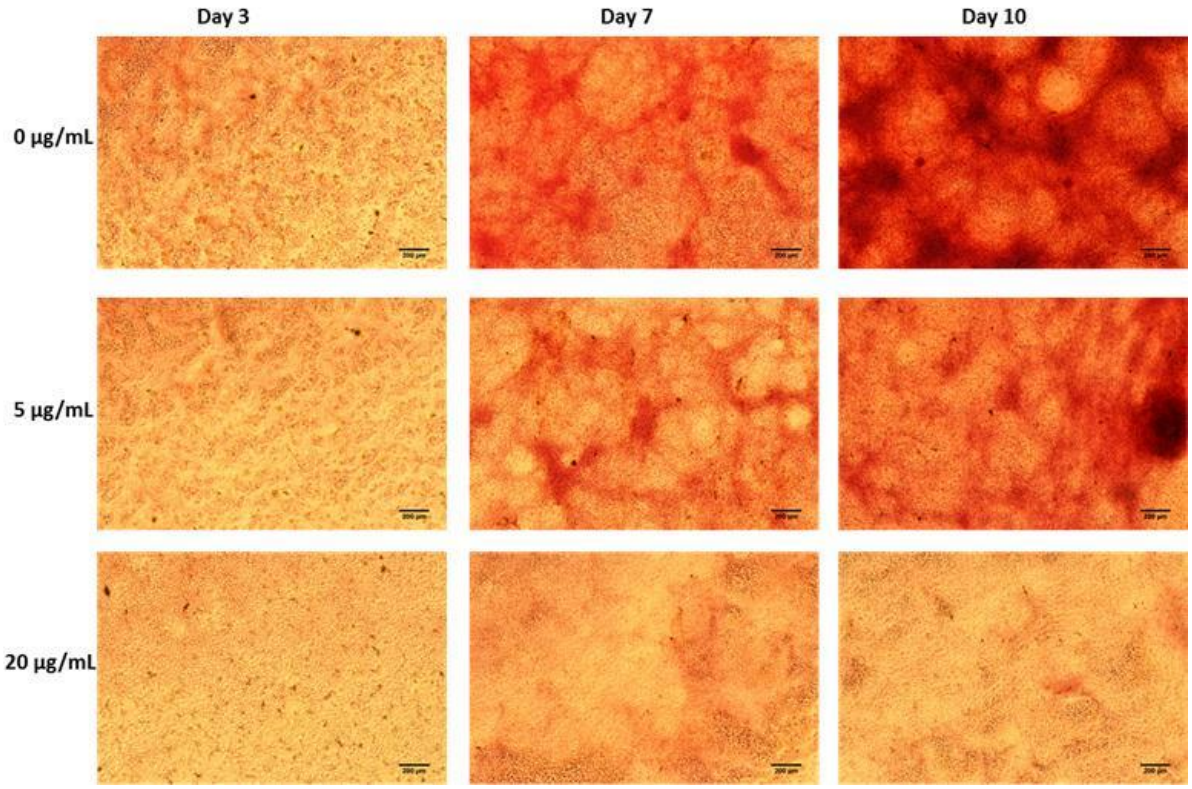

Figure 3.9: The effect of 0, 5 and 20µg/ml orthosilicic acid on calcium deposition in MC-3T3 cells. Calcium deposition was determined with the Alizarin Red S stain, Scale bars denote 200µm.

Cultures treated with 0, 5 and 20µg/ml of OSA, were stained with alizarin red and indicated the presence of mineralised nodules. Cultures treated with no OSA and 5µg/ml of OSA showed the presence of calcium deposits over 10 days in osteoblast like cells, however cells treated with 20µg/ml OSA did not demonstrate calcium deposition, illustrated in Figure 3.9. Quantitative analysis was carried out to determine the actual amount of calcium present in the cell cultures when treated with orthosilicic acid (Figure 3.10).

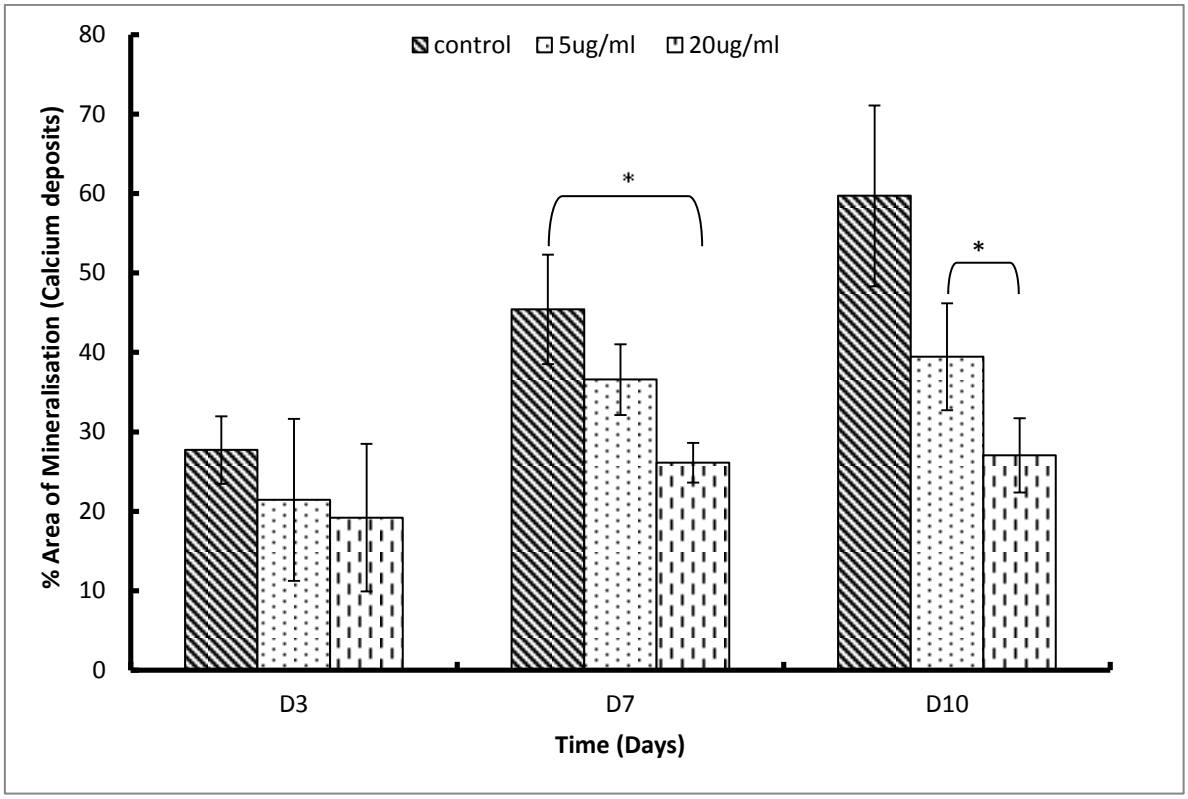

Figure 3.10: Quantifying the calcium deposits in MC-3T3 cells cultured with 0, 5 and 20μg/ml of OSA. Each result is the mean of three observations. Error bars represent standard deviations. The % area of mineralisation was measured using the software ImageJ. Results that a significantly different ($p<0.05$) are marked with an asterisk (*).

Initially, there is little increase in the deposition of calcium for both the non-treated and treated samples. There is no significant difference ($p>0.05$) in the amount of calcium determined in the cells cultured without OSA and those treated with 5μg/ml on day 7. There is a decrease, however, in the amount of calcium present when cells are treated with 20μg/ml of OSA on day 7, when compared to the non-treated cultures (Figure 3.10).

Osteoblasts treated with the highest concentration of OSA, that is, 20μg/ml show significantly less calcium deposition on day 10 however this could be caused by the accumulated concentration of OSA, as fresh culture media containing 20μg/ml of OSA was added over the

time of the investigation. This is interesting that the presence of low concentrations of OSA, may aid in the initiating of nodule formation however if the concentration of OSA continues to increase this can inhibit nodule formation and therefore decrease the deposition of calcium. It is noteworthy however, that this investigation was carried out when cells were cultured without osteogenic media, hence showing the direct effect of OSA on calcium deposition without the presence of osteogenic promoters. Finally a decrease in calcium deposition, from both the concentrations of OSA, that is, 5 and 20µg/ml on day 10 further elucidates the point that the effect of OSA on mineralisation in osteoblast cells is certainly dose dependent.

3.3.3 RT-PCR analysis

The expression of proliferating cell nuclear antigen (PCNA), and osteogenic markers; osteopontin, alkaline phosphatase (ALP), osteocalcin and collagen type 1 (COLL-1) were quantified in the rat bone marrow cells (rBMCs). Which were induced to proliferate *in vitro*, in the presence of 0, 5 and 20μg/mL of OSA, cultured with or without the presence of osteogenic mediators (OM), Ascorbic acid (AA, 200mM), Dexamethasone (Dex, 10^{-7}M) and β- Glycerophosphate (β-GP, 10mM).

Ascorbic acid, Dexamethasone and β- Glycerophosphate have shown to promote the expression of the osteoblastic phenotype in most bone cells. A series of experiments were carried out to evaluate the direct effect of OSA on rBMCs mineralisation as well as its effect in synergy with the osteogenic mediators. This was done so as to elucidate the pathway in which OSA contributes to cell mineralisation.

3.3.3.1 Expression of proliferating cell nuclear antigen (PCNA)

Proliferating cell nuclear antigen (PCNA) is a protein associated with the cell cycle. It is known to interact with many components of the cells replication and signalling machinery. In this case the expression of PCNA was used to determine the rate of proliferation in rBMCs cultured in s-DMEM and treated with orthosilicic acid.

Visual representation for the expression of PCNA was evaluated when rBMCs were cultured without (Figure 3.11) and with (Figure 3.12) the osteogenic mediators, ascorbic acid, β-glycerophosphate and dexamethasone. All images presented are from one gel image for reliable comparison.

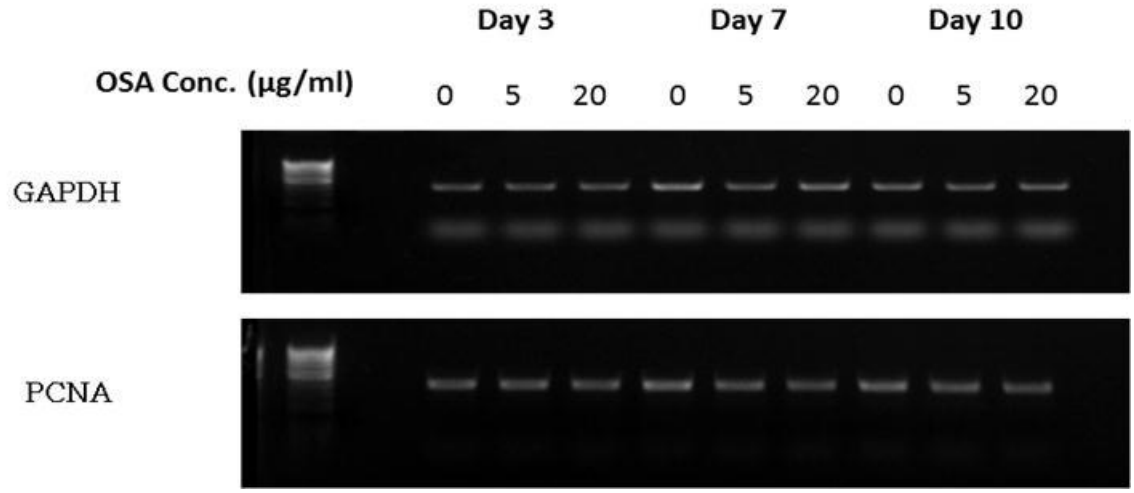

Figure 3.11: RT-PCR analysis of GAPDH and PCNA expression by rBMCs following incubation with 0, 5 and 20ug/ml of OSA for 10 days. Transcription of genes was analysed without the presence of osteogenic mediators (OM).

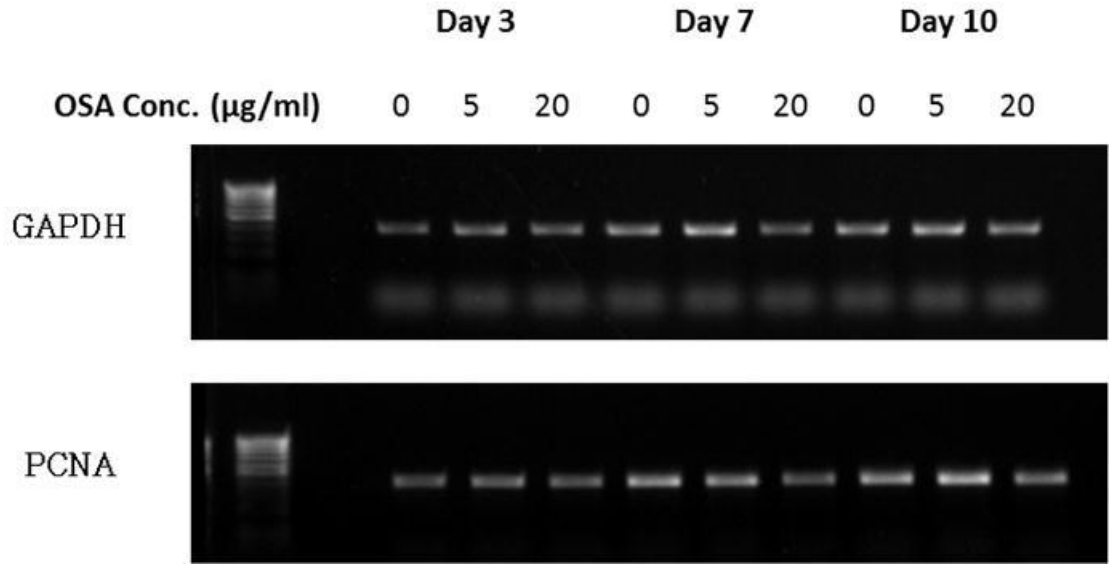

Figure 3.12: RT-PCR analysis of GAPDH and PCNA expression of rBMCs cultured with osteogenic mediators and treated with orthosilicic acid.

Semi-quantitative analysis was determined according to the band intensity and relative PCNA expression was determined after being normalised against the house keeping gene, GAPDH.

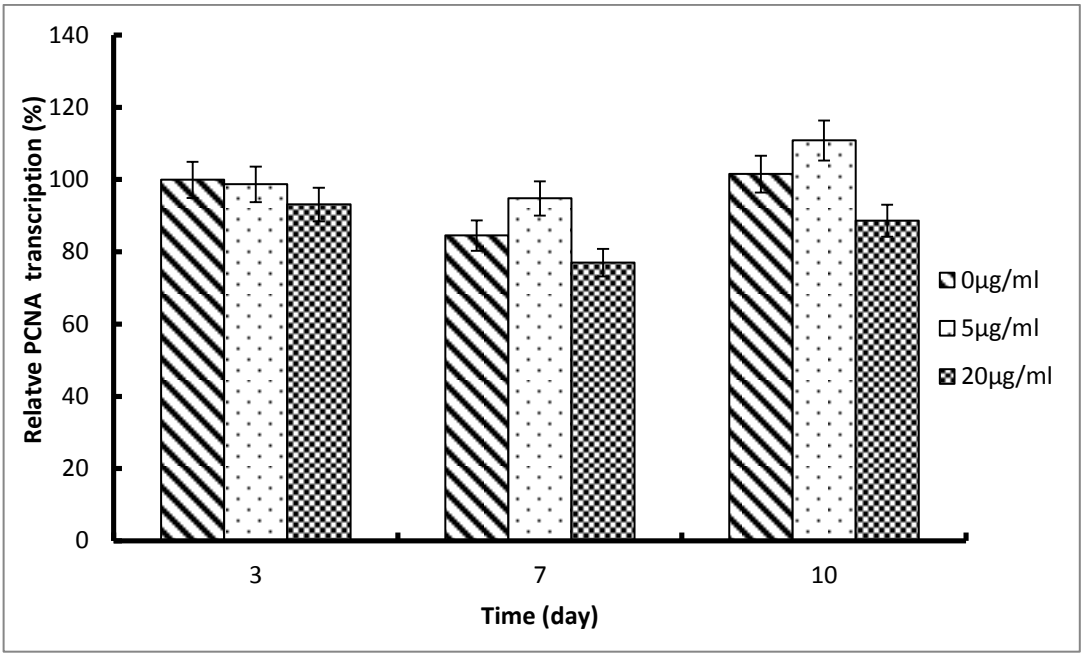

Figure 3.13: Relative transcription (%) of PCNA normalised against the housekeeping gene GAPDH. rBMCs were cultured without OM and doped with 0, 5 and 20ug/ml. The error bars represent the standard deviation of the mean.

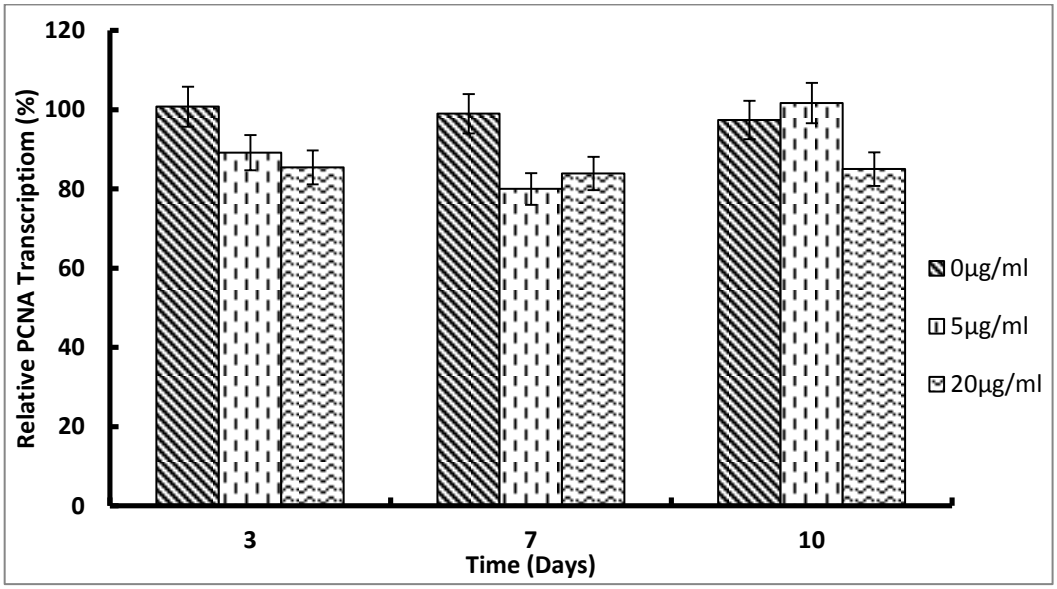

Figure 3.14: Relative transcription of PCNA normalised against the housekeeping gene GAPDH. Rat BMCs were cultured with OM and treated with various concentrations of OSA. The error bars represent the standard deviation of the mean.

Cells cultured without AA, β-GP and Dex, showed little significant change in the expression of PCNA when cells were treated with and without OSA (Figure 3.13). The relative transcription for the control and 5μg/ml OSA was 100% and 98% respectively on day 3, indicating that OSA had little effect in PCNA expression at this time point. There was a decrease in the expression of PCNA expression on day 7 from when cells were treated with 5μg/ml and 20μg/ml OSA when compared to non-treated samples. PCNA expression increased by day 10 for osteoblasts treated with 5μg/ml of OSA. The relative transcription for the control sample was approximately 97% and 102% in cells treated with 5μg/ml. Throughout the 10 day period cells doped with 20μg/ml showed a reduction in PCNA expression (Figure 3.13). Thus indicating, high concentrations of OSA reduce the transcription of PCNA, a protein which is synthesised during the S-phase of the cell cycle and is found in the nucleus of dividing cells. These results corroborate with those obtained from the viability tests (Figure 3.5)

Cells cultured with osteogenic mediators and 5μg/ml of OSA showed an approximately 10% decrease in the relative PCNA expression when compared to the control on day 3 and a 19% decrease on day 7. Cells treated with the highest concentration of OSA showed little change or a decrease in PCNA expression throughout the 10 day period when compared to the control. This could be attributed to the presence of dexamethasone, a glucocoticoid, which has shown to reduce cell proliferation and stimulates differentiation of the rBMCs towards the osteogenic lineage.

3.3.3.2 Expression of osteopontin, alkaline phosphatase, osteocalcin and collagen type1

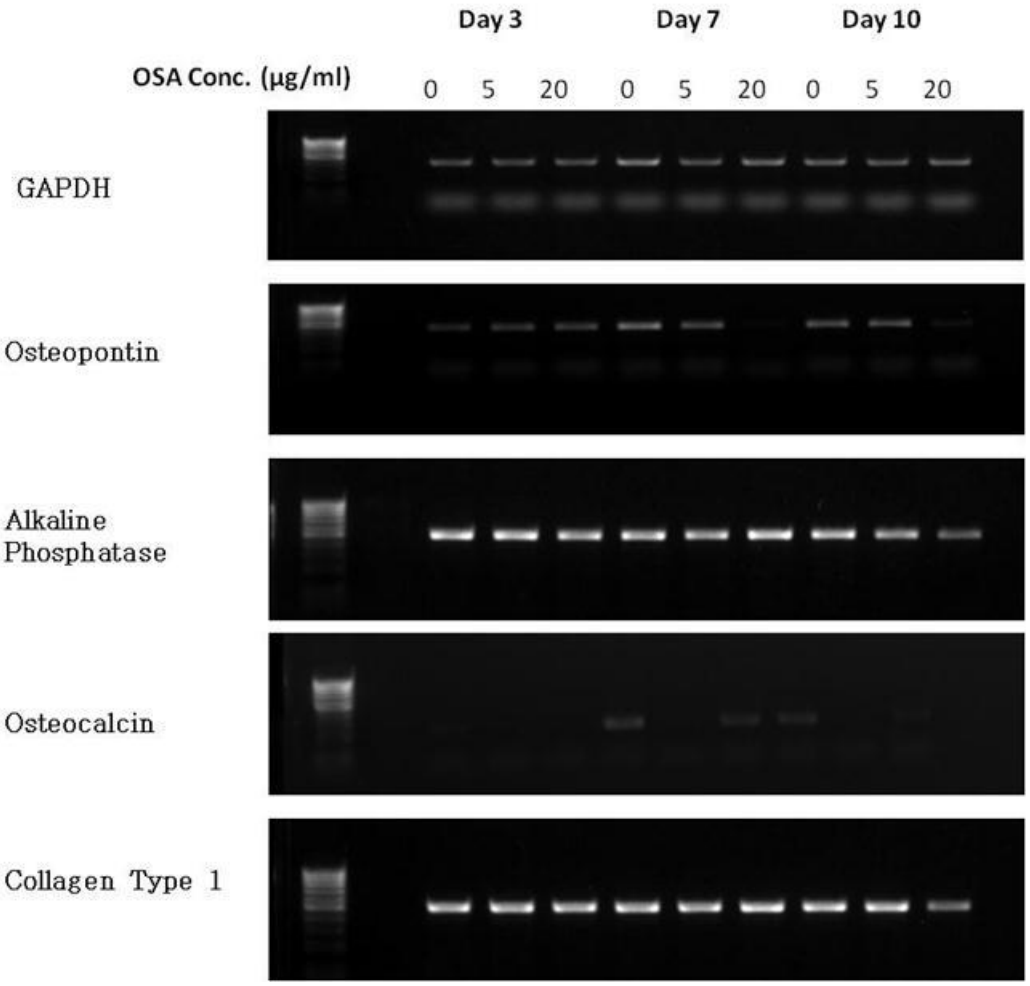

Figure 3.15: RT-PCR of mRNA expression of the house keeping gene GAPDH, osteopontin, alkaline phosphatase, osteocalcin and collagen type 1 in rBMCs when cultured without OM and treated with OSA at 0, 5 and 20μg/ml for 10 days.

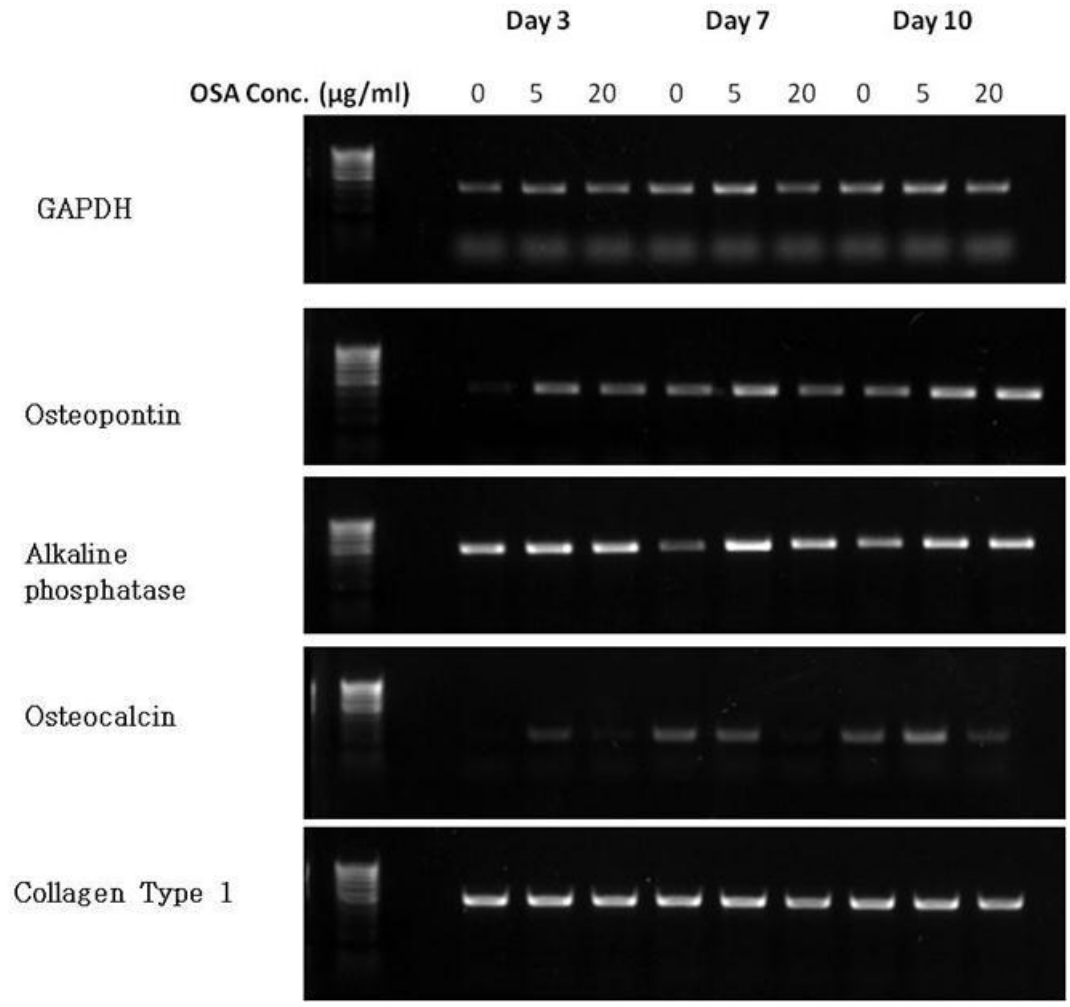

Figure 3.16: RT-PCR analysis of GAPDH, Osteopontin, Alkaline phosphatase, Osteocalcin and Collagen type 1, after rBMCs were treated with osteogenic mediators and 0, 5 and 20μg/ml of OSA for 10 days.

Visual examination of the gels in Figure 3.15 and 3.16 show the expression of osteopontin, alkaline phosphatase, osteocalcin and collagen type 1, when cells are treated without OM and with OM respectively. The relative transcription of all the osteogenic primers was determined according to band intensity and normalised against the house keeping gene, GAPDH.

3.3.3.3 Relative osteopontin transcription

a)

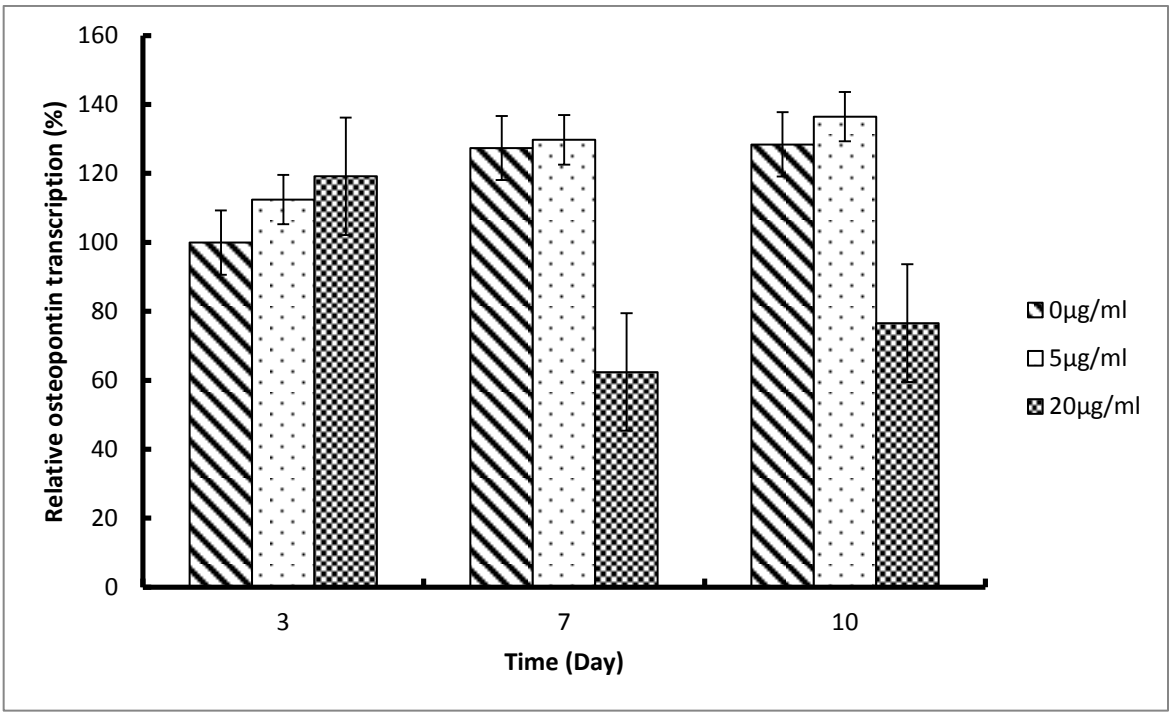

b)

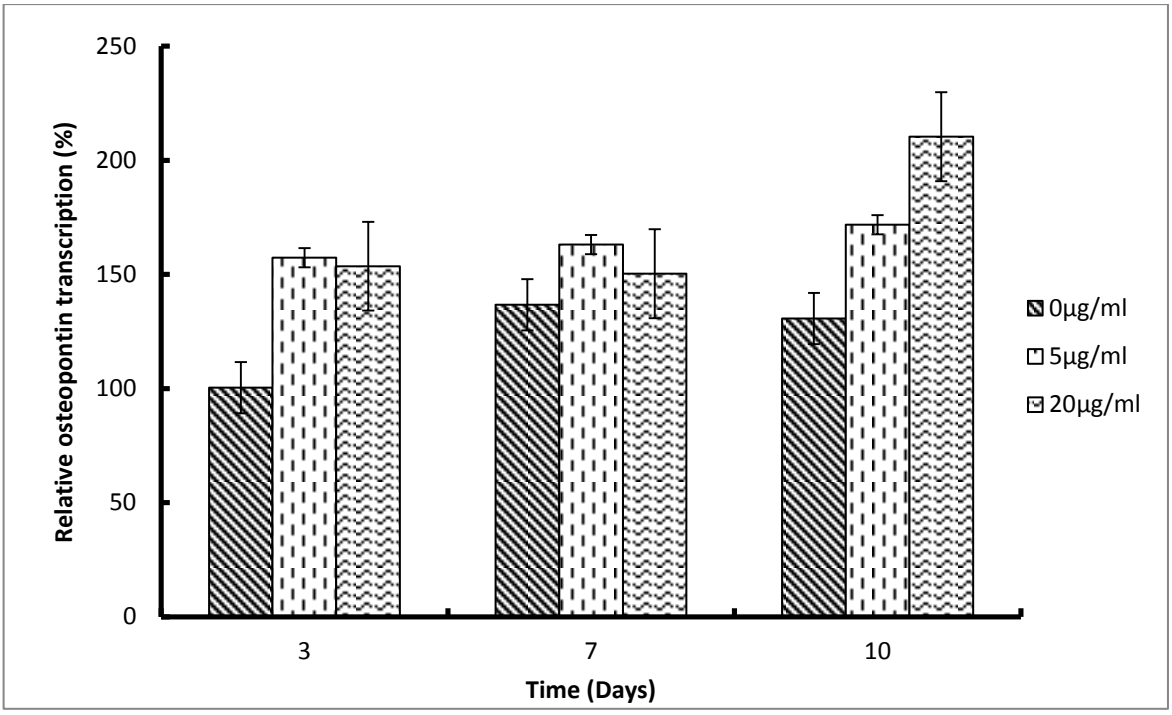

Figure 3.17: RT-PCR analyses of osteopontin expression after rBMCs were cultured without OM (a) and with OM (b) as well as being treated with OSA. Error bars represent the standard deviation of the mean.

Osteopontin is mostly involved in the regulation of bone resorption as it has shown to promote osteoclast differentiation (Rosenthal et al. 2007) and acts as a potent inhibitor of HA, therefore inhibiting the mineralisation process (Standal et al. 2004). The relative osteopontin expression in rBMCs showed to have no significant effect when treated with the low concentration, 5μg/ml, when compared to the control sample. The relative transcription at day 7 for the non-treated sample was 127% and 129% for the cells treated with 5μg/ml OSA. When cells were treated with 20μg/ml OSA, however, relative OPN transcription reduced over the 10 day when compared to the cells treated with 5μg/ml or without OSA (Figure 3.17a).

In the presence of osteogenic media, the cells stop proliferating and differentiation of cells is enhanced. Osteopontin also contains the Arg-Gly-Asp (RGD) sequence which acts as a cell binding motif which allows for adhesion molecules to bind to the surface of the extracellular matrix. Therefore, it has previously been suggested that osteopontin may have a role in the attachment of bone cells to the matrix (Roach 1994) and thus leading to an increase in OPN levels prior to bone mineralisation and as seen in Figure 3.17 b. OPN levels further increase in the osteogenic mediators as well as in the presence of OSA. When rBMCs were doped with 5μg/ml OSA on day 3 a 57% increase was seen when compared to the control, and cells doped with 20μg/ml showed approximately 53% increase on the same day. On day 7, the cells treated with 5μg/ml showed a 26% increase in osteopontin expression and cells with 20μg/ml showed an approximately 14% increase in expression when compared to the control. Overall, samples treated with OSA showed to have a significant effect on osteopontin transcription during the 10 day study, when compared to the control. A similar trend was seen on day 10, whereby samples treated with 5μg/ml showed a 40% increase in OPN transcription and a

significant increase of 80% were seen in samples treated with 20µg/ml OSA, when compared to the control (Figure 3.17b).

3.3.3.4 Relative alkaline phosphatase transcription

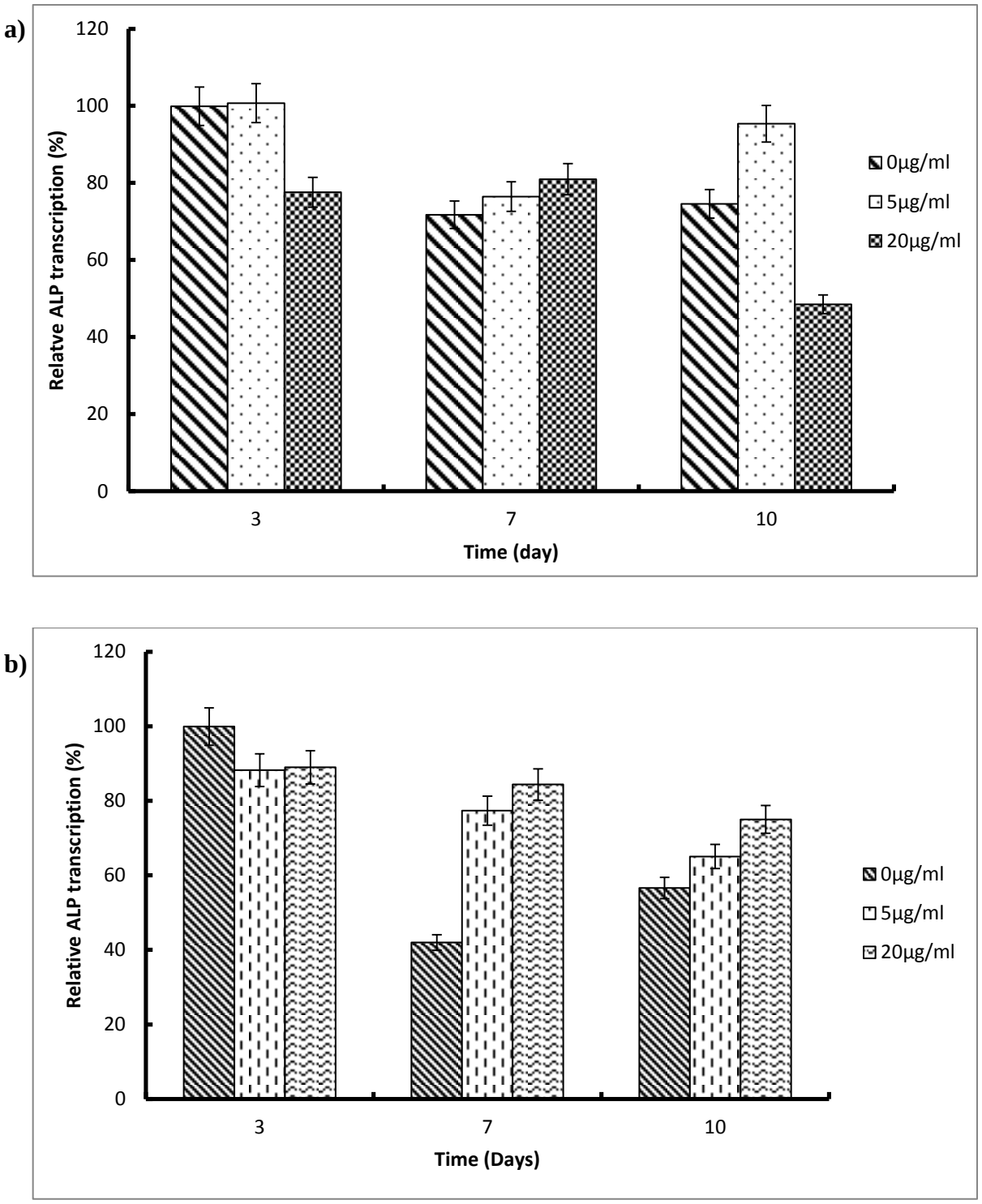

Figure 3.18: Relative alkaline phosphate transcription (%) of rBMCs cells treated with OSA, cultured without OM (a) and with OM (b). The error bars represent the standard deviation of the mean.

Alkaline phosphatase expression is known to increase during osteogenic differentiation and decreases during the formation and mineralisation of the extracellular matrix. Cells treated without osteogenic mediators and with OSA showed a decrease in ALP expression over the 10 day period, that is, ALP expression decreased from 100% on day 3 to 72% on day 7 and remained at approximately 75% on day 10. ALP expression increased however, from 76% on day 3 to 95% on day 10 when cells were treated with 5µg/ml OSA. When cells were treated with the high concentration of OSA, ALP expression decreased by 20% when compared to samples treated with 5µg/ml OSA. This further decreased to 49% on day 10, noticeably less when compared to the non-treated samples and those samples treated with 5µg/ml OSA (Figure 3.18a).

Osteogenically induced cells treated with orthosilicic acid showed an increase in ALP expression on day 3, that is, cells treated with 5µg/ml OSA showed nearly a two fold increase in ALP expression, when compared to the control, a similar trend was seen in cells when treated with 20µg/ml OSA. These results suggest that the high concentration of OSA does not influence ALP expression in the presence of osteogenic mediators, instead may act in synergy to promote osteogenic differentiation of the rBMSCs (Figure 13.8b). High concentrations of OSA, on the other hand, show a decrease in the expression of ALP without the presence of osteogenic mediators, indicating that orthosilicic acid on its own may aid in the formation and mineralisation of the extracellular matrix.

3.3.3.5 Relative osteocalcin transcription

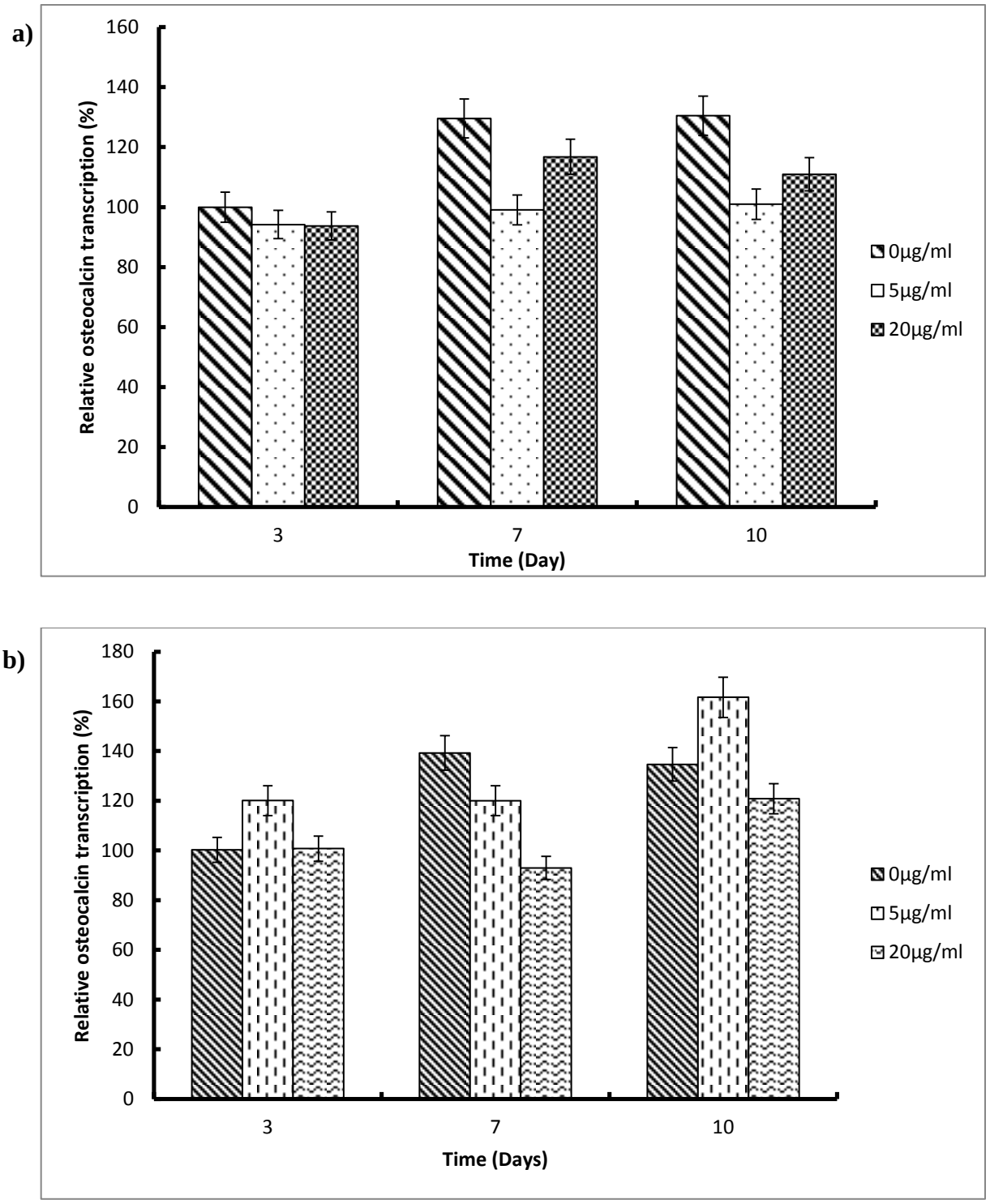

Figure 3.19: Relative osteocalcin transcription (%) of rBMCs cells treated OSA, cultured without OM (a) and with OM (b). The error bars represent the standard deviation of the mean.

Osteocalcin a non-collagenous protein is secreted by osteoblasts and plays a vital role in the body's metabolic regulation as well acting as a marker for early bone mineralisation (Neve et al. 2011). Rat BMSCs treated without OSA remained at an average of 120% in osteocalcin expression throughout the 10 day period. A similar trend was observed in the relative expression for rBMSC treated with 5μg/ml during the 10 day treatment, at approximately 98%. Cells have shown to have a higher expression of osteocalcin when doped with 20μg/ml, that is, 116% on day 7 and 110% at day 10, whereas cells treated with 5μg/ml osteocalcin expression remained at approximately 100% over the same time period. This suggests that OSA on its own when compared to the osteocalcin expressions obtained from the non-treated samples may have little effect on early bone mineralisation, however may still have an effect in conjunction with osteogenic mediators (Figure 3.19a).

The addition of ascorbic acid, β-GP and dexamethasone to the cells, enhanced the relative expression of osteocalcin by day 10 with 5μg/ml of OSA. Initially on day 3 and 7 osteocalcin expression remained at approximately 120% on both days, when doped with 5μg/ml OSA and increased to 161% at day 10. Non-treated samples expressed 100% of osteocalcin on day 3 and approximately 140% for both days 7 and 10. Indicating there was little up-regulation of osteocalcin without the presence of OSA. A noticeable increase was seen with 5μg/ml OSA where the expression remained approximately the same for day 3 and 7 at 120% and increased to approximately 161% on day 10, nearly 27% more than the control.

3.3.3.6 Relative Collagen transcription

a)

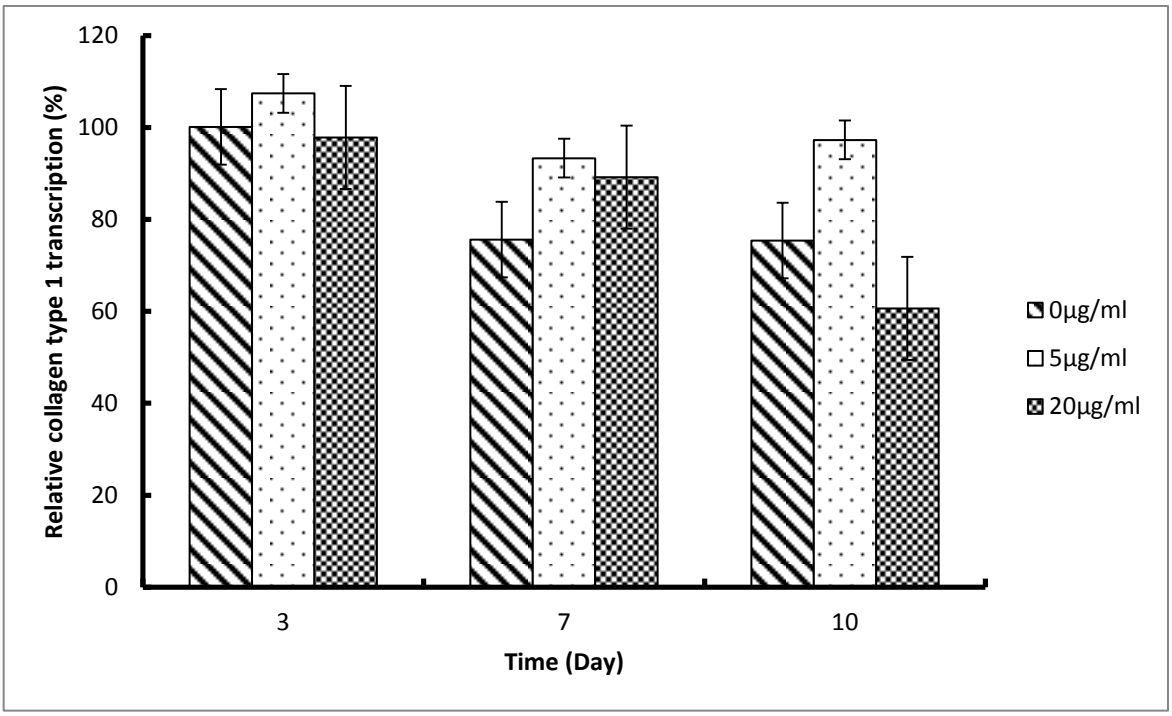

b)

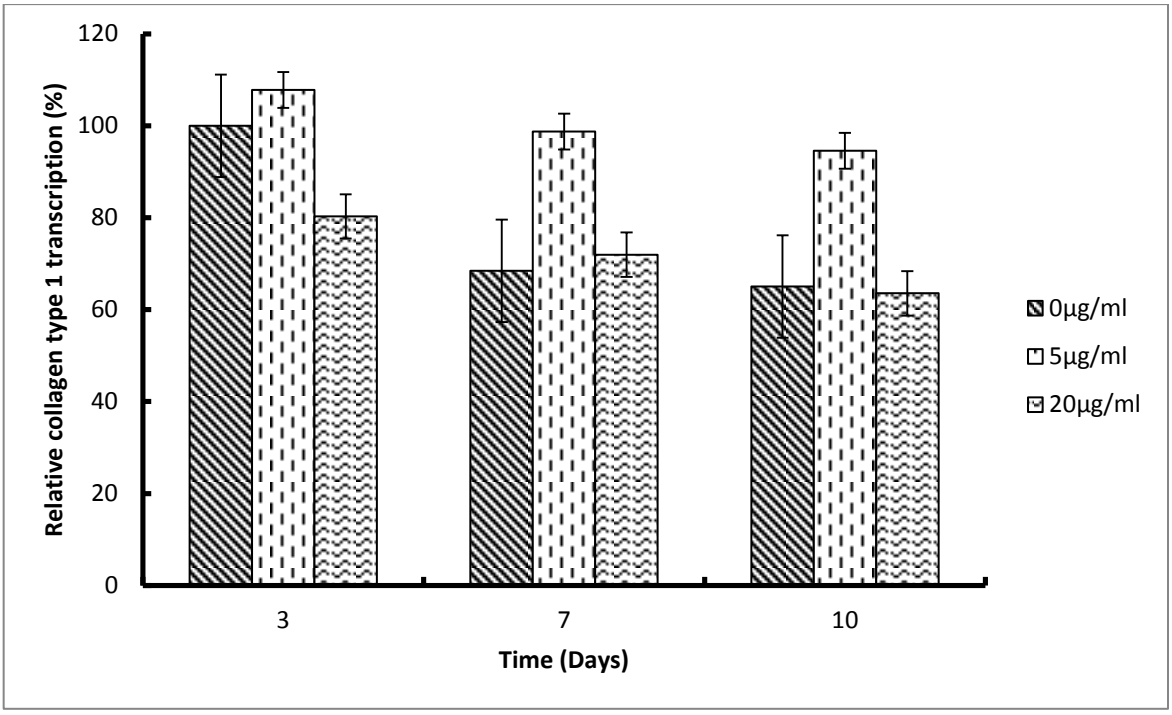

Figure 3.20: Relative collagen type 1 transcription (%) of rBMCs treated with OSA, cultured without OM (a) and with OM (b). The error bars represent the standard deviation of the mean.

Type 1 collagen is a dominant fibrous protein not only in connective tissues but also present in the hard tissues such as bone, and dentine (Viguet-Carrin et al. 2006). It is also present in the mineralising cartilage of the epiphyseal growth plates. Collagen is predominantly present in the form of elongated fibres known as fibrils, which provide structural strength within tissues and form a framework within which other components of the extracellular matrix can interact (Landis et al. 2006). Orthosilicic acid treated cells had a significant increase in the expression of collagen type 1. 5µg/ml treated cells expressed up to 18% and 22% more collagen on days 7 and 10 respectively when compared against the control cultures. This increase in transcription indicated that orthosilicic acid on its own, that is, without the presence of osteogenic mediators played a fundamental role in matrix formation leading to early bone matrix synthesis. A decreasing trend was noticed when cells were doped with the highest concentration of orthosilicic acid similar to the expression of osteopontin and alkaline phosphatase when cells were cultured without osteogenic mediators (Figure 3.20a).

Figure 3.20b, indicated that collagen type 1 expression is comparable to the expression obtained when cells were cultured without osteogenic mediators and with osteogenic mediators. There is an overall increase in the relative transcription of collagen when cells are treated with 5µg/ml OSA when compared to the control. Little difference was seen in cells treated with 20µg/ml, when compared to the non-treated cultures, on day s 7 and 10. This indicates that orthosilicic acid concentrations play a vital role in collagen type 1 expression, therefore an important role the early mineralisation of osteoblast-like cells as well as a fundamental role in initial bone formation (Figure 3.20b). To further investigate the role of orthosilicic acid on bone modelling, the mechanism of collagen fibrillogenesis was evaluated in the presence of orthosilicic acid.

3.3.4 Effect of orthosilicic acid on collagen fibrillogenesis *in vitro*

Collagen is the most common protein in the organic scaffold of mineralised connective tissues and acts as a means for strain energy storage and mechanical support (Heinemann et al. 2011). Type 1 collagen has been widely investigated due to its self-organisation properties (Kadler et al. 2008). Previously in this chapter it has been shown that the soluble form of silicon, orthosilicic acid, augments bone mineralisation, by up-regulating the osteogenic markers, osteopontin, osteocalcin as well as type 1 collagen. Hereon interactions between silicon species and collagen are investigated via *in vitro* analysis of the effect of orthosilicic acid in a range of different concentrations on collagen fibril formation. These include; turbidity profiles, determining the rate of fibril formation, analysing fibril morphology using AFM and evaluating the thickness of collagen fibres in various OSA concentrations.

3.3.4.1 Turbidity profiles

Type 1 collagen kinetics profiles were determined by carrying out turbidity measurements. This measured the rate of assembly of the collagen fibrils as well as the amount of fibrillar material formed.

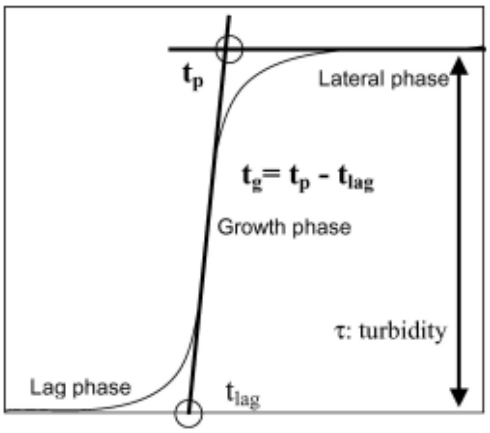

Figure 3.21: A typical turbidity profile of collagen fibrillogenesis (Kuo et al. 2005).

Under typical assembly conditions, the absorbance curve is a function of time and with a sigmoidal profile (Figure 3.21). In general, there are 3 phases;

- Lag phase – whereby triple helices undergo a conformational change and little or no aggregation occurs, leading to no significant change in turbidity.
- Growth phase – represents the occurrence of fibril formation, producing nano/micro meter fibres and leading to a rapid increase in turbidity.
- Lateral phase – fibril association leads to gelation which causes the turbidity to reach a constant value.

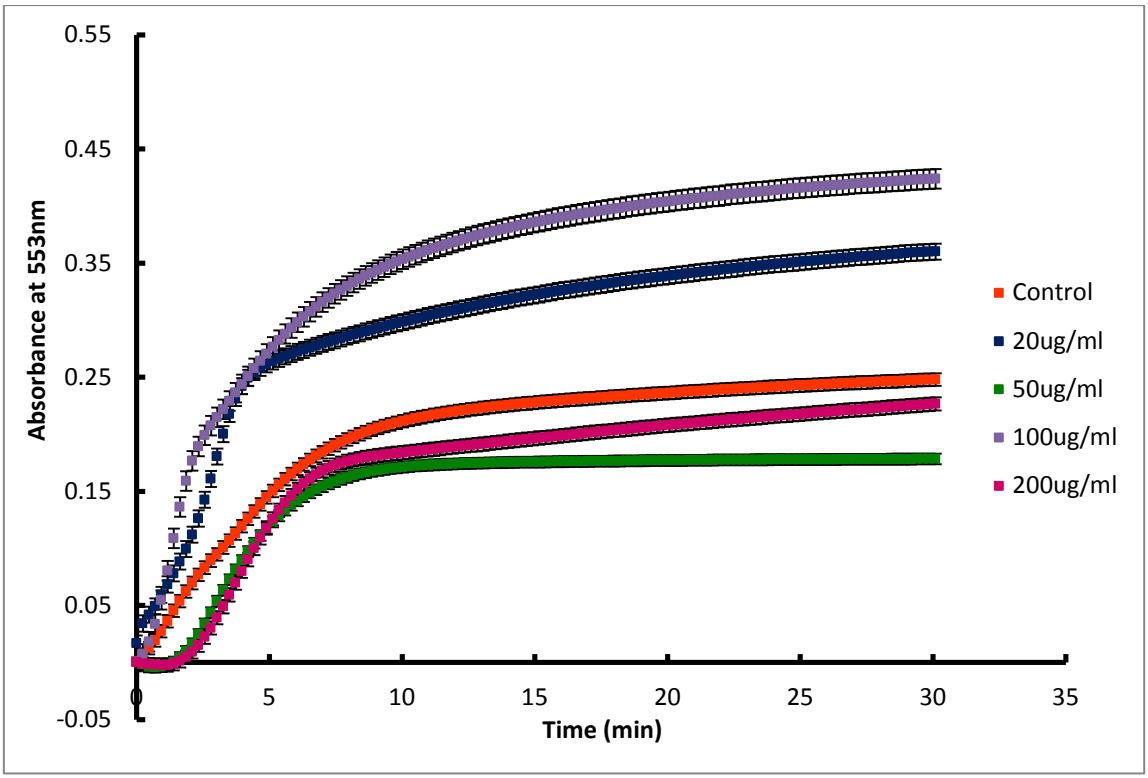

Figure 3.22: Turbidity measurements carried out for 30 minutes, of collagen type 1 fibril formation in the presence of increasing concentrations of OSA. Error bars indicate the standard deviation of the mean (n=4)

Collagen is soluble at a low pH and can be reconstituted to fibrils by neutralisation, for example with the addition of sodium hydroxide. The fibril formation is associated with a strong increase of the viscosity of the solution and leads to a 3D network of collagen fibrils, which exhibit ‘gel-like’ properties.

Turbidity measurements from Figure 3.22 showed typical sigmoidal curves for the collagen gels, with and without orthosilicic acid. The lag phases are comparable, however, the lag phases for the control and collagen with 20µg/ml OSA were shorter than the gels synthesised with higher concentrations of orthosilicic acid that could not be quantified. Collagen gels with 50, 100 and 200µg/ml of OSA, showed to have an increase in lag phase as the concentrations increased, that is, 1.4 minutes for 50µg/ml , 1.63 minutes for 100µg/ml and approximately 2 minutes for collagen gels prepared with 200µg/ml OSA. Indicating that OSA increases the time needed for the collagen triple helices to undergo conformational change. This interaction, however, is highly dependent on the concentration of the silicon source, as in the presence of high concentrations of OSA the association of the protein chains is hindered.

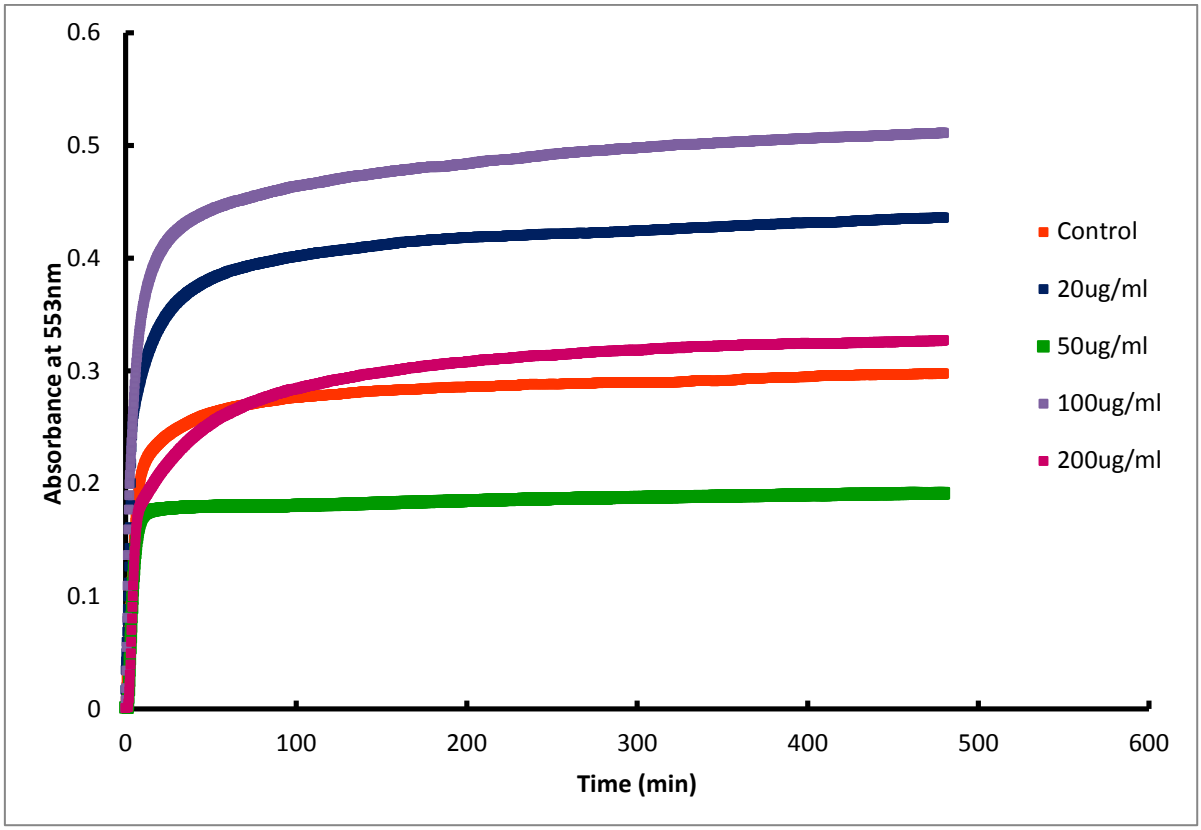

Figure 3.23: Complete turbidity profiles of the type 1 collagen gels prepares with increasing concentrations of OSA.

During the fibrillogenesis phase sodium silicate modifies the fibrillogenesis process at low concentrations. A rapid increase in turbidity was noticed after the lag phase, signifying the formation of the fibres of the collagen gel. The growth phase of the collagen gels was quantified from the turbidity profiles using the following equation:

$$t_g = t_p - t_{lag}$$

t_g – growth phase

t_p – lateral phase

t_{lag} – lag phase

Equation 3-4

Collagen gels prepared with orthosilicic acid decreased the growth phase when compared to the control. The growth phase decreased as the concentration of OSA increased from 20 – 100µg/ml, however increased in the presence of 200µg/ml of OSA. The decrease in the growth phase indicated that OSA increased the rate of fibril formation (Figure 3.23).

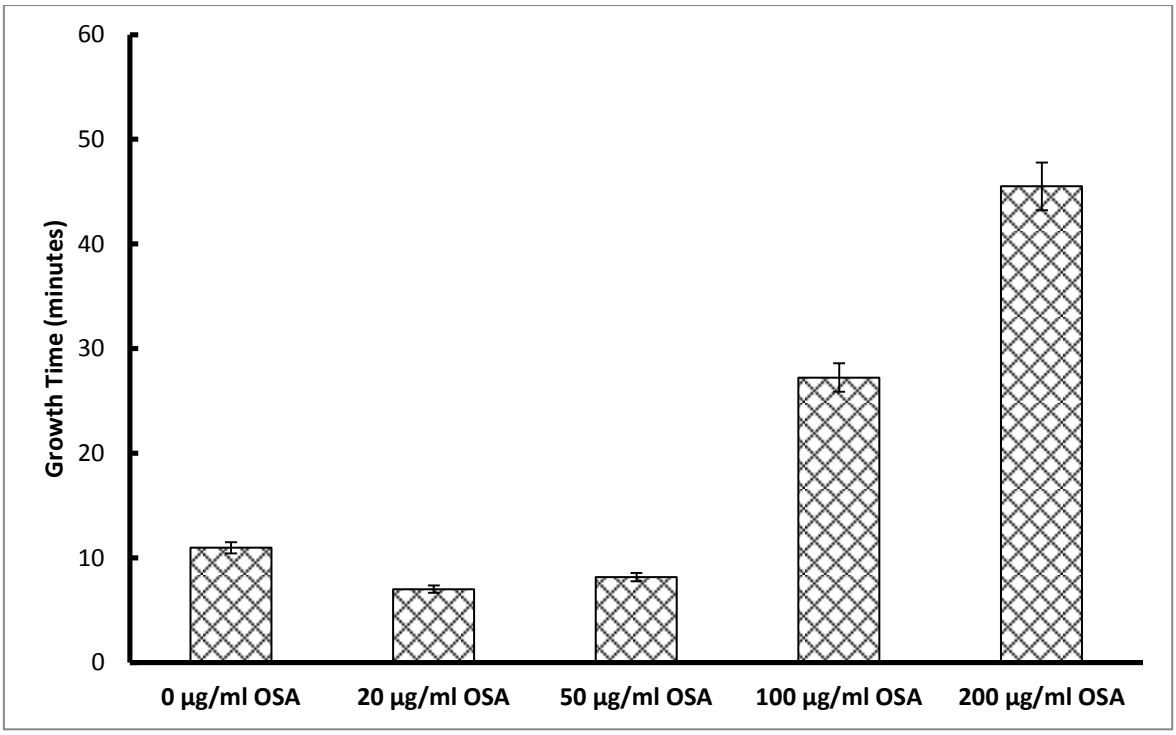

Figure 3.24: Growth time of fibril formation of collagen gels in the presence of various concentrations of OSA

The time needed for fibrils to form decreased significantly in the presence of orthosilicic acid (Figure 3.24). Collagen fibrils formed in approximately 10.96 minutes without the presence of OSA and this time decreased to approximately 7 minutes when supplemented with 20µg/ml. The growth time for fibril to form in the presence of 50µg/ml increased slightly to 8.16 minutes; however this was still lower when compared to collagen fibril growth produced without OSA. When the concentration of OSA was increased to 100µg/ml and 200µg/ml the time required for fibril was significantly higher and increased to 27.23 and 45.5 minutes

respectively. Indicating that collagen degradation occurs in the presence of higher concentrations of OSA, however the presence of OSA in optimum concentrations between 20-50µg/ml the rate of fibril formation is increased. This was further investigated by observing the morphology of the fibres in the presence of various concentrations of OSA.

3.3.4.2 Collagen fibril morphology using AFM

The morphology of the collagen fibres varied depending on the concentration of orthosilicic acid. Fibrils with variable diameter sizes were formed at different concentrations of OSA. Figure 3.25 illustrates the fibril network in the collagen gels.

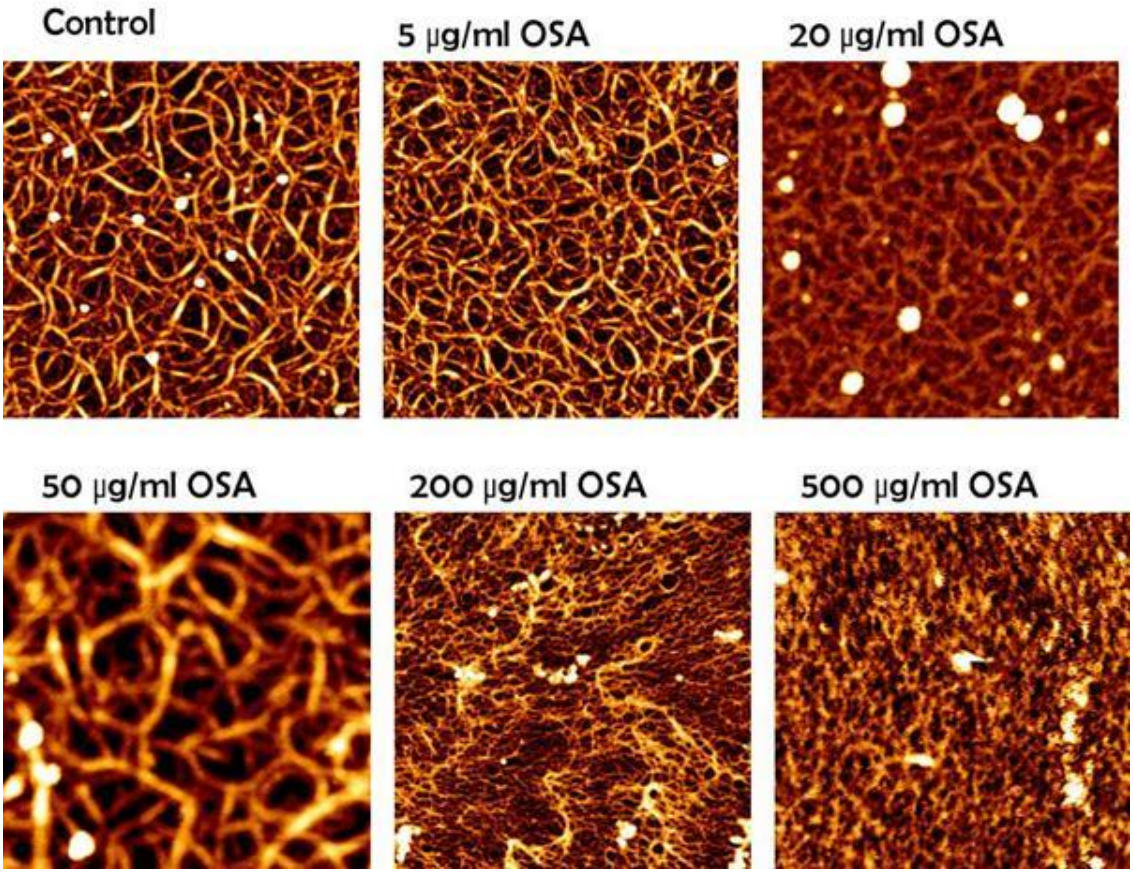

Figure 3.25: AFM images of collagen fibres when collagen gels prepared with various concentrations of OSA

It can be seen that collagen fibrils are a densely packed in the presence of OSA when compared to the control. Collagen gels made with 5-50µg/ml of OSA showed a more intricate network of fibres when compared to gels made without OSA. The collagen gels made with higher concentrations, that is, with 100 and 200µg/ml of OSA led to the degradation of the gel, indicating that OSA in lower concentrations modifies the collagen fibril network, however, in supra-physiological condition may inhibit fibril formation and collagen gel production. This is also evident when determining the growth time for fibril formation, as the fibres take longer to form or may not have formed at all in these concentrations. The effect OSA on collagen fibre diameter was further determined from the AFM images (Figure 3.26).

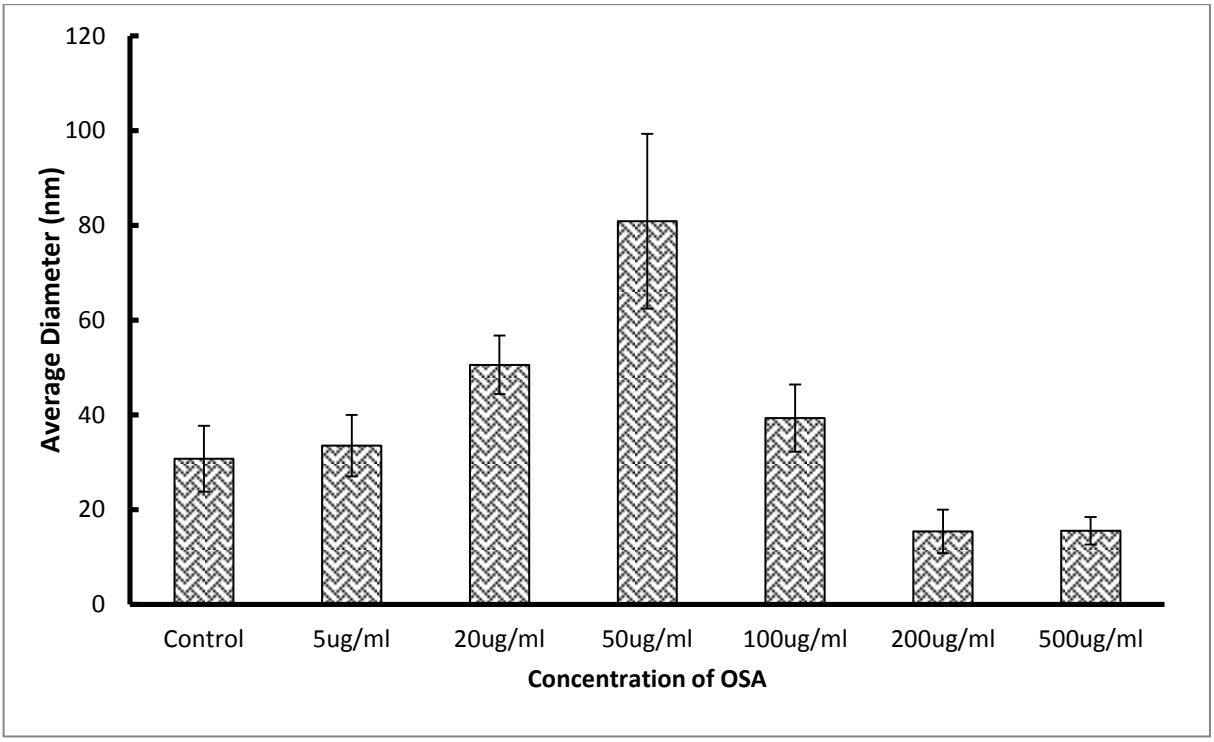

Figure 3.26: Diameter of collagen fibres determined in the presence of various concentrations of OSA.

The presence of OSA in collagen gel formation demonstrated a significant effect in the diameter sizes of the fibrils formed. Gels produced with, 5µg/ml OSA, have shown no significant effect in the fibril diameter size when compared to the control, that is, the diameter was approximately 30.72nm for the collagen gels only and 33.5 ± 3nm for the gels produced with 5µg/ml OSA, however, it was noticed that with the presence of 5µg/ml OSA the gels formed a more intricate network of fibres and visually, more branching was seen when comparing the images to the control collagen sample (Figure 3.25). The diameter size further increased to 50.56nm when 20µg/ml of OSA was added, and 81nm in the presence of 50µg/ml of OSA. In the higher concentration of OSA, that is, between 100-500µg/ml, the collagen gels begin to degrade and thinner fibres were formed, and collagen formed a weak gel. This illustrates that OSA at lower concentrations, plays a key role in the conformation of collagen fibres as well as the branching and the network of the gel *in vitro* and may play a similar role in collagen balance *in vivo.*

3.4 Discussion

Previously, it has been demonstrated that silicon regulates early bone homeostasis *in vivo* (Carlisle, 1976). In this chapter it has been shown that silicon in its soluble form as orthosilicic acid, promotes early bone mineralisation by enhancing the expression of early osteogenic markers as well as having a significant effect on collagen type 1 fibrillogenesis.

The concentration-response relationship of orthosilicic acid on osteoblast cells was determined and the optimum concentration for cell survival and mineral deposition was evaluated *in vitro*. In the presence of high concentrations, there is a decrease in cell proliferation (Figure 3.6) however in the presence of an appropriate OSA concentration (5μg/ml) osteoblast proliferation was promoted. It has been suggested that OSA stimulates the entry of cells into the S phase whereby DNA synthesis takes place as well as the G_2 phase, the gap between DNA synthesis and mitosis, of the cell cycle (Shie et al. 2011). Higher concentrations than 5μg/ml of OSA were shown to cause cell death.

To assess the role of OSA in cell function, the effect on mineralisation was determined. Early phosphate and calcium deposition were simultaneously seen in the presence of 5μg/ml concentration of OSA (figures 3.7 – 3.10). Cells treated with 20μg/ml OSA showed an inhibition of the mineralisation and nodules formation over the 10 day period, as well as cell death; this is in agreement with the proliferation studies carried out. The presence of mineral deposits indicates that Si in the form of orthosilicic acid initially plays a role in early bone mineralisation as well as nodule formation in osteogenic cells. Higher concentrations of OSA have shown to affect the cell cycle and lead to cell death, on the other hand lower concentrations of OSA, such as 5μg/ml, can act as a regulating factor for the deposition of calcium and phosphates in bone tissue.

Rat bone marrow cells were induced to differentiate to the osteogenic lineage in the presence of osteogenic mediators; ascorbic acid, β-glycerophosphate and dexamethasone. The effect of OSA was evaluated when rBMCs were cultured with or without the osteogenic mediators and the expression of osteogenic markers; osteopontin, alkaline phosphatase, osteocalcin and collagen type 1 were evaluated.

The relative osteopontin expression in rBMCs showed to have no significant effect when treated with the low concentration, 5μg/ml, when compared to the control sample. When cells were treated with 20μg/ml OSA, however, relative OPN transcription reduced over the 10 day when compared to the cells treated with 5μg/ml or without OSA (Figure 3.17a). Osteopontin also contains the Arg-Gly-Asp (RGD) sequence which acts as a cell binding motif which allows for adhesion molecules to bind to the surface of the extracellular matrix. Therefore, it has previously been suggested that osteopontin may have a role in the attachment of bone cells to the matrix (Roach 1994) and thus leading to an increase in OPN levels prior to bone mineralisation. OPN levels further increase in the osteogenic mediators as well as in the presence of OSA (Figure 3.17b).

Alkaline phosphatase is an enzyme that is normally present in high concentrations in growing bone and is often used as a marker to indicate bone mineral deposition. Orthosilicic acid in low concentrations of 5μg/ml increased ALP expression, without cells being osteogenically induced after 10 days in culture (Figure 3.18a). Rat BMCs induced with osteogenic mediators however, demonstrated a significant effect in ALP expression, this could be attributed to the presence of β-glycerophosphate which promotes mineralisation in the differentiated osteoblasts as it is rapidly hydrolysed in the presence of alkaline phosphatase within the cell, thus producing high levels of phosphate ions and creating an ideal environment for mineral

deposition (Rupani et al. 2012). When the cells were osteogenically induced, OSA further increased ALP expression, when compared to cells treated without OSA. Anderson et al (2008) suggested that the cells absorb the orthosilicic acid present, which further promote nodule formation of the minerals, leading to an increase in ALP expression both in osteogenic induced cells (Anderson et al. 1998).

Although orthosilicic acid has shown to be an essential element in bone formation, with the analysis of osteogenic markers such as ALP and Collagen type 1, little evaluation has been carried out to determine whether OSA effects early bone mineralisation. RT-PCR analysis on osteocalcin expression was carried out as it is an early mineralisation marker for the reason that it is a key Ca-binding protein that is exhibited when early mineralisation takes place (Varanasi et al. 2011). Interestingly, when cells are treated with OSA and when no osteogenic mediators are present, osteocalcin expression is down regulated, suggesting that, high concentrations of OSA on its own may actually be toxic to cells therefore leading to cell death (Figure 3.19a). In the presence of osteogenic mediators on the other hand, an up-regulation of osteocalcin was observed in the presence of 5µg/ml, showing that OSA and osteogenic mediators act in synergy to promote early bone formation (Figure 3.19b). The presence of ascorbic acid in the osteogenic media is known to aid in the formation of the collagen extracellular matrix which is connected to an increase in alkaline phosphatase activity and therefore associated in forming the mineralised matrix. The addition of the glucocorticoid, dexamethasone induces cell differentiation into the osteogenic lineage, therefore indicating an increase in osteocalcin expression when cells were treated with osteogenic media.

An up-regulation of collagen type 1 was observed in cells treated with OSA and without the presence of osteogenic mediators (Figure 3.20). These results are in agreement with Reffit et

al (2003), whereby, they showed that physiological concentrations of soluble silicon enhance the synthesis of collagen type 1 in osteoblastic cells. Collagen is secreted into the extracellular space during the hydroxylation of proline residues of the collagen chains, a reaction catalysed by prolyl hydroxylase, an enzyme involved in the production of collagen. An increase in prolyl hydroxylase activity was observed when Si was added into the diets of Si-deficient animals, therefore it has been suggested that Si may affect the rate of synthesis of collagen. The up-regulation of collagen is further induced by the presence of ascorbic acid which at the same time induces osteocalcin. Since collagen and osteocalcin expression were up-regulated in the presence of ascorbic acid, it is possible that Si ions play an integral role in intracellular and extracellular pathways in osteogenesis (Varanasi et al. 2011)

The direct interaction between silicic acid and collagen type 1 was investigated, when a significant up-regulation of collagen was seen in the presence of orthosilicic acid. The mechanism of collagen self-assembly is entropy driven (Kadler et al. 2008) whereby, there is a loss of solvent molecules from the surface of the collagen molecule (Kadler et al. 1996) leading to fibril formation. The presence of low concentrations of orthosilicic acid speeded the fibril formation process; however concentrations higher than 100µg/ml inhibited collagen self-assembly (Figure 3.25). It has been suggested that orthosilicic acid interacts through hydrogen bonding between the specific sites on the protein helices. On the other hand, concentrated orthosilicic acid, is mainly constituted of negatively charged poly-silicic acids and these interfere with the triple helices assembly via electrostatic interactions (Coradin et al. 2006). A change in morphology of collagen fibres in the presence of OSA was observed. The collagen fibres were thicker and a more intricate network of fibres was formed when OSA was added (Figure 3.25). It has been suggested that orthosilicic acid may induce a conformation change in collagen maybe by modifying its hydration state through changes in

hydrogen bonding between helices and localised water molecules; this slows the process down and allows for better packing of the triple helices within the fibres, hence showing a compact fibril network. Silicon is also known to cross-link between collagen proteoglycans, therefore resulting in the stabilisation of bone matrix molecules and preventing their enzymatic degradation (Reffitt et al. 2003).

3.5 Conclusion

The effect of orthosilicic acid was investigated on osteoblast response *in vitro*. The optimum concentration of OSA was determined for cell survival and differentiation. The presence of orthosilicic acid in osteoblast like cells, led to the early formation of calcium and phosphate nodules, indicating OSA plays a key role in early mineralisation of osteoblast cells. It is important to note, however, non-quantifiable silicon was present within the mineral composition of the cells.

RT-PCR analysis showed that OSA induces differentiation in rat bone marrow cells by up-regulating early osteogenic markers. A significant effect on collagen type 1 expression was noted when cells were treated with orthosilicic acid and further investigations were carried out to determine the direct interactions between collagen and silicon.

Collagen fibril formation was altered with the addition of OSA, which formed a compact collagen network, illustrating that, the presence of silicon is essential for early bone formation and for continuous bone remodelling and healing.

By determining the optimum concentration for cell survival, will allow for the development of silicon-containing biomaterials, which will have a more tailored release of $Si(OH)_4$ and therefore creating an ideal environment, for cell survival and differentiation and ultimately bone formation.

4. Comparing the release of orthosilicic acid from silicate containing biomaterials

4.1 Introduction

In recent years there has been a great interest in the influence of silicon on the formation of biological minerals (Perry & Keeling-Tucker 1998). In the previous chapter it has been shown that the soluble form of silicon, orthosilicic acid [$Si(OH)_4$], has a positive impact on bone mineralisation. Silicon in its various forms such as silicate (SiO_4^{4-}), silica, porous silicon and orthosilicic acid has been incorporated into biomaterials, for example hydroxyapatite (Patel et al. 2002), Bioglass® (Xynos et al. 2000), and calcium phosphate cements (Guo et al. 2007). These silicon containing biomaterials have shown to enhance the attachment and proliferation of osteoblast-like cells (Heinemann et al. 2011; Bosetti et al. 2003; Ni et al. 2008) There has been little systematic investigation, however to determine whether it is the silicon causing these positive biological effects from the biomaterial or other materials present within the silicon based biomaterial, for example, the release of calcium ions from silicon-substituted calcium phosphates. In this chapter, the therapeutic delivery of silicon in the form of orthosilicic acid was evaluated, when it is incorporated into PLGA microspheres.

4.1.1 Choice of material

Microspheres have received considerable attention due to their potential importance in the area of microencapsulation (Wang et al. 2009). Biodegradable synthetic and natural polymers have been used in the fields of orthopaedics (Gunatillake & Adhikari 2003), controlled delivery systems (Jain 2000) and reconstructive surgery (Mano et al. 2007). To date, however, time and site of the delivery of silicon is still one of the prominent challenges in regenerative medicine. Controlled silicon delivery, via silicon based biomaterials, can effectively enhance bone mineralisation by reducing the release of high concentrations of silicon at a given time, which may cause toxicity within the target site (Shi et al. 2009). Time-controlled delivery can be achieved by embedding or encapsulating orthosilicic acid within the polymeric matrix, therefore allowing the release of OSA in a manner tailored to a particular application.

4.1.1.1 Synthetic Polymer - Poly lactic-*co*-glycolic acid (PLGA)

Poly lactic-co-glycolic acid (PLGA) has shown potential as a drug delivery vehicle as well as a scaffold in tissue engineering (Wischke & Schwendeman 2008). PLGA is a FDA (Food and Drug Administration) approved polymer, and it has been widely used as a delivery vehicle for drugs (Yunos et al. 2008), proteins (McGinity & O'Donnell 1997) and cells (Chun et al. 2004). It is often favoured over other biodegradable polymers due to its established uses, favourable degradation characteristics as well as possibilities for sustained drug delivery. It can be also implanted or injected in the site of interest without the need for major surgical procedures (Xue et al 2004).

PLGA is a co-polymer of poly-lactic acid and poly-glycolic acid, during polymerisation these monomers are linked together via ester bonds, yielding a linear aliphatic polyester (Figure 4.1) (Makadia & Siegel 2011). Many forms of PLGA can be formed with various lactide and glycolide ratios, leading to an amorphous material (Gabler et al. 2007).

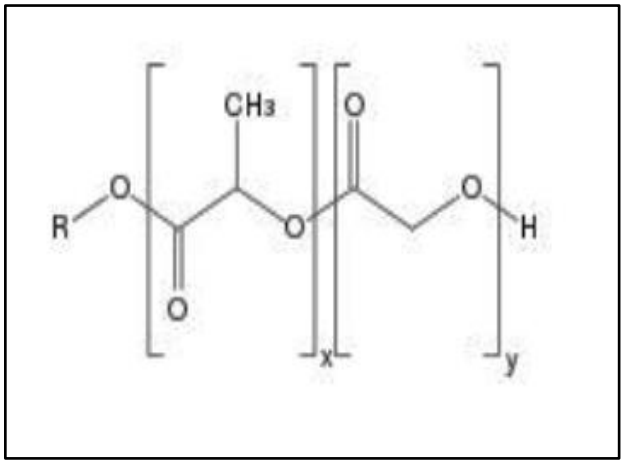

Figure 4.1: Structure of PLGA, whereby X is the number of lactic acid units and Y is the number of glycolic acid units (Makadia & Siegel 2011)

PLGA degrades by the hydrolysis of its ester bonds in the presence of water. It's toxicologically safe by-products; glycolic acid and lactic acid, are broken down to CO_2 and water by the normal metabolic pathways in the body (Figure 4.2), thus making it suitable for use *in vivo* (Zolnik & Burgess 2007).

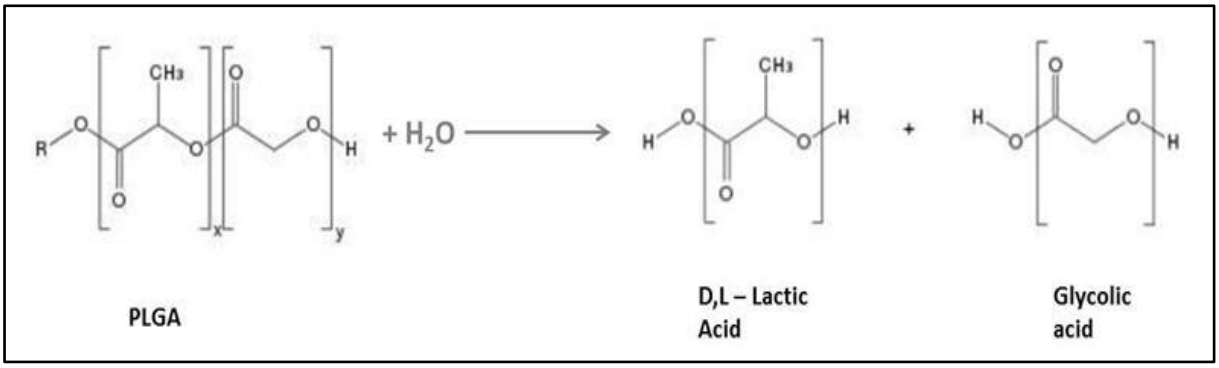

Figure 4.2: Hydrolysis of PLGA in the presence of water, yields lactic acid and glycolic acid monomers (Makadia & Siegel 2011).

4.1.1.2 Calcium silicate cements

The bioactivity of silicon was first discovered in Bioglass® (Xynos et al. 2000) which has been incorporated into various calcium based cements such as β-dicalcium silicate which is the most reactive constituent in Portland cements (Guo et al. 2007). Silicate cements are mouldable and have been assessed as drug delivery devices. β-dicalcium silicate, for example, has many advantageous characteristic when compared to other inorganic cements, such as, reduced setting time *in vitro* and *in vivo* and increased mechanical properties close to that of cortical bone (Wang et al. 2006). Recent studies have shown the β-dicalcium silicate may be used as a potential candidate for hard tissue repair, as the release of silicon and calcium from the material have shown to enhance osteogenesis. Both the calcium and silicon ions are important to nucleation and growth of apatite and influence the biological metabolism of osteoblastic cells, leading to mineralisation and bone-bonding (Su et al. 2010).

In this chapter β-dicalcium silicate was used as an alternative source to sodium metasilicate forming a biocomposite with the biodegradable polymer, PLGA. The combining of bioactive cements and polymers, has been of great interest in recent years as these biocomposites appear to be more beneficial than conventional ceramics or polymer biomaterials alone.

Here we have compared the release of OSA from PLGA spheres using a soluble form of OSA, sodium metasilicate and a sparingly soluble source, β-dicalcium silicate. The encapsulation efficiency of orthosilicic acid into these delivery mechanisms was determined and the morphology and size distribution was also evaluated. Furthermore MC-3T3 cell attachment and proliferation in the presence of calcium silicate cements was examined. The overall aim of this work was to exert some control over the release rate and enable controlled delivery of OSA from these delivery systems.

4.2 Materials and methods

4.2.1 Synthesis of PLGA microspheres

All chemicals and reagents were purchased from Sigma-Aldrich (Gillingham, UK), unless stated otherwise. 2% (w/w) poly(lactic-co-glycolic acid) (PLGA) 50:50 with acid end groups (Lakeshore Biomaterials, Germany) was prepared by dissolving the polymer in dichloromethane (DCM) for 4h at room temperature. 0.5% w/v Poly-vinyl alcohol (PVA) solution was prepared in distilled water and stirred for 3h at 200^{o}C on a hot plate magnetic stirrer (Bibby-B212, UK). The sources of orthosilicic acid were either sodium metasilicate nanohydrate ($Na_2SiO_3.9H_2O$) to form a water/oil/water (w/o/w) emulsion or calcium silicate for a solid/oil/water (s/o/w) emulsion.

4.2.2 Synthesis of β-dicalcium silicate

The Pechini technique was used for the preparation of calcium silicate powder (Tan et al. 2010). Whereby, a 2:1 ratio of calcium nitrate tetra-hydrate and colloidal silica were dispersed in distilled water separately. 2M citric acid ($C_2H_6O_7.H_2O$) prepared in distilled water was then added to the solution. The solution was stirred until clear and 4M ethylene glycol (C_6H_6O) was added to the solution. The mixing solution was placed on a hot-plate stirrer (Heidolph, Germany) at 90˚C, overnight, in a fume cupboard to evaporate the excess solvent. The resultant white cloudy residue was dried overnight in a furnace (Carbolite-CWF 1300, UK) at 150˚C. The dried residue was ground to a fine powder and calcined at 800˚C for 3h.

4.2.3 Characterisation of β-dicalcium silicate using XRF and XRD

The calcined powder was characterised by X-ray diffraction (XRD; Bruker, UK) and X-ray fluorescence (XRF; Bruker, UK) to determine the phase purity of β-dicalcium silicate and elemental composition of the powder respectively.

4.2.4 Solvent evaporation method

In the solvent evaporation method, the polymer is dissolved in suitable water immiscible solvents such as dichloromethane and water soluble 'drugs'. In this case the silicon source is dissolved in the polymeric solution, the resultant solution is then emulsified in an aqueous phase for example PVA to form droplets. For microspheres to form the organic solvent, DCM diffuses into the aqueous solvent and evaporates at the water/air interface.

4.2.4.1 Microsphere production using the w/o/w emulsion technique

Sodium metasilicate (134mg/ml) as a source of orthosilicic acid, was encapsulated into PLGA microspheres using the $w_1/o/w_2$ technique illustrated in Figure 4.3a, whereby a 4:1 polymer: sodium metasilicate solution ($w_1/o_)$ was homogenised (IKA®, Germany) for 25s at 24,000rpm and added into 200ml of 0.5% v/v PVA solution ($w_{2)}$ and stirred continuously at 700rpm for 3h. After complete evaporation of the solvent (DCM) the microspheres were vacuum filtered using a 0.2µM filter paper (Millipore, UK), washed three times with distilled water, to ensure any excess DCM was removed, and left to dry at room temperature overnight (Figure 4.3b).

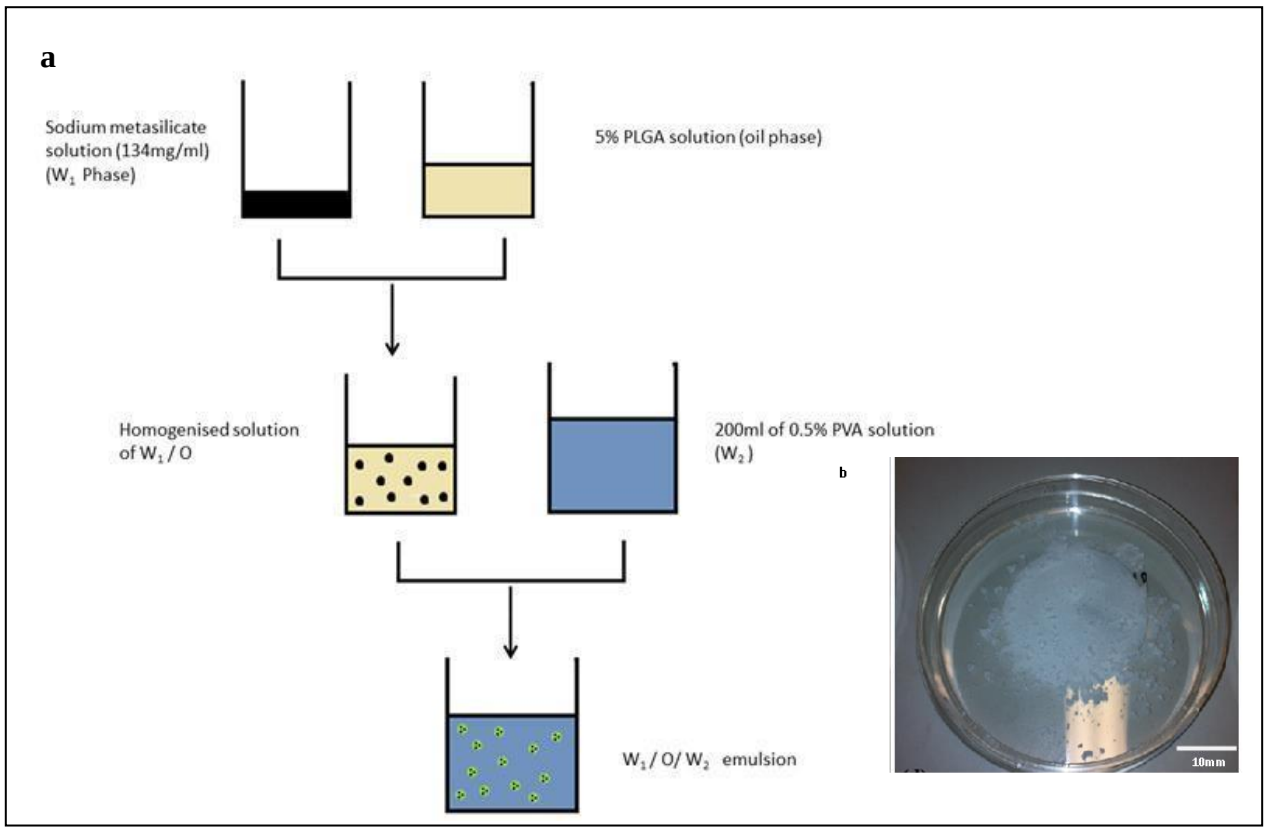

Figure 4.3: Schematic diagram illustrating microsphere production (a) and image of microspheres after production (b)

4.2.4.2 Microsphere production using the s/o/w emulsion technique

Various amounts of β-dicalcium silicate powder (Table 4.1) were encapsulated into PLGA microspheres using the solid/oil/water (s/o/w) emulsion technique. A similar technique was used as described in Section 4.2.4.1.; however the sodium metasilicate was replaced with calcium silicate, hence encapsulation of a solid into the oil phase.

Table 4.1: Masses of polymer and $CaSiO_3$ used in the fabrication of micro-particles

Sample	Amount of polymer (PLGA+DCM) (g)	Amount of $CaSiO_3$ (mg)
A	4.9	100
B	4.8	200
C	4.95	50
D	4.98	20
E	4.99	10

4.2.5 Characterisation of microspheres

4.2.5.1 Determining the morphology of the microspheres

The external morphology of the microspheres was examined using a scanning electron microscope (SEM), whereby the microspheres were mounted onto a stub and coated with gold (EMSCOPE, UK) and viewed using the SEM (Jeol 6060LV, Japan).

4.2.5.2 Laser diffraction particle size distribution

The particle size was determined using a Mastersizer2000 (Malvern, UK). The measurements were carried out in distilled water, which acted as the background solvent. The samples were measured 10 times and the average particle size distribution was determined.

4.2.6 Determining the concentration of OSA – Molybdenum blue method

For the determination of OSA, the silicomolybdate method showed to be the most suitable as it measured the monomeric form of silicon, that is, orthosilicic acid rather than elemental Si. The reaction of molybdic acid with $Si(OH)_4$ produced a yellow complex, it is often used when the concentration of OSA is higher than 1 part per million (ppm).. The reaction of molybdic assay in the presence of OSA is shown in equation 4-1.

$$7Si(OH)_4 + 12H_6Mo_7O_{24}.4H_2O + 126H_2O = 7H_8Si(Mo_2O^{7+})_6.28H_2O$$

Equation 4-1

Orthosilicic acid depolymerises slowly and reacts with molybdic acid leading to the formation of silicomolybdate thus producing a yellow complex. When the concentration of OSA is only a few ppm the absorbance detected by the yellow complex is often insufficient, therefore for accurate measurement, the yellow complex is reduced to molybdenum blue using a reducing agent, 1-amino-2-naphtol-4-sulphonic acid which increases the sensitivity of analysing OSA (Iler 1955).

The reagents required for the colourimetric assay include; 1N hydrochloric acid (HCl) (Fisher Scientific, UK). 100mg/ml ammonium molybdate (Sigma-Aldrich, UK), was prepared in distilled water and the pH was adjusted between 7 and 8 with 2M NaOH (Fisher Scientific, UK). 100mg/ml of oxalic acid (Fisher Scientific, UK) was prepared in distilled water. The reducing agent was prepared by dissolving 500mg of 1-amino-2-naphthol-4-sulfonic acid (Sigma-Aldrich, UK), and 1g of sodium sulphate (Sigma-Aldrich, UK) in 500ml of distilled water. A second solution made up of 30g of sodium bisulfite (Sigma-Aldrich, UK) was

dissolved in 150ml of distilled water and the two solutions were mixed, filtered and refrigerated to avoid exposure to light.

Ammonium molybdate reacts with hydrochloric acid to form molybdic acid and ammonium chloride (Equation 4-2):

$$(NH_4)_6Mo_7O_{24}.4H_2O + 6HCl \rightarrow H_6Mo_7O_{24}.4H_2O + 6NH_4Cl$$

Equation 4-2

Molybdic acid also reacts with phosphates yielding phosphomolybdic acid and this can interfere in the determination of orthosilicic acid. Oxalic acid was added to remove any phosphates if present.

The concentration of the OSA was determined using the molybdenum blue colourimetric assay which includes 60µl of 1M hydrochloric acid (HCl), 120µl of ammonium molybdate reagent, 90µl of oxalic acid and 120µl of the reducing agent 1-amino-2-napthol-4-suphonic acid (Kortesuo et al. 2000). The absorbance of the solution was determined at 650nm using a UV spectrophotometer (Cecil Instruments, UK).

4.2.7 Determining the encapsulation efficiency of OSA in the microspheres

The amount of OSA entrapped within the polymeric matrix was determined by dissolving the PLGA microspheres in DCM and distilled water. The mixture was vortexed and left at room temperature for 1h. The aqueous phase (water phase), containing the hydrophilic silicon, was collected and the concentration of orthosilicic acid was determined using the colourimetric method previously described (4.2.6). The encapsulation efficiency (EE) was calculated as the ratio of total amount of orthosilicic acid entrapped in the microspheres to total amount of orthosilicic acid used in production (Equation 4-3).

EE (%) = (Mass of OSA determined) / (Mass of OSA added) x 100

Equation 4-3

4.2.8 Determining the release of OSA

To determine the release of OSA from the PLGA microspheres and composites, a known mass of microspheres was suspended in 100ml of dissolution medium, in this case distilled water, which was placed in a shaker (Gallenkamp, UK) at 150rpm at 37^{o}C. 3ml of distilled water was taken from the flask at specified time intervals and passed through a 0.22µM filter. To maintain a constant volume of the dissolution medium, 3ml of fresh distilled water was replaced after each measurement. The concentration of OSA was determined using the molybdenum blue colourimetric assay.

4.2.9 Determining the response of MC-3T3-E1 cells to calcium silicate composites

The attachment and proliferation of MC-3T3 cells on the calcium silicate composites was determined over 7 days using a blue fluorescent 4'6-diamidino-2-phenylindole (DAPI) nucleic stain (Invitrogen, UK). MC-3T3-E1 cells were seeded onto the surface of the composites as described in section 3.2.2. A 5mg/ml DAPI stock solution was prepared according to the manufacturer's instructions (Invitrogen, UK). For the staining of cells, the DAPI stock solution was diluted to a concentration of 300nM in PBS. The samples were rinsed 3 times in PBS and 2ml of DAPI/PBS stain was added onto the sample and left for 3 minutes in the dark. The excess stain was removed after 3 minutes and the samples rinsed in PBS. The samples were mounted onto a slide and a drop of ProLong Gold antifade (Invitrogen, UK) reagent was added and the sample covered with a cover slip. The stained samples were observed using a confocal microscope (Leica, UK).

4.3 Results

4.3.1 Incorporation of sodium metasilicate into PLGA microspheres

In this section the results regarding the release of OSA from microspheres encapsulated with sodium metasilicate are described.

4.3.1.1 Synthesis of micro-particles and encapsulation efficiencies

A saturated solution of sodium metasilicate at a concentration of 134 mg/ml was used as the initial source of OSA. This concentration was used as it was necessary to encapsulate a high concentration of OSA into the PLGA microspheres.

Various formulations of microspheres were made in order to entrap the maximum amount of OSA possible into the PLGA microspheres. This was achieved by changing the experimental conditions to increase the encapsulation of OSA without compromising the size and morphology of the particles. The encapsulation efficiencies are listed in Table 4.2 in accordance with change in formulation of the PLGA microsphere.

To begin with no change to the sodium metasilicate (134mg/ml) and PVA solutions was made, the pH was left at 13.42 for the sodium metasilicate and pH 7 for the PVA solution, however when the microspheres were dissolved in DCM and the encapsulation efficiency calculated, no OSA was detected within the PLGA microspheres.

A 0.09% encapsulation efficiency was calculated when the pH of sodium metasilicate was changed from pH 13.42 to pH 7 (Experiment 2). Sodium metasilicate is a salt formed by the alkali metal Na^+ and the silicate SiO_3^{2-}. This silicate is soluble in water and is hydrolysed in aqueous yielding orthosilicic acid as shown in equation 4-4 (Iler, 1979).

$$SiO_3^{2-} + 3H_2O \rightarrow Si(OH)_4 + 2OH^-$$

Equation 4-4

The pH of sodium metasilicate was therefore adjusted to pH 7 so as to achieve maximum encapsulation within the polymeric matrix. Mostly, basic solutions such as sodium metasilicate are more soluble in acid and neutral conditions and tend to diffuse into the PVA solution (pH 6.78) from the PLGA microspheres leading to low encapsulation efficiencies within the microspheres. By decreasing the pH of the sodium metasilicate salt close to neutral with hydrochloric acid (HCl), the sodium metasilicate did not diffuse into the larger water phase (Experiment 2).

Table 4.2: The various formulations used to increase encapsulation efficiency of OSA

Experiment	pH of sodium metasilicate solution	Continuous phase (large W_2 Phase)	EE (%)
1	13.42	PVA 0.5%	0
2	7	PVA 0.5%	0.09
3	7	PVA 0.5% saturated with sodium metasilicate	No microspheres
4	7	PVA 0.5% saturated with colloidal silica pH 6	0.52
5	13.42	PVA 0.5% saturated with colloidal silica pH 6	1.19

The addition of HCl into sodium metasilicate produced a silica gel, which was encapsulated into the PLGA microspheres. The reaction between sodium metasilicate and HCl can be represented as (Equation 4-5) (Ruiz-Hitzki et al., 2008);

$$NaSiO_3 + 2HCl + H_2O \rightarrow Si(OH)_4 + 2NaCl$$

Equation 4-5

0.09% is a relatively low encapsulation of sodium metasilicate into PLGA microspheres. This could be due to the silicate salt diffusing quickly from a high concentration in the polymer solution to a lower concentration in the large water phase (PVA), before the microspheres are fully formed. To reduce this diffusion rate of the metasilicate from the PLGA solution the large PVA solution was saturated with sodium metasilicate (experiment 3). The addition of sodium metasilicate to the PVA solution changed its pH from 6.78 to 13.57, and as a result no microspheres were produced. It has previously been suggested the PLGA degrades in high acid and basic condition (Zolnik & Burgess 2007).

To maintain the same pH of the PVA but saturate the large water phase with silicon, by means of reducing diffusion of OSA from the PLGA solution, the source of orthosilicic acid was replaced with colloidal silica and the pH was adjusted with sulphuric acid 5% v/v (H_2SO_4) to pH 6. The encapsulation efficiency further increased to 0.52% (Experiment 4). Indicating that by saturating the larger water phase reduces the diffusion of sodium metasilicate into the PVA solution, therefore being encapsulated into the PLGA microspheres. By maintaining the pH of sodium metasilicate at 13.42 and forming the PVA and colloidal silica dispersion, the encapsulation efficiency increased to 1.2% (Experiment 5).

As a result, formulations from experiments 4 and 5 were carried out and were compared here on. Although it can be argued that these encapsulation are low, the actual concentration of OSA measured from the microspheres were, 5µg/ml from the microspheres with sodium metasilicate at pH 7 and 12.77µg/ml from microspheres containing sodium metasilicate at pH 13.42. These concentrations are ideal for cell viability as described in the previous chapter. Indeed, at high concentration, OSA can lead to cell apoptosis (Shie et al. 2011). It is therefore important that the concentration of orthosilicic acid released from the microspheres is of a therapeutic concentration leading to a positive biological effect.

4.3.1.2 Morphology and size

Scanning electron microscopy (SEM) images showed the morphology and micro-structure of the PLGA microspheres produced with the different pH of sodium metasilicate.

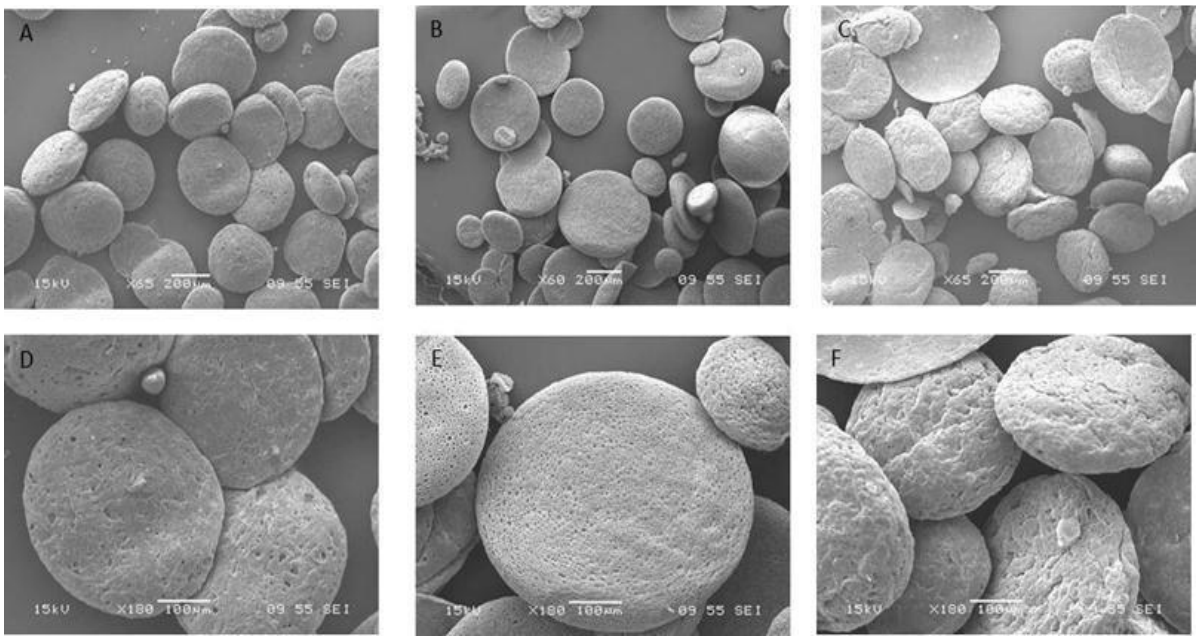

Figure 4.4: SEM images of PLGA microspheres produced without sodium metasilicate (A and D), with sodium metasilicate at pH 7 (B and E) and sodium metasilicate at pH 13 (C and F)

As shown in Figure 4.4, the microspheres produced with sodium metasilicate at pH 7 were larger in size and looked to be more porous than the microspheres produced with sodium metasilicate at pH 13.42, which showed to have a more close knit structure similar to that of the control. The particles were of disc shape morphology, rather than complete spheres. This could be attributed to the stirring speed while forming the microspheres. It has previously been suggested that the stirring speed determines the size and shape of the microspheres (Song et al. 2006).

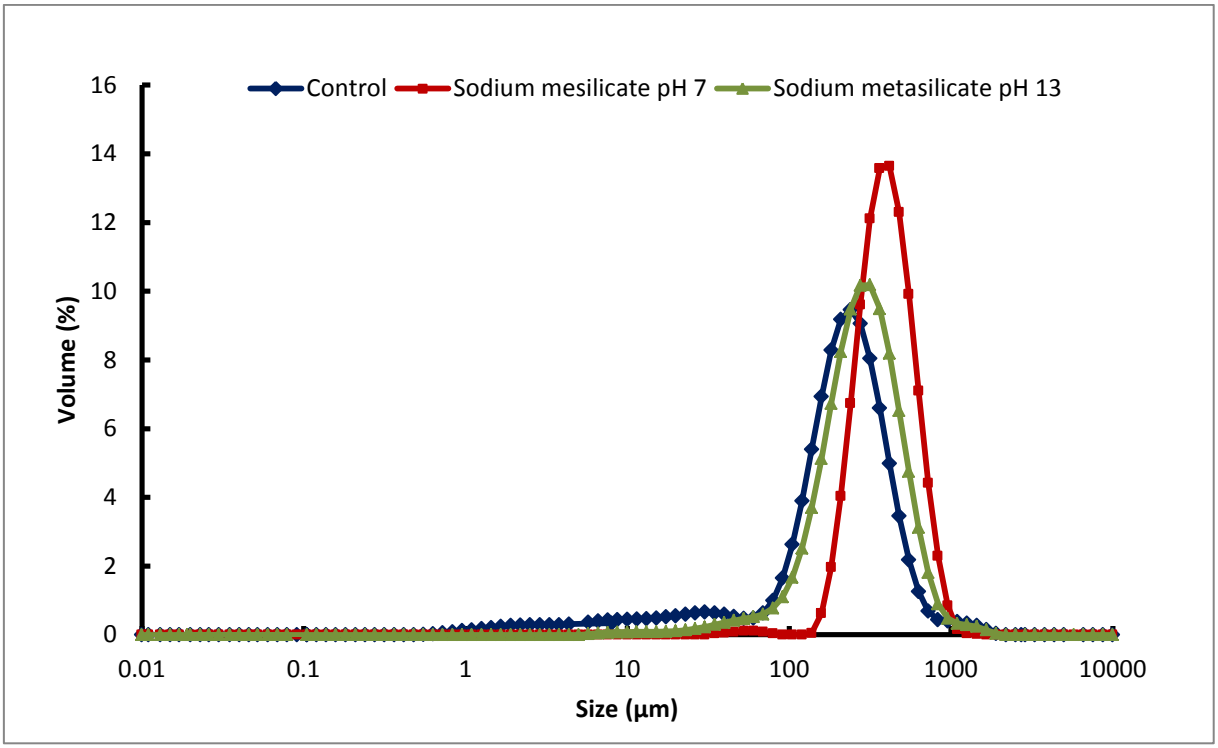

Figure 4.5: Particle size distribution curves for PLGA microspheres without sodium metasilicate, with sodium metasilicate and pH 7 and pH 13.

The particle size distribution is displayed as a Gaussian function which defines the normal distribution of a certain population. In this case the median diameter for each formulation was determined: indicating that half the microspheres lie below 50% (D_{50}). Similarly 90% of the microspheres lie below the D_{90} and 10% lie below the D_{10} (Figure 4.5).

Table 4.3: The D_{10}, D_{50} and D_{90} values of PLGA micro-particles, from which the particle size distribution span is calculated.

	D_{10}	D_{50}	D_{90}	Span (D_{90}-D_{10}/D_{50})
Control	35µm	232µm	472µm	1.88
pH 6.87	255µm	420µm	689µm	1.03
pH 13.4	137µm	301µm	580µm	1.47

The D_{50} (50%) for the microspheres formed with sodium metasilicate at pH 7 was 420µm and 302 µm for pH 13.42. These results were in accordance with the observations from the SEM images (Figure 4.4). The microspheres containing no sodium metasilicate were smaller in size when compared to the microspheres produced with sodium metasilicate. There was no significant difference, however, in the particle size distribution when microspheres were produced with varying pH of sodium metasilicate (Table 4.3), these results are in accordance with the observations from the SEM images. Indicating that sodium metasilicate at pH 7 and pH 13 does not change the size of the microspheres; instead the changes in pH alter the surface topography of the microspheres, seen in Figure 4.4.

4.3.1.3 *In vitro* release of sodium metasilicate from PLGA microspheres

In vitro release studies were carried out to determine the release of sodium metasilicate, in the form of orthosilicic acid from the PLGA microspheres. It is important to tailor the release of orthosilicic acid from silicon containing biomaterials in order to have a positive biological effect in bone repair, rather than a toxic effect. The amount of OSA encapsulated into the PLGA microspheres was determined by dissolving them in DCM and measuring the OSA released from the polymeric matrix. Release of OSA was determined over time and the concentration determined using the colourimetric assay is described in section 4.2.6. The results are summarised in Table 4.4

Table 4.4: Actual amount of OSA entrapped in microspheres, concentration of OSA from microspheres after 600H and cumulative % release determined.

	Sodium metasilicate at pH 13	Sodium metasilicate at pH 7
Actual concentration of OSA entrapped in microspheres (µg/ml)	12.78	6.95
Concentration of OSA released after 600h (µg/ml)	9.82	6.75
% release of OSA after 600h (%)	77	97

The release of OSA from PLGA microspheres prepared with sodium metasilicate at pH 13 and pH 7 was determined. The actual amount of OSA determined after dissolving the PLGA microspheres was 12.78µg/ml, when prepared with sodium metasilicate at pH 13. The release

of OSA from the microspheres after 600h was 9.82µg/ml, that is, approximately 77% of the OSA was therefore released from the microspheres after 600h (Table 4.4).

Microspheres prepared with sodium metasilicate at pH 7 had a lower encapsulation efficiency compared with microspheres prepared with sodium metasilicate at pH 13. The actual concentration of sodium metasilicate entrapped within the microspheres was 6.95µg/ml. After 600h, approximately 97% of OSA was released from within the PLGA microspheres (Table 4.4).

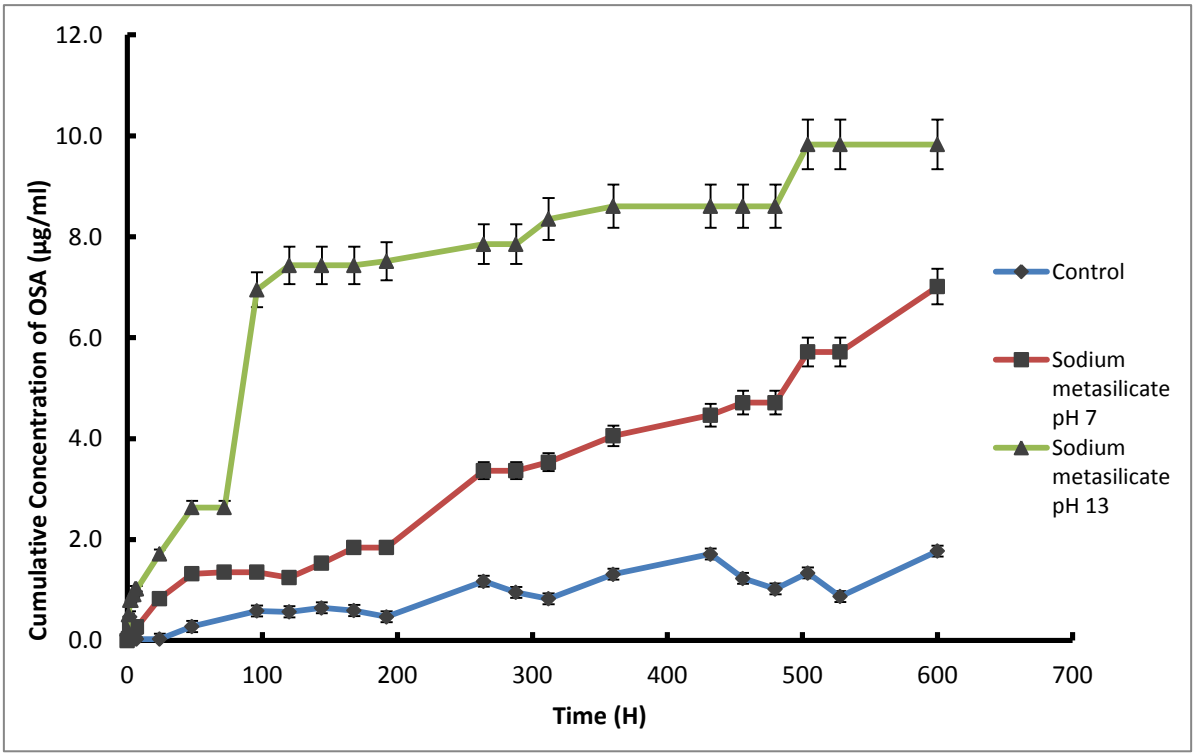

Figure 4.6: Release of orthosilicic acid (µg/ml) from PLGA microspheres loaded with sodium metasilicate at pH 7 and 13. Each point represents the average of 3 tests. Error bars indicate the standard deviation of the mean.

Dissolution studies were carried out to observe the release of orthosilicic acid, *in vitro*. The release was carried out over a period of 25 days and the cumulative concentration was determined (Figure 4.6).

The release of orthosilicic acid from microspheres prepared with sodium metasilicate pH 7 and pH 13 showed similar release profiles, which can be divided into a biphasic release, whereby initially a rapid release, was observed during the first 50h of the study. This initial burst of release can be attributed to the presence of sodium metasilicate either on the surface of the microspheres, or near the exterior surface of the polymer. The release of OSA from the PLGA matrix is released as a function of solubility as well as the penetration of water into the polymeric matrix. The second phase after 50h, demonstrates that OSA is released progressively as the PLGA polymer starts to degrade, as the dissolution medium starts to hydrolyse the polymer into soluble oligomeric and monomeric products. The degradation of the polymer therefore creates a passage for OSA to diffuse out of the polymer and into the dissolution medium. The biphasic release profile in Figure 4.6 shows an initial zero-order release profile, whereby a constant rate of OSA is release independent of the initial OSA concentration in the microspheres (equation 4-6), this was then followed by a progressive release and after 50h a constant amount of OSA was observed.

$$Q_t = Q_o + K_o t$$

Q_o – initial amount of drug

Q_t – cumulative amount of drug released at time t

K_o – zero order release constant

t - time in hours

Equation 4-6

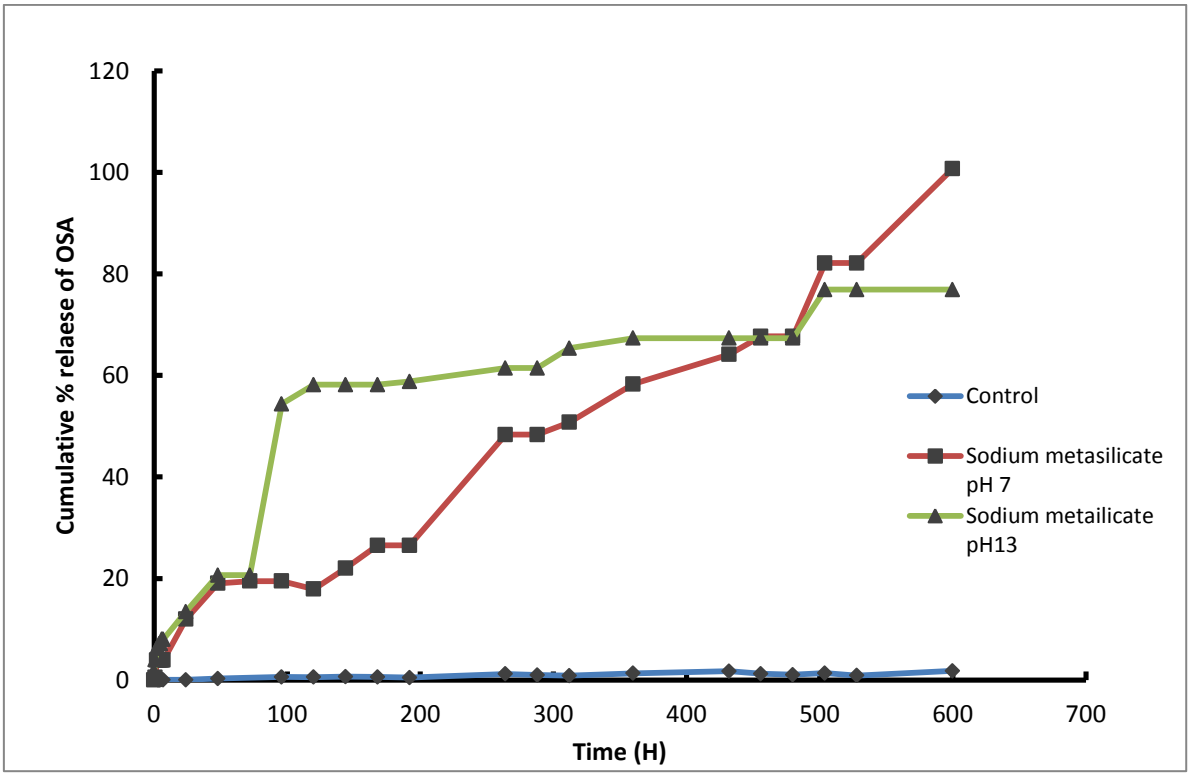

Figure 4.7: Cumulative (%) release of OSA from PLGA microspheres loaded with sodium metasilicate at pH 7 and 13

The cumulative percentage release of OSA was compared from the two types of microspheres formed, that is, with sodium metasilicate at pH 7 and 13 (Figure 4.7). Microspheres prepared with sodium metasilicate at pH 7 released approximately 97% of the OSA, indicating that almost all the OSA entrapped within the microspheres was released after 600h in dissolution media (Figure 4.7). Microspheres prepared with pH 13, however, released approximately 76% of the OSA entrapped during the same time period. This difference in % release can be attributed to the morphology of the microspheres. The microspheres prepared with sodium metasilicate at pH 13, were less porous and had a more intricate network compared to those prepared with sodium metasilicate at pH 7. The decrease in number of pores reduced the diffusion rate of OSA, therefore slowing the release of OSA. It is also known that basic drugs such as sodium metasilicate at pH 13, may react with the terminal carboxyl group of PLGA

creating strong ionic interactions between the polymer and OSA, thus resulting in an incomplete release of OSA. OSA was easily diffused, however, from the micro-particles prepared with pH 7 sodium metasilicate due to an increased number of pores, as well as, a faster rate of erosion of the polymer.

4.3.2 Synthesis of β-dicalcium silicate and PLGA microspheres

Calcium silicate / PLGA (CS/PLGA) composites were fabricated as microspheres, by encapsulating calcium silicate into PLGA using the s/o/w emulsion technique (Section 4.2.4.2.), to further investigate the *in vitro* release of OSA. Initially calcium silicate was characterised using XRF and XRD analysis. The effect of cell survival was observed on the CS only composites before its encapsulation into the polymer PLGA. Various amounts of CS were encapsulated into the PLGA microspheres and the encapsulation efficiency was calculated. Microspheres size and morphology were determined, followed by the release of OSA from the CS/PLGA composites.

4.3.2.1 Characterisation of β-dicalcium silicate

X-ray diffraction patterns of β-dicalcium silicate synthesised using the Pechini method, showed the phase purity of sintered calcium silicate (Figure 4.8), without the production of lime and other unreacted materials. Sharp peaks indicate pure β-dicalcium silicate powder. The results are in accordance with other published data (Tan et al. 2010).

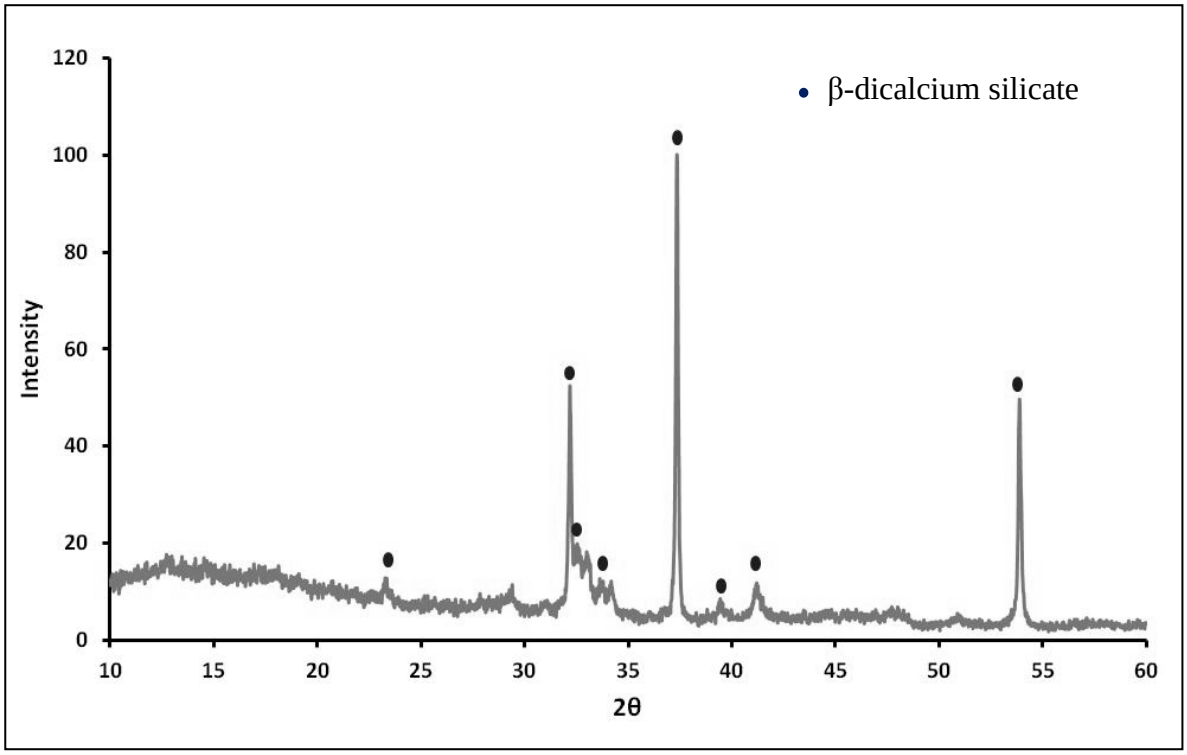

Figure 4.8: XRD pattern of calcium silicate produced by the Pechini method; calcined at 800°C for 3 hours.

Elemental analysis using X-ray fluorescence (XRF) of β-dicalcium silicate showed sharp peaks representing the presence of calcium and silicon in the sintered powder (Figure 4.9). The amount of oxides and elements present in the calcined powder are shown in Table 4.5. The concentration of CaO and SiO_2 are highest accounting to the total of 82.7% and 16.5% respectively.

Table 4.5: XRF analysis of oxides and elements present in β-calcium silicate powder

Chemical composition	CaO	SiO_2	Element	Ca	Si
Concentration (%)	82.72	16.5	Concentration (%)	89.69	9.70

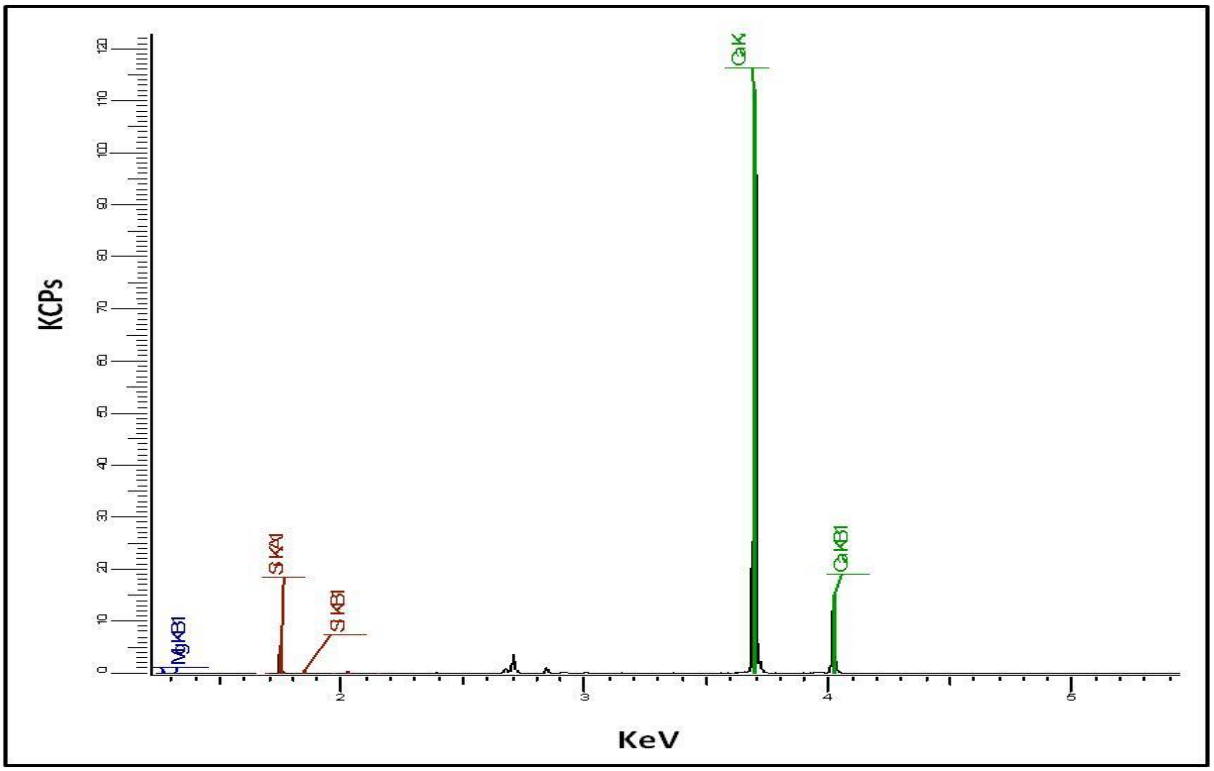

Figure 4.9: X-ray fluorescence (XRF) peaks indicative of elemental calcium and silicon.

4.3.2.2 Response of osteoblasts to CS composites

Calcium silicate composites were made in disc shapes and MC-3T3 cells were seeded onto the samples. The response of these cells was evaluated using DAPI staining, whereby, cell attachment and cell proliferation was determined over a period of 7 days.

It was important to determine the effect of calcium silicate on cell survival before incorporating it into the PLGA polymer. Figure 4.10 illustrates that initially MC-3T3 cells attached onto the surface of the composite at day 1, however cell attachment and proliferation decreased on the surface of the composite, during day 3, 5 and 7.

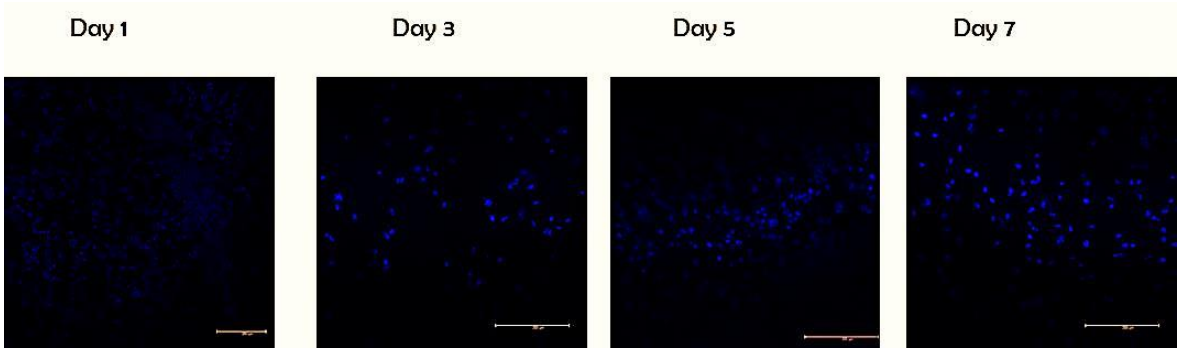

Figure 4.10: Response of MC-3T3 cell attachment and proliferation to calcium silicate cements. Scale bar denotes 200μm

The decrease in cell attachment could be attributed to two factors; an increase in concentration of orthosilicic acid in the growth medium as well as the production of calcium hydroxide when CS become hydrated, leading to either a highly acidic or alkaline environment for the cells to survive. The release of OSA from the calcium silicate composites was determined, shown in Figure 4.11.

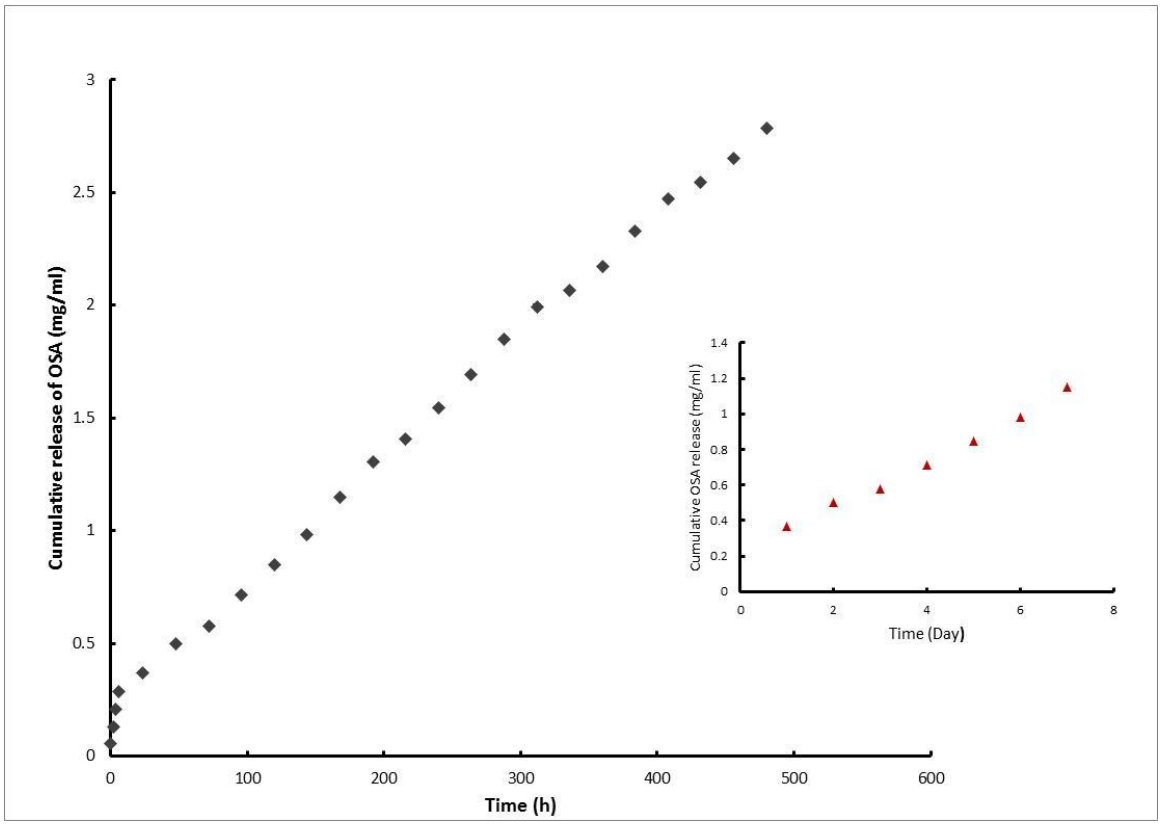

Figure 4.11: Cumulative release of OSA from calcium silicate only composites. Error bars indicative of the standard deviation. Each point represents an average of 3 tests.

The cumulative concentration of OSA released from the calcium silicate composites was approximately 2.9mg/ml after 600h release; the release of orthosilicic acid was of zero order kinetics, whereby the elimination of orthosilicic acid from the calcium silicate composites is independent of concentration of silicon in the composite for the 600h release. Once all the OSA is released from within the composite and the maximum concentration is released the graph should start to plateau. Therefore, this reaction is of zero-order kinetics for only a limited time.

When comparing the release of OSA to osteoblast cell response to the composite, it was illustrated that cell attachment and proliferation decreased over the 7 day period. This was attributed to the high concentration of orthosilicic acid at these time points, that is, the

concentration of orthosilicic acid was approximately 1mg/ml at day 7 (Figure 4.11 (inset graph)). In the previous chapter it has been shown, that high concentrations of orthosilicic acid can have a toxic effect on cells, leading them to apoptose. The high concentrations of orthosilicic acid present in the PLGA/calcium silicate composite prevent cell attachment and proliferation.

Calcium silicate was therefore encapsulated in the PLGA polymer, which acts a diffusion barrier for the release of OSA and hence creating a sustained release of orthosilicic acid at low concentrations.

4.3.2.3 Synthesis and encapsulation efficiency of calcium silicate/PLGA composites

The PLGA/CS microspheres were synthesised using the s/o/w evaporation technique, various amounts of calcium silicate was incorporated into the microspheres to obtain the maximum encapsulation efficiency. It was noted that the morphology of the microspheres depends on the amount of calcium silicate present as it was seen that excess calcium silicate, led to the production of damaged microspheres. Initial stirring speeds and polymer concentration were optimised during particle formation. It was seen that high stirring speeds and high concentrations of polymer, led to the agglomeration of the microspheres.

Agglomerated PLGA/CS microspheres were formed when prepared with 200mg and 100mg of CS, (Figure 4.12, A and B). PLGA/CS microspheres formed with 50mg and 20mg of CS however, produced homogenous microspheres with little presence of excess calcium silicate on the exterior of the microspheres.

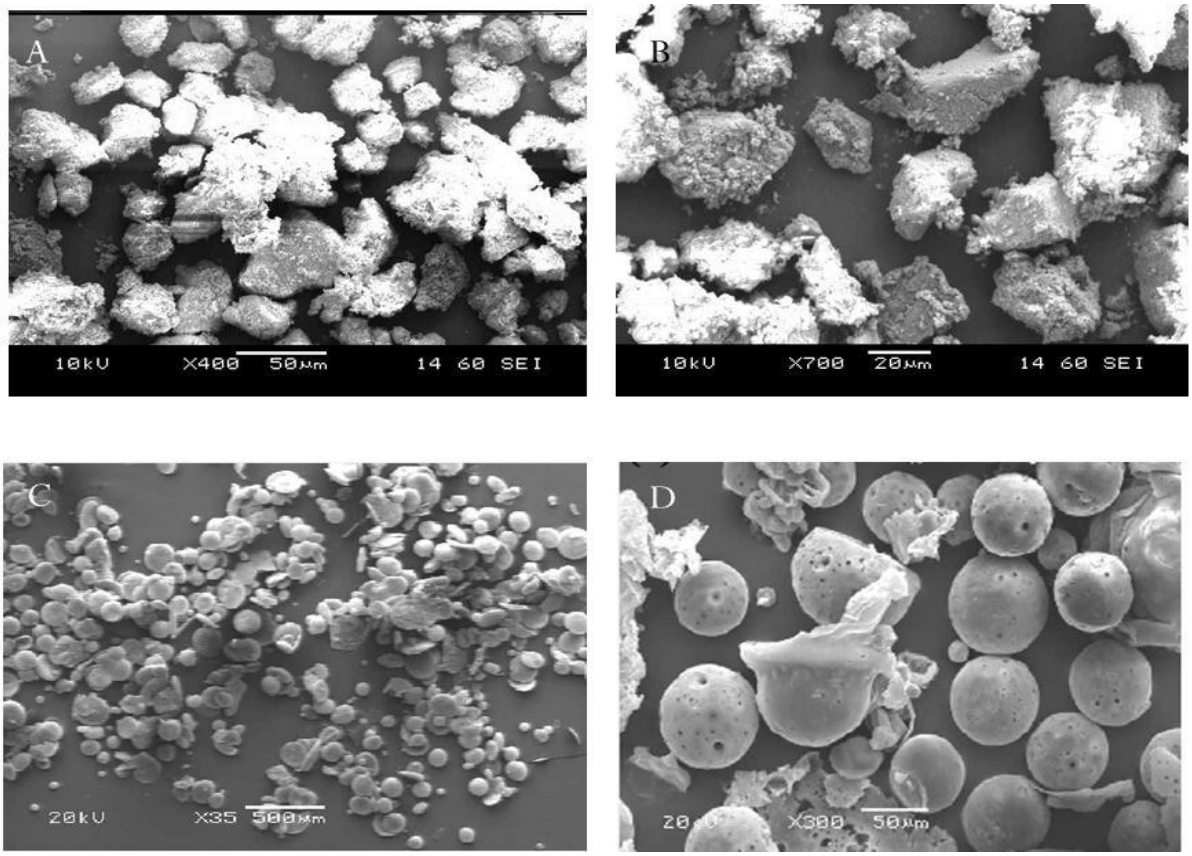

Figure 4.12: SEM images of damaged PLGA/CS microspheres prepared with excess amounts of calcium silicate, A – 200mg of CS, B – 100mg, C-50mg, D- 20mg.

The encapsulation efficiencies were determined with the various amounts of CS added into the polymer, for microspheres production, after washing the microspheres with distilled water, this removed the excess calcium silicate present on the surface of the microspheres. The microspheres were then dissolved in DCM to degrade the polymer and release the calcium silicate into the water phase, the amount of OSA present was measured using the colourimetric assay (Section 4.2.6).

Table 4.6: Encapsulation efficiency of the amount of calcium silicate entrapped within the PLGA microspheres.

Amount of CS (mg)	Encapsulation Efficiency (%)	Mass encapsulated (mg)
200	1.21	2.42
100	2.28	2.28
50	2.34	1.17
20	5.67	1.13
10	6.07	0.607

Microspheres produced with 20 and 10mg of CS showed to have the highest encapsulation efficiency at 5.7% and 6.1% respectively. These microspheres were used here-on to determine the release of OSA from these PLGA/CS composites.

4.3.2.4 Size and morphology of PLGA/CS microspheres

The particle size distribution of the microspheres prepared with 10mg and 20mg of calcium silicate was determined. There was no significant difference in the size of the microspheres prepared with calcium silicate, whereby 50% of the microspheres were 106µm and 104µm for the microspheres prepared with 10mg and 20mg of CS (Table 4.7).

Table 4.7: Size distribution of PLGA/CS composites. D_{10}, D_{50} and D_{90} values of PLGA microspheres from which the particle size distribution span is calculated.

	D_{10}	D_{50}	D_{90}	Span (D_{90}-D_{10}/D_{50})
Control	2µm	169µm	423µm	2.48
10mg CS	51µm	106µm	342µm	2.75
20mg CS	50µm	104µm	331µm	2.69

Microspheres of each sample were measured 10 times and each coloured line represents one measurement, from Figure 4.13 it can be seen that the measurements and methods were reproducible.

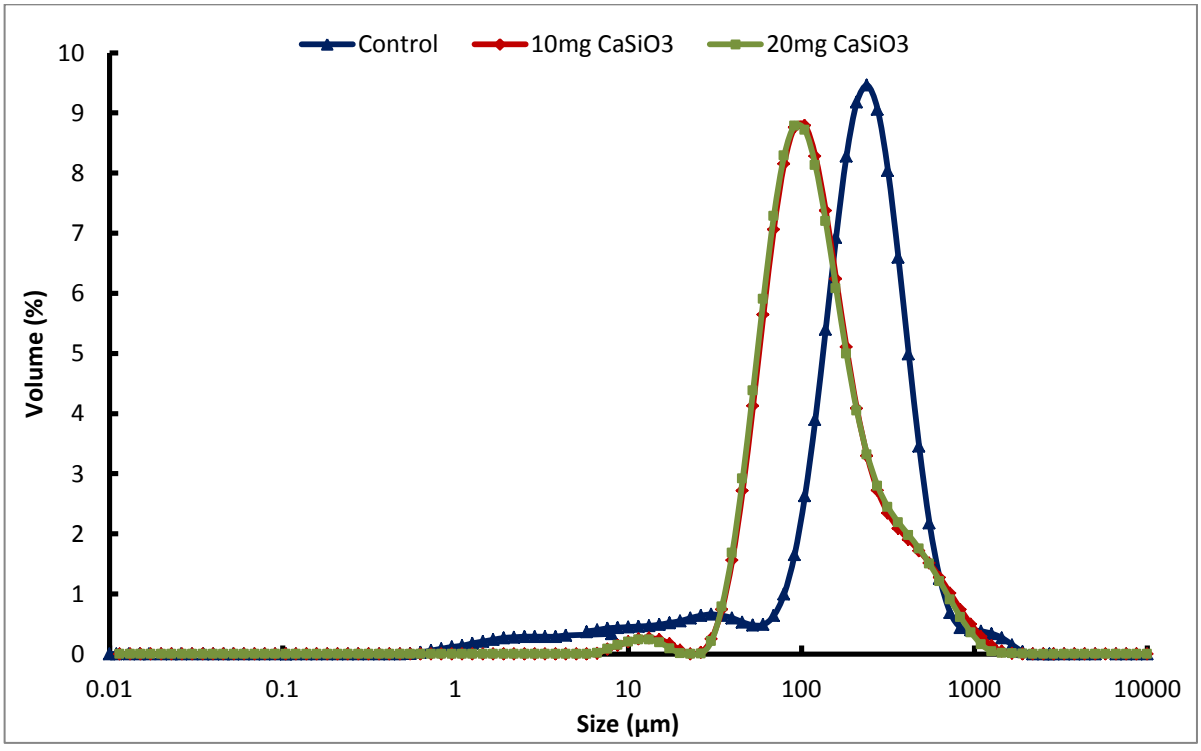

Figure 4.13: Size distribution pattern of microspheres produced with 10mg and 20mg of CS. Each sample was measured 10 times.

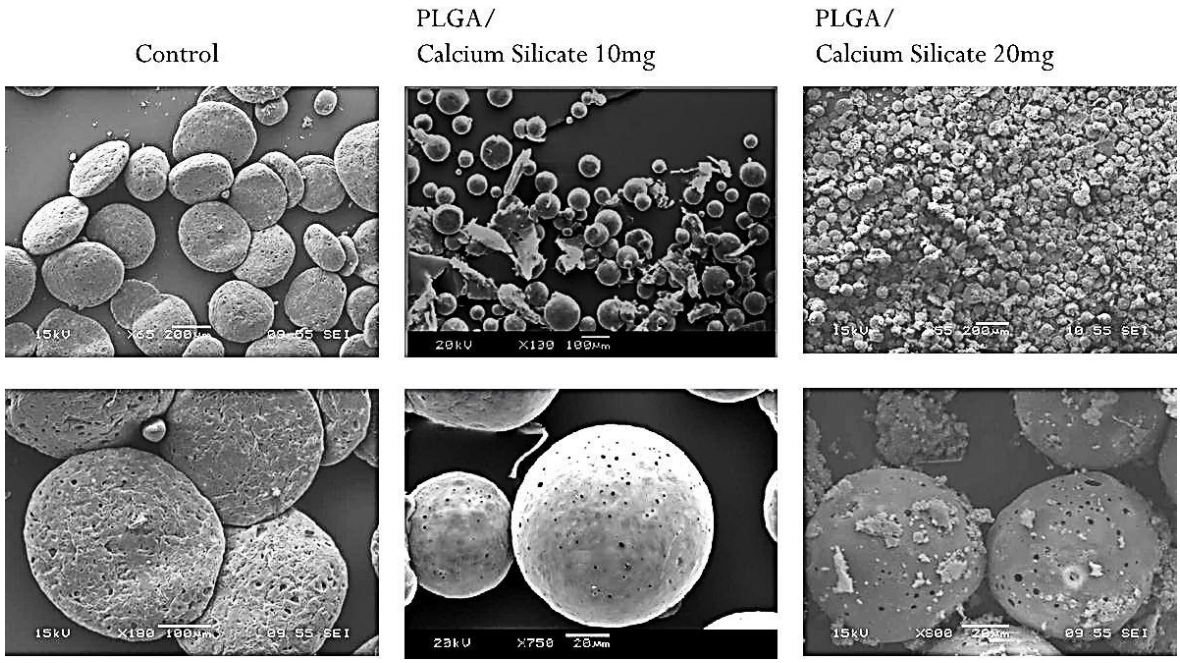

Figure 4.14: SEM images of PLGA/CS composites formulated with various amounts of CS. Excess calcium silicate can be seen on the surface of the microspheres produced with 20mg of calcium silicate.

The morphology of the microspheres was examined using the SEM, the microspheres formulated without CS were more of a disc shape rather than spherical, this could be due to the formation of a vacuum formed inside the SEM equipment (Figure 4.14). Another factor attributing to this morphology could be the speed used when initially forming the microspheres. The microspheres produced with CS, however, showed to be spherical in shape, with some pores present on the surface. Excess calcium silicate was present on the surface of the PLGA/CS microspheres prepared with 20mg calcium silicate, when compared to those prepared with 10mg of calcium silicate.

4.3.2.5 *In vitro* release of OSA from PLGA/calcium silicate microspheres

Dissolution studies were carried out on PLGA/CS microspheres whereby the release of OSA was determined over time.

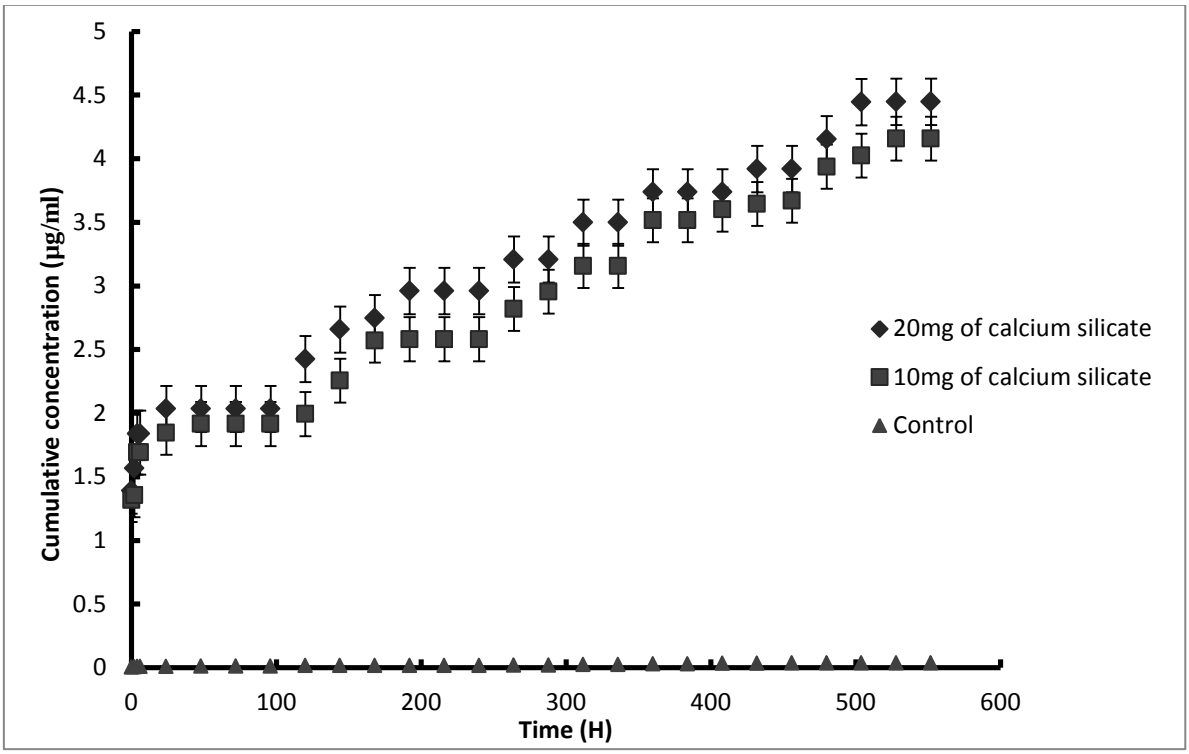

Figure 4.15: Cumulative release of OSA from PLGA/CS composites over time. Each point represents an average of 3 tests. Error bars represent the standard deviation of the mean.

In vitro release of OSA from PLGA/CS microspheres was determined and is shown in Figure 4.15. The release of OSA over the 552h was a linear, first order relationship between the loading and the release of calcium silicate. The initial amount of calcium silicate added into the emulsion for the production of microspheres, had no significant effect on the amount of OSA released at a given time, that is, approximately the same concentration of OSA was released from both the batches at any given time.

The PLGA coating decreased the amount of OSA released from the calcium silicate, when compared to the release of OSA from calcium silicate only (Figure 4.11). The release profile can be divided into stages, whereby the initial release of OSA is from the surface of the particles. The second phase is the diffusion of OSA from within the PLGA microsphere as it degrades over time.

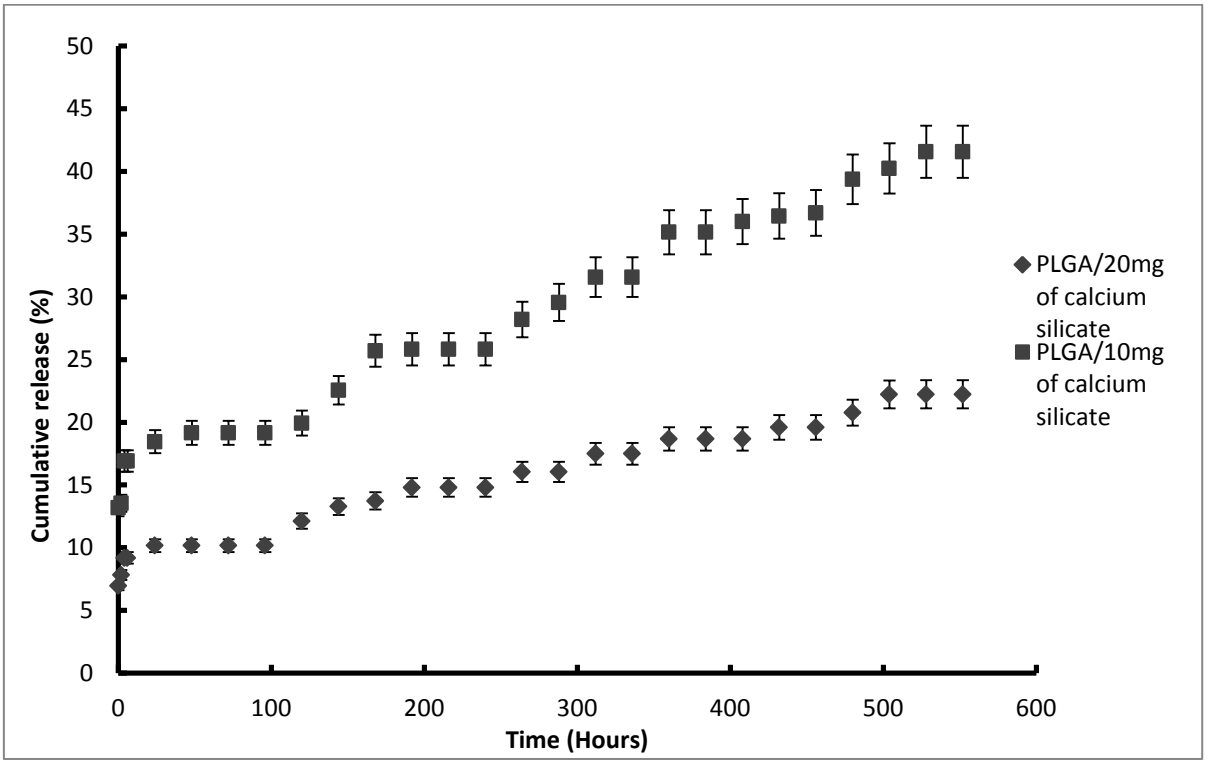

Figure 4.16: Cumulative (%) release of OSA from the PLGA/CS microspheres. Each point represents an average of 3 tests. Error bars indicate the standard deviation of the mean.

The maximum OSA released from the microspheres after 552h was approximately 46% for the microspheres with 10mg of calcium silicate and 22% with those prepared with 20mg. There is a steady release of OSA from these PLGA/CS microspheres, from both batches, independent of the amounts of CS used in the formation of these particles (Figure 4.16).

The amount of OSA released at a given time is at a therapeutic dose for cell survival indicating that the PLGA coating surrounding calcium silicate modifies the release of OSA *in vitro*.

4.4 Discussion

The aim of this investigation was to assess PLGA as a delivery mechanism for orthosilicic acid, to be further applied in orthopaedic reconstruction. Sodium metasilicate or calcium silicate was entrapped into the polymeric matrix and the encapsulation efficiency and the rate of release of OSA was determined.

Different formulations to incorporate silicon into the PLGA microspheres using the w/o/w emulsion-solvent evaporation method were investigated. Little or no OSA was detected when the microspheres were formed with PLGA and sodium metasilicate at pH 13.42, it has been suggested that silica acts as an emulsifier to PLGA particles, whereby silica particles reside exclusively on the interface between the PLGA oil droplet and PVA solution, and therefore very few silica particles are encapsulated into the sphere after solidification, this is often known as the Pickering effect (Li et al. 2011).

Various pH conditions were investigated to increase the encapsulation of sodium metasilicate into the polymeric matrix. The pH of sodium metasilicate was changed from 13.42 to 7 and the diffusion of sodium metasilicate into PVA was reduced by saturating the large water (W_2) phase with a Si source. By 'ion-trapping' the sodium metasilicate salt into the PLGA polymer, increased OSA encapsulation. Prior to any pH changes, the sodium metasilicate salt would easily diffuse from the PLGA into the PVA solution. OSA is hydrophilic, therefore diffuses out of the partition from the dispersed oil phase (PLGA) into the continuous phase (PVA), and therefore leads to poor encapsulation efficiency (Jain 2000).

Calcium silicate ceramics have shown to possess excellent bone regeneration ability, as they have shown to enhance the proliferation of osteoblasts and promote osteogenesis when compared to calcium phosphate cements alone. Calcium silicate ceramics are also well tolerated *in vivo*. Recently there have been some studies in the literature focussing on the composites created by combining polymers and calcium silicate, in this case the polymer used is PLGA. The high ionic dissolution of calcium silicate, leads to a high local pH environment, which results in an adverse cellular response, and may not be suitable for tissue engineering applications. This limitation of calcium silicate can therefore be mitigated by developing CS/polymer composites (Zhao et al. 2011).

Calcium silicate was encapsulated into PLGA micro-particles using the solid/oil/water emulsion technique. This solvent-evaporation technique is often used when a 'drug' such as calcium silicate cannot be dissolved in a carrier solvent. The s/o/w method requires a very low drug particle size in order to allow for a complete encapsulation of the drug crystals. Excess calcium silicate to polymer ratio that is 200mg and 100mg disrupted the formation of micro-particles, however by reducing the amount of CS added into the polymer to 10 and 20mg, formed porous microspheres between 104-106µm in diameter. The encapsulation efficiency of calcium silicate was significantly higher, when compared to that of sodium metasilicate; the CS particles are entrapped in the polymeric matrix rather than adhering to the surface of PLGA microspheres like the silicate salt.

The key advantage of forming microspheres is that they have the potential to accommodate high 'drug' loadings and are able to supply continuous and sustained dosages. Micron size or less, delivery particles can often be injected at a targeted site of a patient, where it will have a localised effect and therefore increases patient compliance, the polymeric matrix also protects the bioactive agent *in vivo*. Therefore the slow release of orthosilicic acid from the PLGA

microspheres plays an important in the nucleation and growth of apatite, and influence the biological metabolism of osteoblastic cells, which are essential to the mineralisation process and bone bonding mechanism (Wei et al. 2008).

The release of OSA from microspheres prepared with sodium metasilicate is divided into a biphasic release. The initial rapid release is attributed to the silicate salt attached either to the surface of the micro-particles or nearby the exterior surface of the polymer. Metasilicate migrated towards the external aqueous phase of the micro-particles, due to its hydrophilic nature and therefore precipitates on the outer surface of the particles, leading to the initial burst of OSA.

The remaining OSA from within the polymeric matrix is released in the second phase of the release profile, whereby OSA is dissolved and transported out of the microspheres (Xue & Shi 2004). The release can also be due to the degradation of the PLGA polymer, which creates channels allowing the passage of the entrapped OSA.

Various studies have shown that by incorporating calcium silicate into polymers not only induces bioactivity into the composite but also improves the composites mechanical properties and hydrophillicity. The PLGA/CS microspheres were formed because of the Pickering effect, whereby the PLGA solution acts as a ‘glue’ and calcium silicate acts as the stabiliser for the microspheres (Li et al. 2011). The release of Ca and Si ionic products neutralises the acidic by-products from degrading PLGA microspheres and therefore stabilises the pH value of the surrounding environment.

Release profiles for 10mg and 20mg CS loaded calcium silicate microspheres follow the similar release profiles as the microspheres entrapped with sodium metasilicate. The initial rapid burst of OSA due the presence of excess calcium silicate on the surface of the PLGA

microspheres, followed by a progressive release rate for 4h and then a gradual increase as PLGA degrades and subsequent diffusion takes place. Approximately 4.4µg/ml OSA was released over the time period of 552 h, the sustained release can be beneficial for the mineralisation of bone *in vivo*.

Orthosilicic acid was also encapsulated within alginate, a commonly used hydrogel for tissue regeneration; little or no release of OSA was observed from the hydrogel beads. This was further investigated and the results are described in chapter 5, whereby it was observed that OSA has a significant effect on the degradation of alginate.

4.5 Conclusion

Various researchers have developed silicon containing biomaterials and have investigated apatite formation, cell attachment and proliferation, very few however, have observed the ions released from these 'bone graft substitutes' and evaluated the therapeutic levels needed to have a positive biological effect.

A delivery system for the tailored release of orthosilicic acid for bone mineralisation was developed, whereby, sodium metasilicate and calcium silicate were entrapped into PLGA microspheres and the release of OSA was determined. Due to the novel nature of sodium metasilicate/PLGA formulations, there are a very few similar studies to compare the OSA release profiles to. The presence of sodium metasilicate increased the porosity of PLGA microspheres, and released therapeutic levels of OSA suitable for *in vitro* cell survival.

Calcium silicate ceramics were coated with PLGA to modify the release properties of the ceramic. PLGA coating acts as a barrier to CS and the release of OSA is decreased significantly, when compared to the release of CS on its own. In addition the alkaline degradation products of CS are neutralised by the acidic degradation products of PLGA, making it a favourable environment for cell viability.

5. Modification of alginate degradation properties using orthosilicic acid

5.1 Introduction

There is a significant and growing need for the development of materials that can be used in the replacement and regeneration of human tissues (Kamitakahara et al. 2008) At present, the `gold standard' in the regeneration of most tissues require harvesting from the patient's own tissue (autogenic) (Heinemann et al. 2009) Although a range of synthetic materials has been used for tissue regeneration, relatively few have replaced autograft tissues as the `gold standard'. A current area of significant interest is the repair of tissues through the delivery of cells to a specific site in the body (Hunt & Grover 2010). The therapeutic delivery of such cell populations has been proposed to assist in the treatment of autoimmune disorders such as rheumatoid arthritis (Jorgensen et al. 2004) and is also thought to have potential to facilitate the regeneration of connective tissues such as cartilage and bone (Tuan et al. 2003). As a consequence of this, there has been a significant drive towards the development of hydrogels as cell delivery vehicles, since they consist largely of water, enabling good mass transport, and have been proposed to resemble the extracellular matrix (Bhattarai et al. 2006). In this chapter we show that the degradation of an alginate hydrogel can be tailored through the addition of orthosilicic acid.

5.1.1 Biodegradable polymer – Alginate

Alginate is a polysaccharide derived from marine brown algae (Tønnesen & Karlsen 2002), and has been widely used in tissue engineering, wound healing as well as a food additive. Alginate is composed of (1-4) linked β-D-mannuronic acid (M unit) and α-L-guluronic acid (G unit). Alginate hydrocolloid gels ionotropically when combined with divalent cations such as calcium. Gelation of the alginate solution occurs between the G - blocks of adjacent alginate chains, creating ionic interchange bridges (Rowley et al. 1999), also known as egg box junctions.

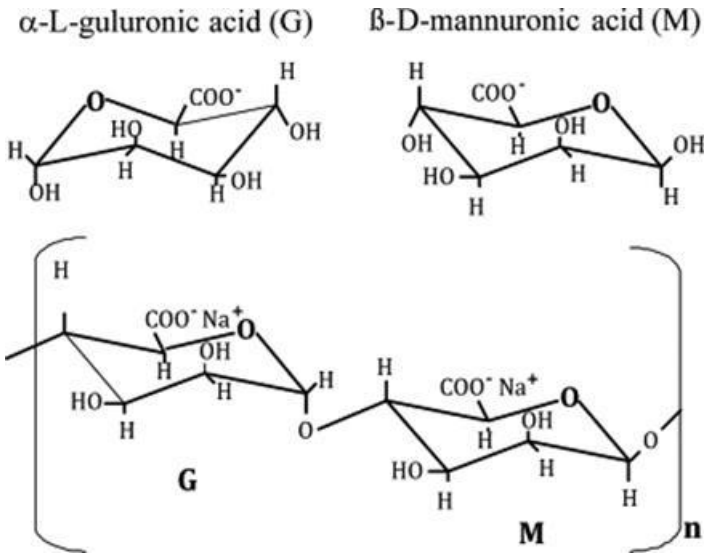

Figure 5.1: Molecular structure and monomer units of alginate; (Jovanovic et al 2012)

While significant progress has been made towards the use of alginate in a clinical context, one major barrier remains the unpredictable degradation rate and often precipitous drop in mechanical properties when maintained in culture conditions or placed in vivo. It has been suggested that this decrease in mechanical properties is usually due to an outward flux of crosslinking ions into the surrounding medium.

A range of modifications have been made to alginate hydrogels to enhance biological function or adjust mechanical properties (Augst et al. 2006), however, relatively little research has been carried out on the control of degradation.

Bioactive molecules are often incorporated with growth factors that can be released from the material to enhance the repair of the tissue specified (Silva et al. 2007) However, trace elements such as silicon have recently become of great interest in regenerative medicine. Silicon has a number of advantages when compared to traditional growth factors, for example it does not induce an adverse immunogenic response and is known to enhance bone formation via both acellular and cellular mechanisms

While authors have previously reported the reinforcement of alginate hydrogels by using silica particles (Coradin 2003; Sakai 2002), there has been little investigation into the incorporation of the soluble form of silicon (orthosilicic acid) into the hydrogel. In this chapter the influence of OSA addition on the degradation and mechanical properties of an alginate hydrogel was evaluated by determining the silicate and calcium release from the gel in the presence of a potent calcium chelator (ethylenediamine tetra-acetic acid; EDTA) and a mechanism for the modification alginate hydrogel properties by interactions between the OSA, calcium and alginate is proposed.

5.2 Materials and methods

5.2.1 Alginate hydrogel preparation

All chemicals and reagents were purchased from Sigma-Aldrich (Gillingham, UK), unless stated otherwise. Alginate hydrocolloid solutions of 2% w/w concentration were made by dissolving sodium alginate (20-40 centipoise (cps) for 2% w/v, Cat. No. 180947, Lot. 08620BJ, MW 102,000-209,000, M:G ratio 1.56) in double distilled water on a heated stirrer plate at 100^{o}C.

Non-modified alginate gels were prepared by the drop-wise method, whereby, the alginate hydrocolloid was added drop-wise using a 10ml plastic syringe into a 100mM calcium chloride, $CaCl_2$, solution, stirred using a magnetic stirrer. The dispersion was allowed to stir overnight, until the beads were fully gelled. For beads that were modified with OSA, 25µg/ml Ammonium hexafluorosilicate (Fisher Scientific) was added to 10mL of the alginate hydrocolloid solution and mixed thoroughly, and the beads were formed as described previously.

5.2.2 Alginate hydrogel bead degradation

The degradation of modified and unmodified beads was determined by suspending the beads in 30mM EDTA solution, and the mean change in diameter was determined with time. The beads were removed from EDTA solution at different time intervals and images of the beads were taken using a digital camera attached to an optical microscope (Carl Zeiss, Welwyn Garden City, UK) at a magnification of 40X. Subsequently the diameter of the beads was determined using ImageJ (National Institute of Health, Maryland, USA).

5.2.3 Calcium release from alginate hydrogel beads

The release of calcium from gelled beads was determined colourmetrically by measuring the intensity of a calcium sensitive dye Arsenezo III (AIII), which undergoes a colour change upon binding with calcium ions. 30µl of sample was taken every 30 minutes for 2 hours and analysed using 4ml of AIII solution, made up with, 400 µM AIII, 300µM NaCl and 200mM HEPES. Followed by the addition of 30µl of 20% (v/v) Triton X – 200 solution. The sample was mixed thoroughly and measured using a UV spectrophotometer at 656nm (Smith et al. 2007).

5.2.4 Orthosilicic acid release from alginate hydrogel beads

To determine the release of OSA from alginate hydrogel beads, a known mass of beads was suspended in 300ml of Dulbecco's Modified Eagle's Medium (DMEM) which was placed in a shaker (Gallenkamp, UK) at 100rpm at 37^0C. 4ml of DMEM was taken from the vessel at specified time intervals and passed through a 0.22µM filter. To maintain a constant volume of the dissolution medium, 4ml of fresh DMEM was replaced after each measurement.

5.2.4.1 Molybdenum blue method – colourimetric assay for OSA detection

The reagents required for the colourimetric assay have been previous described in section 4.2.5. Briefly, to quantify the release of OSA from the alginate hydrogels using the molybedenum blue colourimetric assay, includes 60 µl of 1M hydrochloric acid (HCl), 120µl of ammonium molybdate reagent, 90µl of Oxalic acid and 120µL of the reducing agent 1-amino-2-napthol-4-suphonic acid (Kortesuo et al. 2000). The absorbance of the solution was determined at 650nm using a UV spectrophotometer (Cecil Instruments, UK).

5.2.5 Rheology

Rheology derived from the Greek phrase *panta rei* meaning ‘everything flows’, is the study of deformation and flow of matter, whereby, the relationship between stress and strain within a material can be determined as a function of time, temperature etc. The force per unit area acting on a sample is called stress, measured in Pascals (Pa), this result in the deformation of the sample called strain. Materials can be classified either as solids or liquids depending on their mechanical properties; however materials such as gels are referred to as viscoelastic materials as they have some elastic behaviour (solid) and some viscous behaviour (liquid). Oscillatory shear is used in the characterisation of viscoelastic materials such as biopolymers. In this method, both the stress and strain vary cyclically with time, with sinusoidal variation being the most commonly used. Based on the strain imposed and the stress response, material functions are defined to quantify the material behaviour. G´ the storage modulus and G´´ the loss modulus are defined as stress and strain amplitudes. Storage modulus is based on the amplitude of in-phase stress and loss modulus is based on the out-of-phase stress (Picout & Ross-Murphy 2003).

5.2.5.1 Monitoring alginate hydrogel mechanical properties using small deformation oscillatory rheology

The influence of modification with OSA on the mechanical properties of alginate was determined using small deformation oscillatory rheometry on alginate hydrogel discs. To form the discs, 10ml of alginate 2% (w/w) hydrocolloid, with or without 25µg/ml ammonium hexafluorosilicate was poured into dialysis tubing and then placed into a 100mM $CaCl_2$ to gel via external gelation overnight. The gelled alginate was then cut into 2mm thick discs and placed into un-supplemented DMEM and allowed to age for up to 14 days prior to measurement using a rheometer. All measurements were formed at 37^{o}C using a stress controlled rheometer (TA Instruments, USA). The gels were characterised using 20mm stainless steel parallel plate geometry (sand blasted to prevent slippage) at 0.5% strain, across a frequency ω range of 0.1-100 rad/s. For the determination of G', measurements were carried out at 6.283 rad/s.

5.2.6 Determining the structure of alginate hydrogels

To determine the internal structure of the alginate hydrogels scanning electron microscopy (SEM) was carried out on non-modified and modified hydrogels. The samples were mounted onto a stub and etched at -90^{o}C, to reduce ice crystal formation and were coated with gold (EMSCOPE, UK) before being viewed using the SEM (Philips XL30 ESEM FEG, Netherlands).

5.3 Results

5.3.1 Determining alginate hydrogel degradation

Modification of the calcium alginate hydrogel using the source of OSA made no visual difference to the hydrogel, which remained transparent with the formation of no mineral particulate within the gel matrix. A visual representation of the reduction in diameter of the unmodified and modified beads is shown in Figure 5.2.

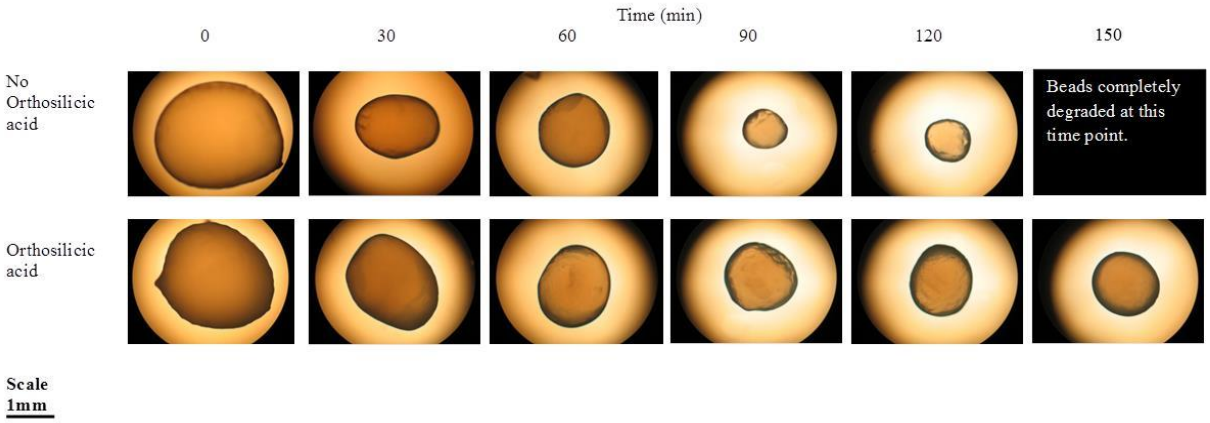

Figure 5.2: Degradation of calcium alginate beads in the presence of EDTA with and without orthosilicic acid addition.

From Figure 5.3 it was seen that on immersion in EDTA, a potent calcium chelator, which breaks the cross-links between the calcium and the alginate, the non-modified hydrogel beads reduced in diameter so that after a period of 150 min of ageing the gel had entirely dispersed within the ageing medium. In the case of the OSA modified gel, the beads lost mass, but at a far slower rate than the control material. After a period of 150 min of ageing in EDTA, the gel beads had only reduced in diameter by 45% (Figure 5.3).

Following further immersion in EDTA, there was no further reduction in average bead diameter and to completely disperse the gel it was necessary to mechanically disrupt the material by sonication followed by further immersion in EDTA.

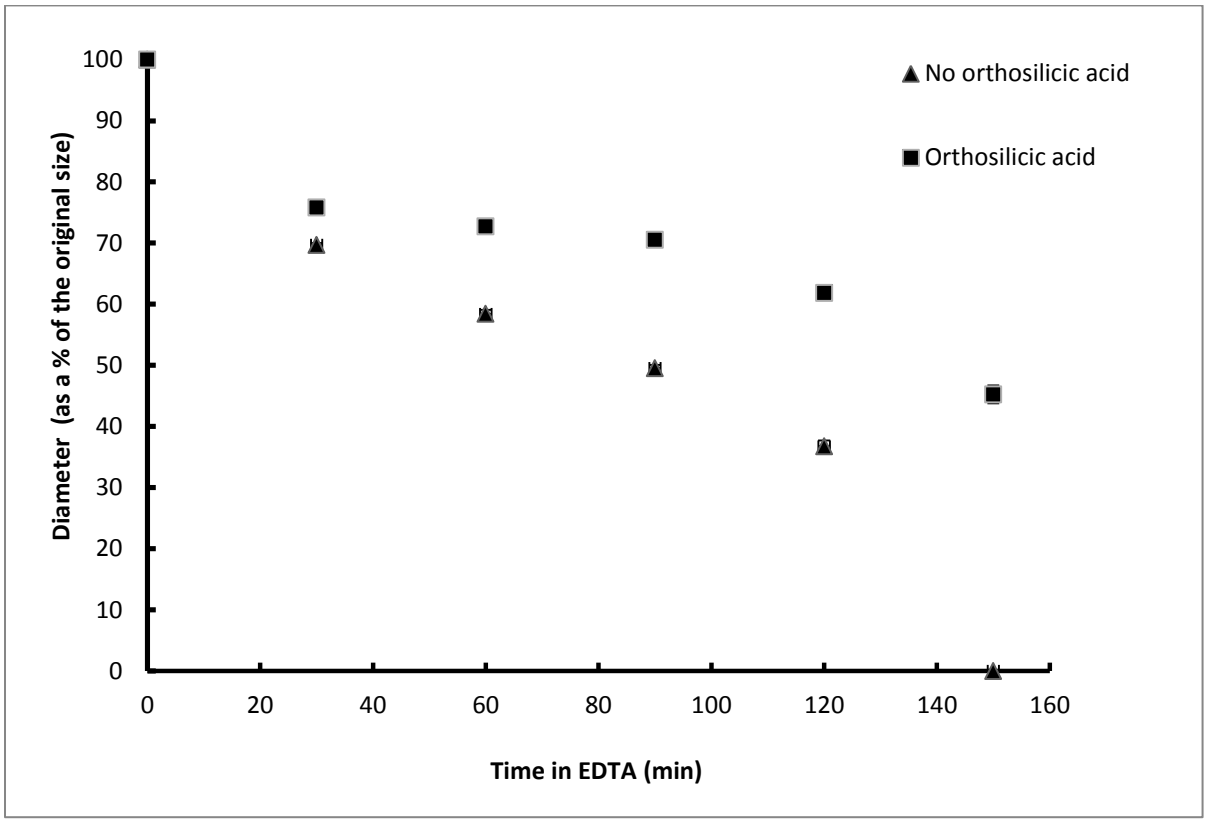

Figure 5.3: Calcium alginate beads were suspended in EDTA and the effect of OSA on the degradation of alginate beads was determined. Each point represents an average of 20 measurements and error bars are indicative of the standard deviations.

5.3.2 Determining calcium release from alginate hydrogels

Since the gel was produced by the formation of cross-links between the calcium ions and the guluronate residues of the alginate polymer and no other cross-linking ions were present, the release of calcium from the modified and non-modified alginate hydrogels was determined. From Figure 5.4 it can be seen that in the case of the non-modified alginate beads, there was an increase in the calcium content of the ageing media up to 120 min when calcium was detectable at a concentration of 60 mM. In comparison, there was little calcium released over a period of 120 min when the hydrogel had been modified using the source of OSA, with only 10 mM detectable in 120 min of ageing (Figure 5.4).

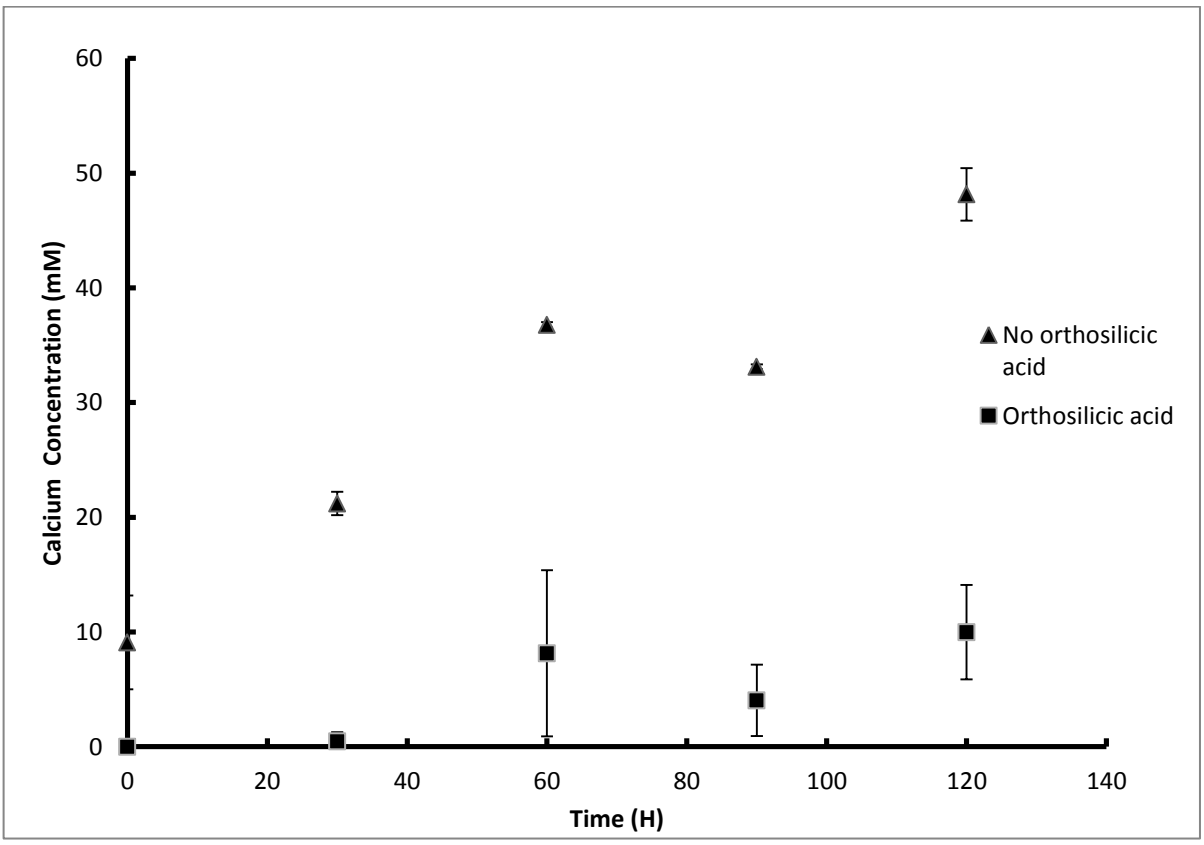

Figure 5.4: Calcium concentration measured when alginate beads were suspended in EDTA. Each point represents the overall mean from 3 experiments and the error bars are indicative of the standard deviation.

5.3.3 Determining the release of OSA from alginate hydrogels

To determine whether OSA was released from the gel on ageing, silicate release from the gels was assayed. Despite a 45% reduction in gel diameter, there was very little OSA released from the alginate hydrogel modified with OSA over 168 minutes (Figure 5.5). Indeed the background concentration of silicate was comparable when there was no OSA loaded into the hydrogel beads.

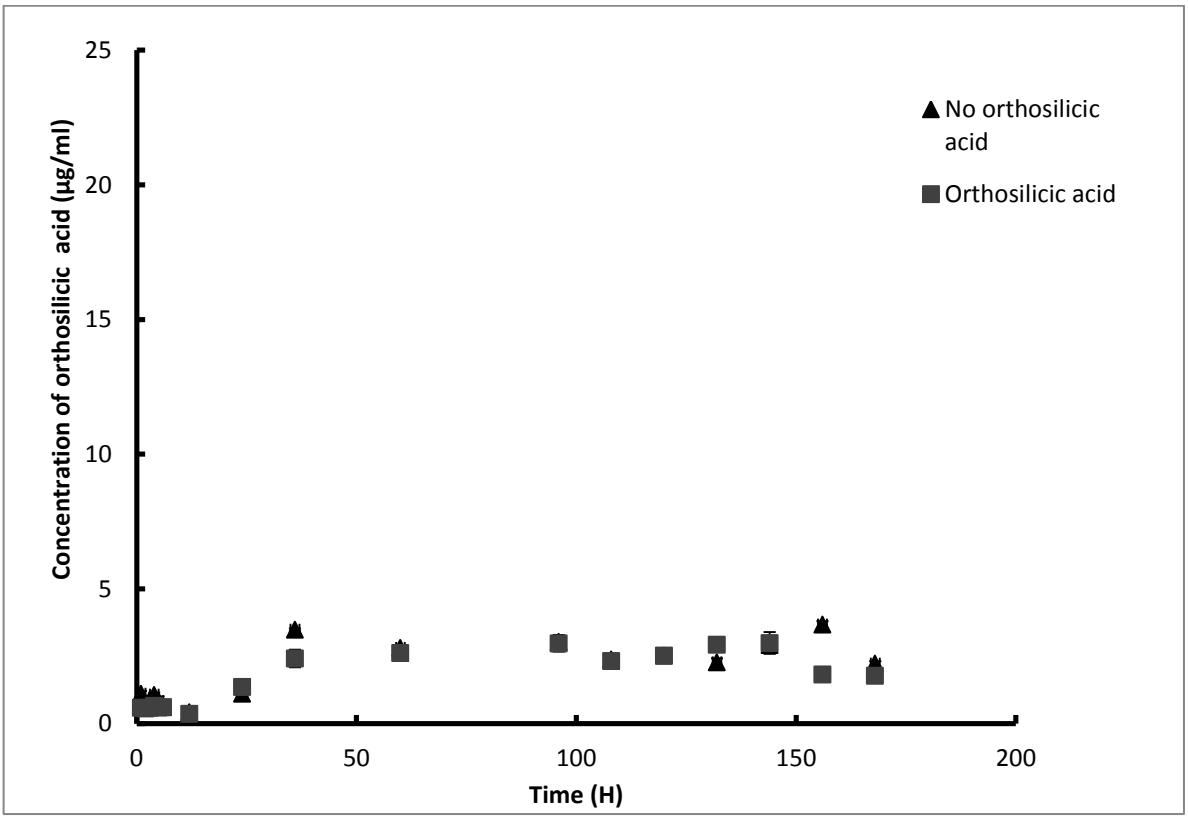

Figure 5.5: The concentration of OSA released from calcium alginate beads, determined using the molybdenum blue assay for orthosilicic acid detection. The error bars represent the standard deviation.

To determine whether the calcium ions were required for the interaction between the OSA and the alginate, alginate hydrocolloid was combined with a solution containing 1mg/ml OSA. The dispersion was left to stand for 1 h and was then centrifuged. The silicate content of the supernatant was shown to be 0mg/ml suggesting that the silicate was immobilised within the hydrocolloid, which was a pale yellow colour, indicating that OSA was present within the hydrocolloid (Figure 5.6).

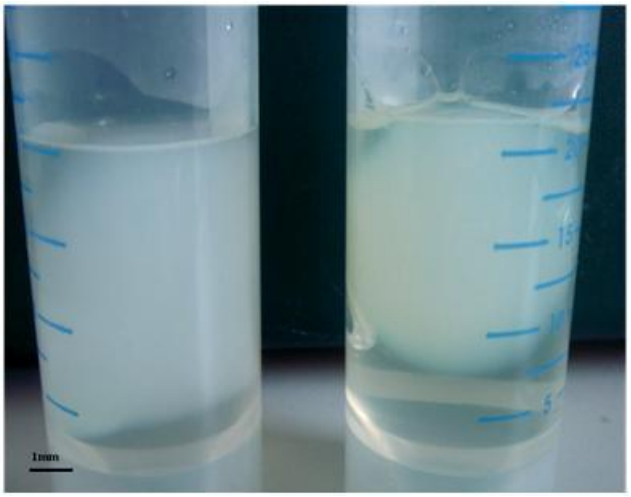

Figure 5.6: The affinity of alginate and OSA was tested with the ammonium molybdate assay.

5.3.4 Determining the microstructure of alginate hydrogels

To further determine the calcium and OSA cross-link network, SEM images of the micro-structure of the OSA modified beads were collected. From figure 5.7 it can be noted that the OSA modified gel has a much smaller and intricate network when compared to the network of the non-modified hydrogel, indicating that although OSA on its own does not gel alginate, in the presence of calcium ions, they form a finer microstructure.

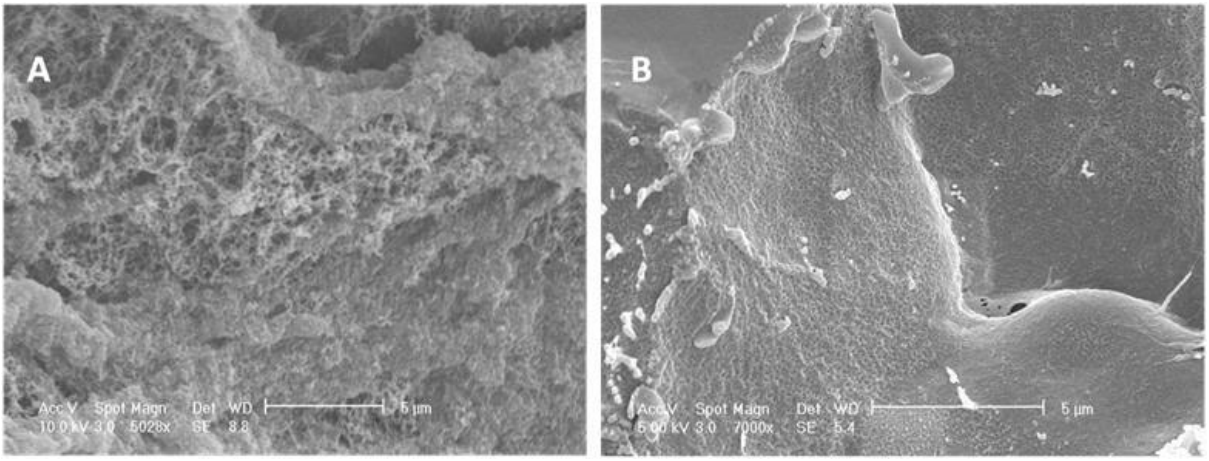

Figure 5.7: SEM images of showing the microstructure of non-modified (A) and modified (B) cross–linked alginate hydrogels.

5.3.5 Determining the mechanical properties of alginate hydrogels

The influence of the OSA on the mechanical properties exhibited by the gel was determined using small deformation oscillatory rheometry. Prior to immersion in DMEM, there was no significant difference between the G' exhibited by the control and the OSA modified alginate hydrogels. In the case of the unmodified alginate, there was a reduction in the G' of the gel over the period of the study from 9000 to 2200 Pa over a period of 14 days of ageing in DMEM (Figure 5.8). This finding is in accordance with that reported by others (Hunt et al. 2010). In comparison, there was relatively little reduction in the G' exhibited by the OSA modified alginate, which was 12000 Pa at both days 0 and 12.

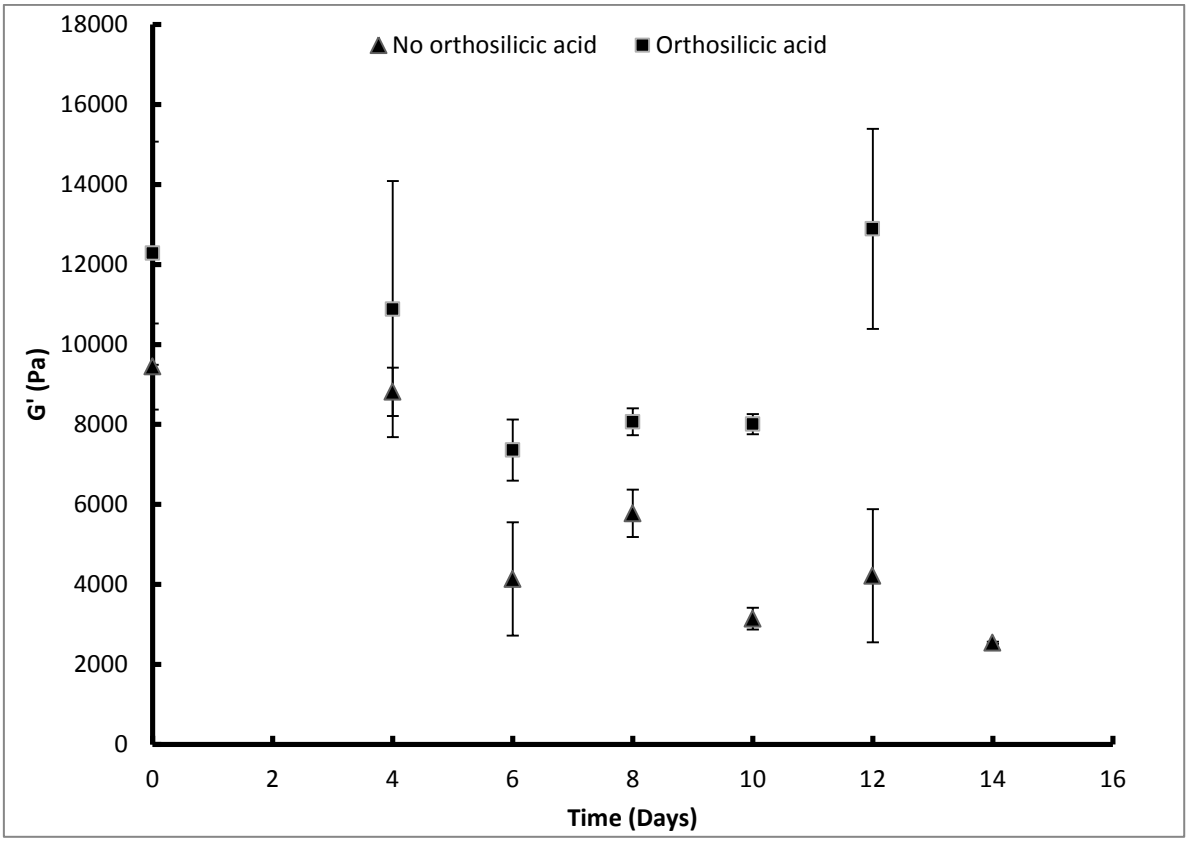

Figure 5.8: Mechanical stiffness, G´ (Pa) of modified and non-modified alginate hydrogels. Anova-two factor with replication was carried out and the p-value calculated at 0.019.

5.4 Discussion

Alginate hydrogels have been used in a variety of medical applications. This is in part because they are tolerated well when placed in contact with the body, but also because they have a similar structure to glycosaminoglycans (GAGs), one important constituent of the extracellular matrix (Bhattarai et al. 2006). As a consequence, alginates have been used for the encapsulation of cells such as chondrocytes, fibroblasts and mesenchymal stem cells for the regeneration of cartilage, skin and bone respectively. One major drawback associated with the use of alginate in the body is that it has a rapid and often unpredictable degradation profile (Hunt et al. 2010). In this study, it has been shown that the degradation of an alginate hydrogel can be retarded by the addition of OSA and that this modification also maintains the

mechanical integrity of the gel when immersed in culture medium. While several authors have previously reported the reinforcement of alginate hydrogel using silicate particles (Coradin et al. 2003; Sakai 2002) to date no-one has evaluated the influence of soluble silicate species on gel properties.

Gelling of alginate occurs as a result of the formation of ionic cross-links between carboxyl groups in guluronic acid residues within the polysacharride. The collection of carboxylic acid groups within the guluronate residue are termed the egg-box junction. Each calcium ion is then chelated by two alginate molecules, forming cross-links, thus resulting in gelation of the hydrocolloid. When immersed in double distilled water alginate will maintain its mechanical properties, however, in the presence of monovalent ions (K^+ or Na^+) ion exchange will occur with the cross-linking Ca^{2+} resulting in a rapid reduction in mechanical properties. Indeed, we have previously reported almost complete degradation within one week of ageing in culture medium. Given the varying ionic concentrations found at different sites in the body and even in different culture media, the degradation properties of the resulting gel can be unpredictable and this remains a major obstacle for the use of alginate hydrogels in medicine.

The addition of OSA to the hydrocolloid enhanced the stability of the hydrogel, and the systematic investigation suggests that this is most likely achieved by each OSA molecule forming an interaction with one or more calcium ions, which prevents them being lost from the structure - even in the presence of the potent calcium chelator EDTA. There have been numerous mentions of the interaction of silica with calcium and alginate in the literature and despite the obvious ionic interactions between OSA and calcium ions in solution, it has been reported that calcium ions can also be adhered onto the surface of OSA through one SiOH group (Perry & Keeling-Tucker 1998) indicating the presence of weak interactions between both of these components. Furthermore, it has been demonstrated that the OSA interacts with

the alginate hydrocolloid (Figure 5.6) and it has previously been reported that silicate species can form strong covalent interactions with alginic acid (Schwarz 1973) or hydrogen bonds between the silanol group and the alginate polymer (Avnir et al. 2006) OSA is negatively charged and so cannot form an association with the egg box junction in the absence of calcium, meaning that it cannot cause cross-linking and therefore gel formation. It is likely therefore, that in the absence of calcium, the OSA interacts via hydrogen bonding on the hydroxyl groups of both the guluronate and mannuronate residues of the alginate. The lack of calcium release in EDTA in the presence of OSA, however, suggests that the OSA may interact with calcium ions that are bound within the egg-box junction. Furthermore, since OSA can polymerise in the pH range of 5-7 (Iler 1955), it is possible that a silicate network could interact with multiple calcium ions, thus augmenting the cross-links between the alginate chains. Indeed, the formation of such complex calcium - silicate networks is the origin of the mechanical integrity of the majority of Portland cement materials. Clearly, the affinity of the OSA and alginate for calcium is higher than the affinity of EDTA for calcium alone. This is illustrated in Figure 5.9, showing the OSA interacting with the mannuronate groups within the cross-linked alginate, and also due to no significant reduction in G' it can be suggested that OSA polymerises on the surface of the gelled hydrocolloid. The minimal release of calcium indicates the interactions between the calcium and OSA.

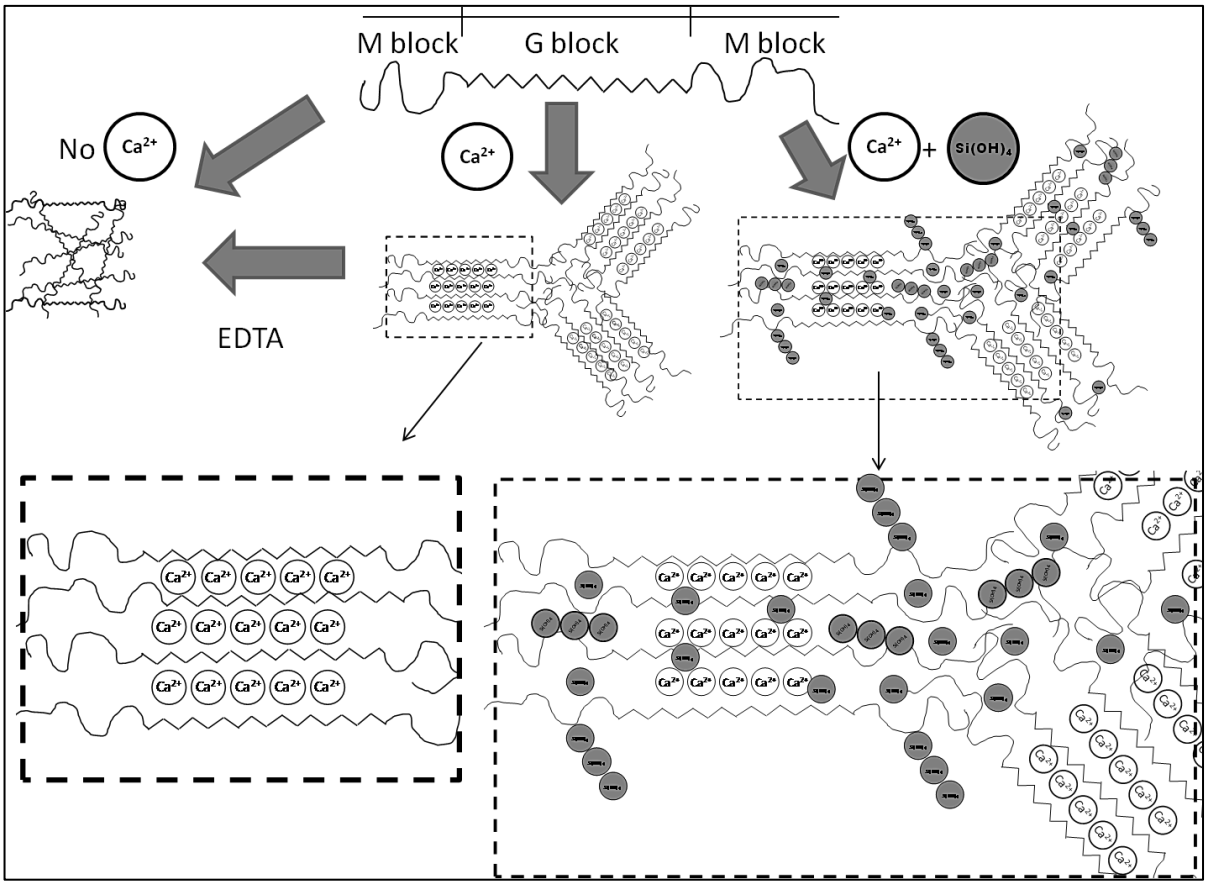

Figure 5.9: Schematic diagram to demonstrate how calcium ions bind to and cross-link the egg-box junctions on the guluronate residues in the alginate polymer enabling gel formation. The addition of calcium chelator EDTA, withdraws the calcium destroying the cross-links and dispersing the gel to reform the alginate hydrocolloid. The addition of OSA to the gel strengthens the interactions between the calcium and alginate holding it in the egg box junction even during aging in EDTA or culture medium, where exchange with monovalent ions can result in extensive degradation.

What is particularly interesting is that although the gel that is formed with OSA reduces in diameter by 45% on immersion in EDTA (Figure 5.3) before plateauing, there is little measurable release of calcium or OSA from the alginate gel into the ageing medium (Figures 5.4 and 5.5). This suggests that the OSA and Ca^{2+} bound in the outer regions of the gel absorbed into the surface of the remaining mass of the bead following material degradation.

This would result in more extensive cross-linking of the remaining gel and may explain why despite there being a reduction in the diameter of the specimens, there was no measurable reduction in the G' of the material over the duration of the study. By maintaining storage modulus and slowing degradation upon immersion in biological fluids, the modification of alginate using OSA may circumvent some of the problems associated with the application of alginate in cell delivery. This is particularly important since cell phenotype is well known to be sensitive to local fluctuation in modulus and in order for cell delivery to be feasible the phenotypic stability of the delivered cells must be guaranteed to prevent potential teratoma formation.

5.5 Conclusion

In this chapter, it has been shown that the addition of OSA to alginate gelled with calcium ions can be used to retard hydrogel degradation, even in a potent calcium chelator (EDTA). It has been demonstrated that this adjusted degradation profile could be attributed to an interaction between the OSA, the hydrocolloid and the cross-linking agent calcium. The ability to adjust the degradation of calcium alginate gels and to maintain mechanical properties even during degradation may help to widen the application of alginate in biomedical applications.

6. Conclusions and Future Works

6.1 Overall Conclusion

The role that silica plays in modifying bone structure was famously reported by Carlisle (1974) and Schwarz et al (1973). They demonstrated that when the levels of silica in an animal's diet were decreased to a critical level, bone and cartilage deformation resulted. Many researchers used this finding as inspiration for the development of a generation of biomaterials, which incorporated silicon into their structure as a means to enhance bone formation. Despite the plethora of biomaterials that now incorporate silicon, little is known, of the biological pathways involved in bone formation that may be influenced by silica.

In this thesis, the role of silicon in early bone mineralisation was elucidated by investigating the dose response and *in vitro* mineralisation of osteoblasts exposed to various concentrations of orthosilicic acid. This led to the development of silicon release systems to provide a controlled dose of OSA. The effect of orthosilicic acid on the degradation properties of the hydrogel, alginate were also evaluated.

In Chapter 3 the effect of orthosilicic acid was investigated on osteoblast responses *in vitro*. The optimum concentration of OSA was determined for cell survival and differentiation. It was noted that osteoblast survival was concentration dependent that is cell proliferation and differentiation increased when treated with of 5µg/ml OSA, however decreased in the presence of 20µg/ml of OSA. The presence of OSA in MC-3T3 cells, led to the early formation of phosphate and calcium nodules, indicating OSA may play a key role in early mineralisation of osteoblast cells. It is important to note, however, that the concentrations of silicon in the deposited mineral were so low as to be non-quantifiable.

RT-PCR analysis showed that OSA induced differentiation in rat bone marrow cells by up-regulating early osteogenic markers such as ALP, osteocalcin, osteopontin and collagen type 1. A significant effect on collagen type 1 expression was noted when cells were treated with OSA and further investigations were carried out to determine the direct interactions between collagen and silicon. OSA was also shown to have a distinct influence on collagen fibril formation, with certain concentrations of OSA producing a compact and irregular collagenous network, when compared with the control. This confirms that OSA may indeed have a critical role in early matrix formation.

Metal ions such as zinc, boron and strontium have also been shown to have a key role in a number of processes associated with bone formation. It has been reported that it is important to control the dosage if metal ions released from biomaterials whereby, the window between efficacy and toxicity is carefully maintained (Lakhkar et al. 2013).

In Chapter 4, a delivery system for the tailored release of OSA for bone mineralisation was developed, whereby, sodium metasilicate and calcium silicate were entrapped into PLGA micro-particles and the release of OSA was determined. The presence of sodium metasilicate increased the porosity of PLGA microspheres when compared with the control, and released therapeutic levels of OSA suitable for *in vitro* cell survival.

Calcium silicate ceramics were coated with PLGA to modify the release properties of the ceramic. The PLGA coating acts as a barrier to CS and the release of OSA was decreased significantly, when compared to the release of OSA from CS on its own. In addition the alkaline degradation products of CS were neutralised by the acidic degradation products of PLGA, reducing the chance of polymer or ceramic degradation causing cytotoxicity *in vivo*.

OSA was also encapsulated in the hydrogel, alginate, however, little or no release of OSA was seen over time. This was further investigated in Chapter 5, where it was demonstrated that the structure of alginate was modified in the presence of OSA. It was shown that the addition of OSA to alginate gelled with calcium ions can be used to stop hydrogel degradation, even in a potent calcium chelator such as EDTA. It was demonstrated that this adjusted degradation profile could be attributed to an interaction between the OSA, the hydrocolloid and the cross-linking agent calcium. The ability to adjust the degradation of calcium alginate gels and to maintain mechanical properties even during degradation may help to widen the application of alginate in biomedical applications.

6.2 Future Work

OSA was shown to up-regulate collagen type 1 expression as well as have a significant effect on collagen fibril formation and diameter. These changes in collagen fibrillogenesis suggest that silicon plays a fundamental role in the development of the extracellular matrix during formation. The next steps to further elucidate the biological pathway of silicon could be to investigate the formation of mineral within the collagen/OSA composite, in an acellular environment (Andre-Frei,1997). Mineral deposition in collagen/OSA composites can further be evaluated using XRD, FTIR and XRF to quantify changes in crystallite structure and composition. Findings from this could suggest that silicon aids in the biomineralisation of collagen, which acts as a template for the deposition of calcium, phosphate and carbonate. TEM imaging would allow for the visualisation of the banding of collagen fibres, which would further enhance the underlying mechanism involved in the interaction between OSA and collagen fibre formation. Furthermore, the production of collagen from osteoblast cells treated with various concentrations of OSA could be assessed using various stains such as

Sirius Red. The effect of OSA on collagen contraction can also be determined by seeding cells either on the surface of the resulting gels or within the collagen gels.

Designing a release system for the dissolution of OSA was also a key part of this investigation. Although PLGA has been shown to be a promising polymer for the delivery of non-toxic doses of OSA, various other polymers could be investigated to tailor the release of OSA from within the polymeric matrix. Other synthetic polymers include poly-ε-carprolactone (PCL) as well as the copolymers of PLGA; poly-lactic acid (PLA) and poly-glycolic acid (PGA), have been demonstrated to be potential polymers used in drug delivery technologies. With variable degradation rates and molecular weights as well as their ability to integrate well with osseous tissue, these polymers can further be investigated as release mechanisms for OSA as well as simultaneously acting as scaffolds for bone regeneration.

PLGA microspheres, entrapped with sodium metasilicate and calcium silicate were fabricated using the water/oil/water and solid/oil/water emulsions, respectively. This method, although successful in forming homogenously sized microspheres, demonstrated a low encapsulation efficiency of OSA. Various other techniques, for example, using solvent casting methods could be employed to enhance the encapsulation efficiency and thus extend the delivery of OSA and making it a more efficient and implantable scaffold/drug delivery composite.

Similar concentrations of OSA released from the PLGA microspheres, were used to evaluate cell mineralisation in vitro (Chapter 3), to further investigate the effect of PLGA/OSA microspheres in cellular conditions would be advantageous. Dose response curves can also be determined for rBMSCs before culturing the cells in trans-well plates and suspending the PLGA/OSA microspheres in the culture media, will allow for the release of OSA and the effect on cell differentiation and mineralisation will be determined. Together with evaluating

the effect of OSA on cell differentiation, the concentration of OSA released from the microspheres could be determined using inductively coupled plasma mass spectrometry (ICP-MS) or atomic absorption spectroscopy (AAS) as it was noted that the ammonium molybdate colourimetric assay had limited usage in various medias, such as PBS and DMEM.

The structure of alginate was modified in the presence of OSA and it has been shown that OSA interacts with the structure of the alginate polymer. Many hydrogels have a similar structure to glycosaminoglycan an important constituent of the extracellular matrix and thus used as a drug and cell delivery vesicles as well as wound dressings. One of the disadvantages of using hydrogels for these applications is that they have unpredictable degradation rates. Orthosilicic acid can therefore be incorporated into other hydrogels such as gellan, pectin, carrageenan and gelatin and their mechanical properties evaluated.

By investigating the above will fully determine the role of orthosilicic acid in mineralisation and will provide a better understanding of the biological pathways involved in bone biology when orthosilicic acid is present. This will further allow in the synthesis of well-tailored silicon containing biomaterials that can be used clinically as bone replacements.

7. References

Anderson, S.I. et al., 1998. Evaluation of the osteoblast response to a silica gel in vitro. *Journal of materials science. Materials in medicine*, 9(12), pp.731–5.

Andreassen, T.T. & Oxlund, H., 2001. The effects of growth hormone on cortical and cancellous bone. *Journal of musculoskeletal & neuronal interactions*, 2(1), pp.49–58.

Anvir, D. et al., 2006. Recent bio-applications of sol – gel materials. *Journal of Materials Chemistry*, 16, pp.1013–1030.

Arcos, D. & Vallet-Regí, M., 2010. Sol-gel silica-based biomaterials and bone tissue regeneration. *Acta biomaterialia*, 6(8), pp.2874–88.

Arumugam, M.Q. et al., 2003. Orthosilicic acid increases collagen type 1 expression in human bone derived osteoblasts in vitro. *Key Engineering Materials*, pp.869–872.

Augst, A.D., Kong, H.J. & Mooney, D.J., 2006. Alginate hydrogels as biomaterials. *Macromol Biosci*, 6(8), pp.623–33.

Avnir, D. et al., 2006. Recent bio-applications of sol–gel materials. *Journal of Materials Chemistry*, 16(11), p.1013.

Barrère, F., van Blitterswijk, C. a & de Groot, K., 2006. Bone regeneration: molecular and cellular interactions with calcium phosphate ceramics. *International journal of nanomedicine*, 1(3), pp.317–32.

Bhattarai, N. et al., 2006. Alginate-Based Nanofibrous Scaffolds: Structural, Mechanical, and Biological Properties. *Adv Mater*, 18(11), pp.1463–1467.

Bonewald, L.F. et al., 2003. von Kossa staining alone is not sufficient to confirm that mineralization in vitro represents bone formation. *Calcified tissue international*, 72(5), pp.537–47.

Bosetti, M. et al., 2003. Type I collagen production by osteoblast-like cells cultured in contact with different bioactive glasses. *Journal of biomedical materials research. Part A*, 64(1), pp.189–95.

Buckwalter, J.A. et al., 2010. Bone Biology. ,pp.1256–1275.

Calomme, M. et al., 2006. Partial prevention of long-term femoral bone loss in aged ovariectomized rats supplemented with choline-stabilized orthosilicic acid. *Calcified tissue international*, 78(4), pp.227–32.

Carano, R.A.D. & Filvaroff, E.H., 2003. Angiogenesis and bone repair Bone healing. , 8(21), pp.980–989.

Carlisle, E.M., 1976. In vivo requirement for silicon in articular cartilage and connective tissue formation in the chick. *Journal of Nutrition*, 106(4), pp.478–84.

Carlisle, E.M., 1972. Silicon: The essential element for the chick. *Science*, 178(4061), pp.619–621.

Chun, K.W. et al., 2004. Biodegradable PLGA microcarriers for injectable delivery of chondrocytes: effect of surface modification on cell attachment and function. *Biotechnology progress*, 20(6), pp.1797–801.

Coradin, T. et al., 2006. Sol-Gel Biopolymer / Silica Nanocomposites in Biotechnology. *Curent Nanoscience*, pp.1-10

Coradin, T. & Lopez, P.J., 2003. Biogenic silica patterning: simple chemistry or subtle biology? *Chembiochem* 4(4), pp.251–9.

Coradin, T., Nassif, N. & Livage, J., 2003. Silica-alginate composites for microencapsulation. *Appl. Microbiol. Biotechnol*, 61(5-6), pp.429–34.

Douthitt, C.B., 1982. The geochemistry of the stable isotopes of silicon. *Geochimica et Cosmochimica Acta*, 46(1449), p.1458.

Ducy, P. et al., 1996. Increased bone formation in osteocalcin-deficient mice. *Letters to Nature*, 382, pp.448–452.

Fan, D. et al., 2012. Mesoporous Silicon-PLGA Composite Microspheres for the Double Controlled Release of Biomolecules for Orthopedic Tissue Engineering. *Advanced Functional Materials*, 22(2), pp.282–293.

Fox, S.W. & Lovibond, A.C., 2005. Current insights into the role of transforming growth factor-beta in bone resorption. *Molecular and cellular endocrinology*, 243(1-2), pp.19–26.

Francis, M.J.O. et al., 2002. ATPase pumps in osteoclasts and osteoblasts. *The international journal of biochemistry & cell biology*, 34(5), pp.459–76.

Fukuoka, H. et al., 2007. Bone morphogenetic protein rescues the lack of secondary cartilage in Runx2-deficient mice. *Journal of anatomy*, 211(1), pp.8–15.

Gabler, F. et al., 2007. Emulsion-based synthesis of PLGA-microspheres for the in vitro expansion of porcine chondrocytes. *Biomolecular engineering*, 24(5), pp.515–20.

Gerber, H.-P. et al., 1999. ARTICLES VEGF couples hypertrophic cartilage remodeling , ossification and angiogenesis during endochondral bone formation. *Nature Medicine*, 5(6), pp.623–628.

Gibson, I.R., Best, S.M. & Bonfield, W., 1999. Chemical characterization of silicon-substituted hydroxyapatite. *Journal of biomedical materials research*, 44(4), pp.422–8.

Golub, E.E. et al., 2007. The role of alkaline phosphatase in cartilage mineralization. *Current opinion in orthopaedics*, 17(2), pp.273–8.

Greenberg, S. a., 1959. The chemistry of silicic acid. *Journal of Chemical Education*, 36(5), p.218.

Grosland, N., 2001. Techniques and applications of adaptive bone remodeling concepts. ... *systems. Techniques and applications*. (3) - Musculoskeletal Models and Techniques CRC Press.

Guénin, S. et al., 2009. Normalization of qRT-PCR data: the necessity of adopting a systematic, experimental conditions-specific, validation of references. *Journal of experimental botany*, 60(2), pp.487–93.

Gunatillake, P. a & Adhikari, R., 2003. Biodegradable synthetic polymers for tissue engineering. *European cells & materials*, 5, pp.1–16.

Gunnarsson, I. & Arnorsson, S., 2000. Amorphous silica solubility and the thermodynamic properties of H4SiO ° 4 in the range of 0o to 350o at Psat. *Geochimica et Cosmochimica Acta*, 64(13), pp.2295–2307.

Guo, D. & Bonewald, L.F., 2009. Advancing our understanding of osteocyte cell biology. *Therapeutic advances in musculoskeletal disease*, 1(2), pp.87–96.

Guo, H. et al., 2007b. Development of calcium silicate/calcium phosphate cement for bone regeneration. *Biomed Mater*, 2(3), pp.S153–9.

H.I.Roach, 1994. Why does bone matrix contain non-collagenous proteins? The possible roles of osteocalcin, osteonectin, osteopontin and bone sialoprotein in bone mineralisation and resorption. *Cell Biology International*, 18(6), pp.617–628.

Hadjidakis, D.J. & Androulakis, I.I., 2006. Bone remodeling. *Annals of the New York Academy of Sciences*, 1092, pp.385–96.

Harvey, N., Dennison, E. & Cooper, C., 2010. Osteoporosis: impact on health and economics. *Nature reviews. Rheumatology*, 6(2), pp.99–105.

Heinemann, S. et al., 2007. A Novel Biomimetic Hybrid Material Made of Silicified Collagen: Perspectives for Bone Replacement. *Adv Eng Mater*, 9(12), pp.1061–1068.

Heinemann, S. et al., 2009. Bioactive silica-collagen composite xerogels modified by calcium phosphate phases with adjustable mechanical properties for bone replacement. *Acta biomater*, 5(6), pp.1979–90.

Heinemann, S. et al., 2011. Effect of silica and hydroxyapatite mineralization on the mechanical properties and the biocompatibility of nanocomposite collagen scaffolds. *ACS applied materials & interfaces*, 3(11), pp.4323–31.

Heinemann, S. et al., 2011. Possibilities and limitations of preparing silica/collagen/hydroxyapatite composite xerogels as load-bearing biomaterials. *Composites Science and Technology*, 71(16), pp.1873–1880.

Hench, L.L., 2009. Genetic design of bioactive glass. *Journal of the European Ceramic Society*, 29(7), pp.1257–1265.

Hing, K. a, 2004. Bone repair in the twenty-first century: biology, chemistry or engineering? *Philosophical transactions. Series A, Mathematical, physical, and engineering sciences*, 362(1825), pp.2821–50.

Hing, K.A., 2005. Bioceramic Bone Graft Substitutes: Influence of Porosity and Chemistry. *International Journal of Applied Ceramic Technology*, 2(3), pp.184–199.

Hogan, H. a, 1992. Micromechanics modeling of Haversian cortical bone properties. *Journal of biomechanics*, 25(5), pp.549–56.

Hunt, N.C. et al., 2010. Encapsulation of fibroblasts causes accelerated alginate hydrogel degradation. *Acta biomater*, 6(9), pp.3649–56.

Hunt, N.C. & Grover, L.M., 2010. Cell encapsulation using biopolymer gels for regenerative medicine. *Biotechnol. Lett.*, 32(6), pp.733–42.

Hunter, G.K. et al., 1996. Nucleation and inhibition of hydroxyapatite formation by mineralised tissue proteins. *Journal of Biochemistry*, 64, pp.59–64.

Iler, R.K., 1955. *The Chemistry of Silica*, Wiley - Interscience.

Jain, R. A, 2000. The manufacturing techniques of various drug loaded biodegradable poly(lactide-co-glycolide) (PLGA) devices. *Biomaterials*, 21(23), pp.2475–90.

Jalili, N. & Laxminarayana, K., 2004. A review of atomic force microscopy imaging systems: application to molecular metrology and biological sciences. *Mechatronics*, 14(8), pp.907–945.

Jones, J.R., 2013. Review of bioactive glass: from Hench to hybrids. *Acta biomaterialia*, 9(1), pp.4457–86.

Jorgensen, C., Gordeladze, J. & Noel, D., 2004. Tissue engineering through autologous mesenchymal stem cells. *Curr. Opin. Biotechnol.*, 15(5), pp.406–10.

Jugdaohsingh, R. et al., 2002. Dietary silicon intake and absorption. *The American journal of clinical nutrition*, 75(5), pp.887–93.

Kadler, K.E. et al., 1996. Collagen fibril formation. *The Biochemical journal*, 316 (Pt 1, pp.1–11.

Kadler, K.E., Hill, A. & Canty-Laird, E.G., 2008. Collagen fibrillogenesis: fibronectin, integrins, and minor collagens as organizers and nucleators. *Current opinion in cell biology*, 20(5), pp.495–501.

Kamitakahara, M., Ohtsuki, C. & Miyazaki, T., 2008. Review paper: behavior of ceramic biomaterials derived from tricalcium phosphate in physiological condition. *Curent Opinion in Biotechnoogy*, 23(3), pp.197–212.

Kaneshiro, E.S. et al., 1993. Reliability of calcein acetoxy methyl ester and ethidium homodimer or propidium iodide for viability assessment of microbes. *Journal of Microbiological Methods*, 17(1), pp.1–16.

Kelm, R.J. et al., 1994. Osteonectin in Matrix Remodeling. *The Journal of Biological Chemistry* , 269(48), pp.30147–30153.

Kempen, D.H.R. et al., 2010. Growth factor interactions in bone regeneration. *Tissue engineering. Part B, Reviews*, 16(6), pp.551–66.

Kirsch, T. et al., 1997. Regulated production of mineralization-competent matrix vesicles in hypertrophic chondrocytes. *The Journal of cell biology*, 137(5), pp.1149–60.

Kortesuo, P. et al., 2000. Silica xerogel as an implantable carrier for controlled drug delivery—evaluation of drug distribution and tissue effects after implantation. *Journal of Biomedical Materials*, 21(2), pp.193–198.

Kuo, A.D. & Carter, D.R., 1991. Computational methods for analyzing the structure of cancellous bone in planar sections. *Journal of orthopaedic research*, 9(6), pp.918–31. Available at: http://www.ncbi.nlm.nih.gov/pubmed/1919856.

Kuo, S.M. et al., 2005. Influence of alginate on type II collagen fibrillogenesis. *Journal of materials science. Materials in medicine*, 16(6), pp.525–31.

Lai, W., Garino, J. & Ducheyne, P., 2002. Silicon excretion from bioactive glass implanted in rabbit bone. *Biomaterials*, 23(1), pp.213–7.

Lakhkar, N.J. et al., 2013. Bone formation controlled by biologically relevant inorganic ions: role and controlled delivery from phosphate-based glasses. *Advanced drug delivery reviews*, 65(4), pp.405–20.

Landis, W.J., Silver, F.H. & Freeman, J.W., 2006. Collagen as a scaffold for biomimetic mineralization of vertebrate tissues. *Journal of Materials Chemistry*, 16(16), p.1495.

Lavernia, C.J. et al., 2004. Bone and tissue allograft use by orthopaedic surgeons. *The Journal of Arthroplasty*, 19(4), pp.430–435.

Lee, a J., Hodges, S. & Eastell, R., 2000. Measurement of osteocalcin. *Annals of clinical biochemistry*, 37 (Pt 4), pp.432–46.

Lee, E.-J. et al., 2009. Membrane of hybrid chitosan-silica xerogel for guided bone regeneration. *Biomaterials*, 30(5), pp.743–50.

Lepage, O.M., Marcoux, M. & Tremblay, a, 1990. Serum osteocalcin or bone Gla-protein, a biochemical marker for bone metabolism in horses: differences in serum levels with age. *Canadian journal of veterinary research = Revue canadienne de recherche vétérinaire*, 54(2), pp.223–6.

Li, D. et al., 2011. Fabrication of poly(lactide-co-glycolide) scaffold embedded spatially with hydroxyapatite particles on pore walls for bone tissue engineering. *Polymers for Advanced Technologies*, (May), p.n/a–n/a.

Lim, S.Y. et al., 2009. Silica-coated alginate beads for in vitro protein synthesis via transcription/translation machinery encapsulation. *Journal of biotechnology*, 143(3), pp.183–9.

Madhumathi, K. et al., 2009. Novel chitin/nanosilica composite scaffolds for bone tissue engineering applications. *International journal of biological macromolecules*, 45(3), pp.289–92.

Makadia, H.K. & Siegel, S.J., 2011. Poly Lactic-co-Glycolic Acid (PLGA) as Biodegradable Controlled Drug Delivery Carrier. *Polymers*, 3(3), pp.1377–1397. A

Maniatopoulos, C., Sodek, J. & Melcher, A.H., 1988. Bone formation in vitro by stromal cells obtained from bone marrow of young adult rats. *Cell and tissue research*, 2(254), pp.317–330.

Mano, J.F. et al., 2007. Natural origin biodegradable systems in tissue engineering and regenerative medicine: present status and some moving trends. *Journal of the Royal Society, Interface / the Royal Society*, 4(17), pp.999–1030.

Matsuno, H. et al., 2001. Biocompatibility and osteogenesis of refractory metal implants, titanium, hafnium, niobium, tantalum and rhenium. *Biomaterials*, 22(11), pp.1253–62.

Matsuo, K. & Irie, N., 2008. Osteoclast-osteoblast communication. *Archives of biochemistry and biophysics*, 473(2), pp.201–9.

Mazzali, M. et al., 2002. Osteopontin--a molecule for all seasons. *QJM : monthly journal of the Association of Physicians*, 95(1), pp.3–13. Available at: http://www.ncbi.nlm.nih.gov/pubmed/11834767.

McGinity, J. & O'Donnell, P., 1997. Preparation of microspheres by the solvent evaporation technique. *Advanced drug delivery reviews*, 28(1), pp.25–42.

McNamara, L., 2011. Bone as a Material. Materials of Biological Origin Elsevier Ltd.

Mohamad Yunos, D., Bretcanu, O. & Boccaccini, A.R., 2008. Polymer-bioceramic composites for tissue engineering scaffolds. *Journal of Materials Science*, 43(13), pp.4433–4442.

Mornet, E. et al., 2001. Structural evidence for a functional role of human tissue nonspecific alkaline phosphatase in bone mineralization. *The Journal of biological chemistry*, 276(33), pp.31171–8.

Navarro, M. et al., 2008. Biomaterials in orthopaedics. *Journal of the Royal Society, Interface / the Royal Society*, 5(27), pp.1137–58.

Nerem, R.M. & Sambanis, a, 1995. Tissue engineering: from biology to biological substitutes. *Tissue engineering*, 1(1), pp.3–13.

Neve, A., Corrado, A. & Cantatore, F.P., 2011. Osteoblast physiology in normal and pathological conditions. *Cell and tissue research*, 343(2), pp.289–302.

Ni, S. et al., 2008. Beta-CaSiO3/beta-Ca3(PO4)2 composite materials for hard tissue repair: in vitro studies. *Journal of Biomedical Materials Research A*, 85(1), pp.72–82.

Niu, T. & Rosen, C.J., 2005. The insulin-like growth factor-I gene and osteoporosis: a critical appraisal. *Gene*, 361, pp.38–56.

Ohlsson, C. et al., 1998. Growth hormone and bone. *Endocrine reviews*, 19(1), pp.55–79.

Ohtsuki, C., Kamitakahara, M. & Miyazaki, T., 2009. Bioactive ceramic-based materials with designed reactivity for bone tissue regeneration. *Journal of the Royal Society, Interface / the Royal Society*, 6 Suppl 3(January), pp.S349–60.

Orimo, H., 2010. The Mechanism of Mineralisation and the Role of Alkaline Phosphatase in Health and Disease. *Journal of Nippon Medical School*, 77(1), pp.4–12.

Palmer, L.C. et al., 2009. NIH Public Access. , 108(11), pp.4754–4783.

Patel, N. et al., 2002. A comparative study on the in vivo behavior of hydroxyapatite and silicon substituted hydroxyapatite granules. *Journal of materials science. Materials in medicine*, 13(12), pp.1199–206.

Perry, C.C., 2010. Silica. *Life Sciences*, pp.1–6.

Perry, C.C. & Keeling-Tucker, T., 1998. Aspects of the bioinorganic chemistry of silicon in conjunction with the biometals calcium, iron and aluminium. *J. Biol. Inorg. Chem*, 69(3), pp.181–91.

Phan, T.C. a, Xu, J. & Zheng, M.H., 2004. Interaction between osteoblast and osteoclast: impact in bone disease. *Histology and histopathology*, 19(4), pp.1325–44.

Picout, D.R. & Ross-Murphy, S.B., 2003. Rheology of biopolymer solutions and gels. *TheScientificWorldJournal*, 3, pp.105–21.

Prasad, S., 1991. Special Discovery of human zinc deficiency human and studies Articles in an experimental.

Raisz, L.G., 1999. Physiology and pathophysiology of bone remodeling. *Clinical chemistry*, 45(8 Pt 2), pp.1353–8.

Reffitt, D.. et al., 2003. Orthosilicic acid stimulates collagen type 1 synthesis and osteoblastic differentiation in human osteoblast-like cells in vitro. *Bone*, 32(2), pp.127–135.

Rimstidt, J.D. & Cole, D.R., 1983. Geothermal Mineralization I: The Mechanism of Formation of the Beowawe Nevada, Siliceous Sinter Deposit. *American Journal of Science*, 283, pp.861–875.

Rosenthal, A.K. et al., 2007. Osteopontin promotes pathologic mineralization in articular cartilage. *Matrix Biol*, 26(2), pp.96–105.

Rowe, M. & Tracey, D., 2005. Mechanosensory perception: are there contributions from bone associated receptors? *Clinical and Experimental Pharmacology and Physiology*, 32, pp.100–108.

Rowley, J. a, Madlambayan, G. & Mooney, D.J., 1999. Alginate hydrogels as synthetic extracellular matrix materials. *Biomaterials*, 20(1), pp.45–53.

Rucci, N., 2008. Molecular biology of bone remodelling. *Clinical cases in mineral and bone metabolism*, 5(1), pp.49–56.

Rupani, A., Balint, R. & Cartmell, S.H., 2012. Osteoblasts and their applications in bone tissue engineering. , pp.49–61.

Sachlos, E. & Czernuszka, J.T., 2003. Making tissue engineering scaffolds work. Review: the application of solid freeform fabrication technology to the production of tissue engineering scaffolds. *European cells & materials*, 5, pp.29–39.

Sakai, S., 2002. Permeability of alginate/sol–gel synthesized aminopropyl-silicate/alginate membrane templated by calcium-alginate gel. *Journal of Membrane Science*, 205(1-2), pp.183–189.

Sapir-Koren, R. & Livshits, G., 2011. Bone mineralization and regulation of phosphate homeostasis. *International Bone and Mineral Society*, 8(6), pp.286–300.

Schwarz, K., 1973. A bound form of silicon in glycosaminoglycans and polyuronides. *Proceedings of the. National Academy of Sciences in the U.S.A.*, 70(5), pp.1608–12.

Sen, C.K. et al., 2002. Copper-induced vascular endothelial growth factor expression and wound healing. *American Journal of Physiology Heart and Circulatory Physiology*, 282, pp.1821–1827.

Shi, X. et al., 2009. Novel mesoporous silica-based antibiotic releasing scaffold for bone repair. *Acta biomaterialia*, 5(5), pp.1697–707.

Shie, M.-Y., Ding, S.-J. & Chang, H.-C., 2011. The role of silicon in osteoblast-like cell proliferation and apoptosis. *Acta biomaterialia*, 7(6), pp.2604–14.

Shoulders, M.D. & Raines, R.T., 2010. Collagen structure and stability. *Annual review of Biochemistry*, (78), pp.929–958.

Silva, G. a, Ducheyne, P. & Reis, R.L., 2007. Materials in particulate form for tissue engineering. 1. Basic concepts. *Journal of Tissue Engineering and Regenerative medicine Med*, 1, pp.4–24.

Smith, A.M. et al., 2007. 3D culture of bone-derived cells immobilised in alginate following light-triggered gelation. *Journal of Control Release*, 119(1), pp.94–101.

Sommerfeldt, D.W. & Rubin, C.T., 2001. Biology of bone and how it orchestrates the form and function of the skeleton. *European Spine Journal* 10 , pp.S86–95.

Song, K.C. et al., 2006. The effect of type of organic phase solvents on the particle size of poly(d,l-lactide-co-glycolide) nanoparticles. *Colloids and Surfaces A: Physicochemical and Engineering Aspects*, 276(1-3), pp.162–167.

Standal, T., Borset, M. & Sundan, A., 2004. Role of osteopontin in adhesion, migration, cell survival and bone remodeling. *Experimental oncology*, 26(3), pp.179–84.

Stenzel, K.H., Miyata, T. & Rubin, a L., 1974. Collagen as a biomaterial. *Annual review of biophysics and bioengineering*, 3, pp.231–53.

Stevens, M.M., 2008. Biomaterials for bone Materials that enhance bone regeneration have a wealth of potential. , 11(5), pp.18–25.

Su, J. et al., 2010. Nanoporous Calcium Silicate and PLGA Biocomposite for Bone Repair. *Journal of Nanomaterials*, 2010, pp.1–9.

Tan, Y. et al., 2010. β-dicalcium silicate., *IEEE*., pp.3–6.

Termine, J.D. et al., 1981. Linking Mineral to Collagen. *Cell*, 26, pp.99–105.

Theriot, E.C. et al., 2012. Diatoms, In: eLS. John Wiley and Sons, Ltd.

Thian, E.S. et al., 2006. The response of osteoblasts to nanocrystalline silicon-substituted hydroxyapatite thin films. *Biomaterials*, 27(13), pp.2692–8.

Tønnesen, H.H. & Karlsen, J., 2002. Alginate in drug delivery systems. *Drug development and industrial pharmacy*, 28(6), pp.621–30.

Towler, M.R. et al., 2009. Comparison of in vitro and in vivo bioactivity of SrO-CaO-ZnO-SiO2 glass grafts. *Journal of biomaterials applications*, 23(6), pp.561–72.

Tuan, R.S., Boland, G. & Tuli, R., 2003. Adult mesenchymal stem cells and cell-based tissue engineering. *Arthritis Research and Therapy*, 5, pp.32-45.

Varanasi, V.G. et al., 2011. The ionic products of bioactive glass particle dissolution enhance periodontal ligament fibroblast osteocalcin expression and enhance early mineralized tissue development. *Journal of biomedical materials research. Part A*, 98(2), pp.177–84.

Verron, E. et al., 2010. Calcium phosphate biomaterials as bone drug delivery systems: a review. *Drug discovery today*, 15(13-14), pp.547–52.

Viguet-Carrin, S., Garnero, P. & Delmas, P.D., 2006. The role of collagen in bone strength. *Osteoporosis international*, 17(3), pp.319–36.

Walschot, L.H.B. et al., 2012. Osteoconduction of impacted porous titanium particles with a calcium-phosphate coating is comparable to osteoconduction of impacted allograft bone particles: in vivo study in a nonloaded goat model. *Journal of biomedical materials research. Part B, Applied biomaterials*, 100(6), pp.1483–9.

Wang, X. et al., 2009. Drug distribution within poly(ε-caprolactone) microspheres and in vitro release. *Journal of Materials Processing Technology*, 209(1), pp.348–354.

Wang, Y. et al., 2006. Examination of mineralised nodule formation in living osteoblastic cultures using fluorescent dyes. *Biotechnology progress*, 22(6), pp.1697–1701.

Wei, J. et al., 2008. Comparison of physical, chemical and cellular responses to nano- and micro-sized calcium silicate/poly(epsilon-caprolactone) bioactive composites. *Journal of the Royal Society, Interface / the Royal Society*, 5(23), pp.617–30.

Whyte, M.P., 2010. Physiological role of alkaline phosphatase explored in hypophosphatasia. *Annals of the New York Academy of Sciences*, 1192, pp.190–200.

Wischke, C. & Schwendeman, S.P., 2008. Principles of encapsulating hydrophobic drugs in PLA/PLGA microparticles. *International journal of pharmaceutics*, 364(2), pp.298–327.

Xue, J.M. & Shi, M., 2004. PLGA/mesoporous silica hybrid structure for controlled drug release. *Journal of Controlled Release*, 98(2), pp.209–17.

Xynos, I.D. et al., 2000. Bioglass 45S5 Stimulates Osteoblast Turnover and Enhances Bone Formation In Vitro: Implications and Applications for Bone Tissue Engineering. *Calcified Tissue International*, pp.321–329.

Yamaguchi, A., Komori, T. & Suda, T., 2000. Regulation of Osteoblast Differentiation Mediated by. *The Endocrine Society*, 21(4), pp.393–411.

Zhao, L. et al., 2011. The influences of poly(lactic-co-glycolic acid) (PLGA) coating on the biodegradability, bioactivity, and biocompatibility of calcium silicate bioceramics. *Journal of Materials Science*, 46(14), pp.4986–4993.

Zolnik, B.S. & Burgess, D.J., 2007. Effect of acidic pH on PLGA microsphere degradation and release. *Journal of Controlled Release*, 122(3), pp.338–44.

8. Appendix

Birdi, G., Bridson, R.H., Smith, A.M., Bohari, S.P., Grover, L.M., (2012) Modification of alginate degradation properties using orthosilicic acid, *Journal of the Mechanical Behaviour and Biomedical Materials* (6) 181-187

Birdi, G., Bridson, R.H., Shelton R.M., Grover L.M., A systematic investigation of orthosilicic acid on bone formation *in vitro* – Poster accepted at the DTC Joint Conference Tissue Engineering and Regenerative Medicine, Keele University, July 2012

Birdi, G., Bridson, R.H., Tan, Y., Grover, L.M., Comparing the release of orthosilicic acid from silicate containing biomaterials – Poster accepted at the 9th World Biomaterials Conference, Chengdu, 2012

Birdi, G., Bridson, R.H., Smith, A.M., Grover, L.M., Mechanical reinforcement of alginate hydrogels using orthosilicic acid – Poster presented at the International Conference on the Mechanics of Biomaterials and Tissues, 2012

Birdi, G., Bowen, J., Smith A.M., Shelton, R.M., Grover, L.M., The Release of Orthosilicic Acid from Silicon Containing Biomaterials and its effect on Collagen Fibril Formation *In Vitro* – Poster presented at the U.K Society of Biomaterials, 2013